



Discovery of a novel dsRNA virus in *Trichomonas gallinae*

Dalal Durzi Ardan

A thesis submitted for the
degree of Doctor of Philosophy

University of East Anglia, School of Biological
Sciences, Norwich, Norfolk, England

September 2022

© This copy of the thesis has been supplied on condition that anyone who consults it is understood to recognise that its copyright rests with the author and that use of any information derived there from must be in accordance with current UK Copyright Law. In addition, any quotation or extract must include full attribution.

Abstract

Trichomonas gallinae is a single-celled protozoan parasite and causative agent of avian trichomonosis, canker or frounce. While a majority of infected birds are asymptomatic, it can be deadly and is the cause of huge die-offs and population declines representing an existential threat to some avian species. Thus understanding the difference between virulent and avirulent strains of this parasite is of considerable interest and importance for its management. Viruses that infect protozoan parasites can modulate virulence, and in the related parasite *Trichomonas vaginalis*, *Trichomonas* viruses are known to affect the pathological outcomes of infection. I set out to determine whether the variation in virulence observed from *T.gallinae* subtypes might be similarly correlated with the presence of viruses. Specifically I undertook to screen an archive of genetically diverse *T. gallinae* isolates from the UK which was hosted from the Tyler laboratory for the presence of viruses. It appeared based on preliminary, standard analyses that the ostensibly avirulent C10 lineage might be host to an active viral infection. I then went on to use Transmission Electron Microscopy and negative staining of supernatants to validate the presence of virus in the isolates identified in the screen. I then evaluated the phenotypic differences between infected and closely related uninfected isolates using Scanning Electron Microscopy and Transmission Electron Microscopy and finally determined the genomic sequence of the novel virus identified from the transcriptome of this isolate. Infected cells were smaller and grew less well than uninfected controls consistent with a fitness deficit from infection. They had a peripheral punctate distribution of virus that was confirmed by Electron Microscopy where the virus could be visualized in the cell periphery and where the infections appeared to affect cellular morphology, topology and ultrastructure, particularly of the Golgi apparatus. Finally, the identity of the virus was confirmed as a member of the *Totiviridae* a dsRNA virus with a close affinity to the TVV1 family of viruses from *T. vaginalis*. The sequence providing support for the idea that contemporary *T. vaginalis* may not have arisen monophyletically but could contain components from more than one *T. gallinae*. In summary, I present evidence for a virus infection in an avirulent *T gallinae* isolate which has considerable implication for the understanding and management of this important avian disease and more broadly for the evolution of the *T. gallinae/T.vaginalis* group of parasites.

Access Condition and Agreement

Each deposit in UEA Digital Repository is protected by copyright and other intellectual property rights, and duplication or sale of all or part of any of the Data Collections is not permitted, except that material may be duplicated by you for your research use or for educational purposes in electronic or print form. You must obtain permission from the copyright holder, usually the author, for any other use. Exceptions only apply where a deposit may be explicitly provided under a stated licence, such as a Creative Commons licence or Open Government licence.

Electronic or print copies may not be offered, whether for sale or otherwise to anyone, unless explicitly stated under a Creative Commons or Open Government license. Unauthorised reproduction, editing or reformatting for resale purposes is explicitly prohibited (except where approved by the copyright holder themselves) and UEA reserves the right to take immediate 'take down' action on behalf of the copyright and/or rights holder if this Access condition of the UEA Digital Repository is breached. Any material in this database has been supplied on the understanding that it is copyright material and that no quotation from the material may be published without proper acknowledgement.

Acknowledgments

First, I would like to express my sincerest gratitude to my UEA supervisory team, Prof Diana Bell (School of Biological Sciences) and Dr Kevin Tyler (Norwich Medical School). I would not have been able to complete this work without their continued guidance, support and encouragement throughout my PhD studies.

I am also grateful for the cooperation of Prof Marlene Benchimol, of the Laboratório de Ultraestrutura Celular Hertha Meyer, at the Instituto de Biofísica Carlos Chagas Filho, UFRJ, Rio de Janeiro, Brazil, who helped me with the TEM. Many thanks are due to Dr Sally Waring and Prof Neil Hall for overseeing the bioinformatic analysis of the *T. gallinae* transcriptome and in particular the identification and assembly of the *T. gallinae* virus. I would like to thank Bertrand Lézé, Head of the Laboratory, at the Technician Science Analytical Facility at the University of East Anglia, Norwich for helping me to observe images using a Zeiss Gemini 300 scanning electron microscope. I would like to thank my past and current lab colleagues, including Dr Éden Ramalho, Georgina Hurle from Norwich Medical School, University of East Anglia. I also want to acknowledge the members of the BMRC floor 01 for their help and support. I also take this opportunity to sincerely acknowledge Hail University for providing financial support, which allowed me to carry out my work in comfort and security. From the bottom of my heart, I would like to thank my beloved husband, Basheer Alshammari, and my children, Ward, Sultan and Rose for their patience and support during my PhD journey. Last but not least, I would like to acknowledge my family in Saudi Arabia, especially my mother, for their sincere encouragement and inspiration throughout my research; I owe them everything.

CONTENTS

Main Contents of Thesis	ii
List of Tables	vi
List of Figures	vii
List of Abbreviations	ix
List of Appendices	xi
Chapter 1: General introduction	1
1.1 Emerging infectious diseases (EIDs)	1
1.2 Emerging infectious diseases of wildlife	2
1.3 SARS_CoV2 and other significant emerging infectious diseases	3
1.4 <i>Trichomonas gallinae</i>	6
1.4.1 <i>T. gallinae</i> Morphology/History	6
1.4.2 Pathogenesis/Pathology of <i>T.gallinae</i>	15
1.5 <i>T. gallinae</i> /virulence/viruses	16
1.6 The aims of this thesis	20
1.7 References	21
Chapter 2: A dsRNA screen of <i>Trichomonas gallinae</i> isolates for potential viral infection	30
Abstract	30
2.1 Introduction	31
2.2 Detection of dsRNA in <i>T.gallinae</i> using monoclonal anti –ds RNA(J2) antibody	32
2.3 Methods	36
2.3.1 Selection of <i>Trichomonas gallinae</i> isolates from the cryobank	36
2.3.2 Medium preparation	38
2.3.3 Giemsa-staining <i>T. gallinae</i>	38

2.3.4 Optimization of growth conditions for RNA extraction	40
2.3.5 Monitoring of <i>T. gallinae</i> culture and counting cells	40
2.3.6 Growth curve for four panel of <i>T. gallinae</i>	40
2.4 Extraction of RNA from <i>Trichomonas gallinae</i> isolates for detection of dsRNA	40
2.5 Material of Immunofluorescence Microscopy Assay	42
2.5.1 Immunofluorescence assay procedure	42
2.5.2 Microscopic images analysis	43
2.6 Northwestern Blotting	43
2.7 Protein concentration assessment	43
2.7.1 SDS - electrophoresis	44
2.7.2 Protein blotting	44
2.8 Antibodies and fluorescent dyes	44
2.9 DotBlot	45
2.10 Statistical Analysis	46
2.11 Results	46
2.11.1 Optimization of growth conditions for RNA extraction	46
2.11.2 Appearance of sub-types of <i>T. gallinae</i> with potential virus	49
2.11.3 The agarose gel electrophoresis	49
2.11.4 Giemsa-staining for the study of morphology <i>T. gallinae</i>	51
2.11.5 Using cell area of <i>T. gallinae</i> subtypes to compare	52
2.11.6 Immunofluorescence microscopy assay	53
2.12 Northwestern blot	57
2.13 Dot blot	57
2.14 Discussion	58

2.15 References	65
Chapter 3: Validating the presence of dsRNA virus in <i>Trichomonas gallinae</i> using Transmission Electron Microscopy	70
Abstract	70
3.1 Introduction	70
3.2 Methods and Buffers	72
3.3 Electron Microscopy Negative Staining Protocol using TEM	73
3.3.1 Protocol (1).	73
3.3.2 Protocol (2).	73
3.4 Using TEM to investigate <i>T. gallinae</i> internal morphology	74
3.5 Field emission Scanning Electron Microscopy	74
3.5.1 Protocol (1).	74
3.5.2 Protocol (2).	74
3.5.3 Protocol (3).	75
3.5.4 Protocol (4).	75
3.6 Cells area comparison of the two sub-types C10 and C4:	75
3.7 Results	75
3.7.1 Negative staining supernatants confirms icosahedral virus-like particles (VLPs) in potentially infected C10 isolate	75
3.7.2 Negative staining of concentrated supernatants reveals abundant exosomes with putative VLPs in infected C10 isolate:	77
3.7.3 Confirmation of virus like particles using TEM of sectioned <i>Trichomonas gallinae</i>	79
3.7.4 Scanning Electron Microscope	81
3.7.5 Results for Protocol 4 Using Osmium tetroxide and Poly L lysine coverslip	84
3.8 Discussion	88
3.9 References	94
Chapter 4: <i>Trichomonas gallinae</i> virus TGV-1 is most closely related to TVV-1.	97

Abstract	97
4.1 Introduction	98
4.1.1 A brief history of transcriptomics	98
4.1.2 RNAseq	101
4.1.3 RNAseq in Trichomonads	104
4.1.4 Trichomonas virus in trichomonad transcriptomes	106
4.2 Materials Methods	107
4.2.1 Earlham institute collaboration	107
4.2.2 Extraction of RNA from <i>Trichomonas gallinae</i> isolates for detection of dsRNA	107
4.2.3 Methods for identification of trichomonas (+virus) RNA-seq	109
4.2.4 Virus genome assembly and identification.	110
4.2.5 Protein alignment and phylogenetic tree.	111
4.3 Results	114
4.3.1 The <i>T.gallinae</i> sample identified as C10 subtype but not those of the C3, C4, or A1 subtypes show high levels of viral transcript.	114
4.3.2 Phylogenetic analysis	117
4.3.3 Design of diagnostics for TVV1 like virus in other <i>T. gallinae</i> strains.	120
4.4 Discussion	124
4.4.1 Surprising phylogeny	125
4.4.2 Future Work	126
4.5 References	127
Chapter 5: General Discussion	131
5.1 Screening an archive of genetically diverse <i>Trichomonas gallinae</i> isolates from the UK.	131
5.2 To use Transmission Electron Microscopy and negative staining of supernatants to validate the presence of virus in the isolates identified in the screen.	132
5.3 To evaluate phenotypic differences between infected and closely related uninfected isolates using Scanning Electron Microscopy and Transmission Electron Microscopy.	133
5.4 To determine the genomic sequences of any novel viruses identified.	135

5.5 Afterword	136
5.6 References	138

List of Tables

Table 1.1 Significant Emerging Infectious Diseases in History	4
Table 1. 2. The literature cited for <i>T. gallinae</i>	9
Table 1.3. Types of viruses of protozoan parasites. (Adapted from Gómez-Arreaza et al., 2017).	18
Table 2.1 A 21 Isolates of <i>T. gallinae</i> obtained from of birds and preserved in cryobank at the University of East Anglia	37
Table 4.1 Measurement of QC of samples for our Low throughput RNA pipeline	107
Table 4.2. TVV genomes used to identify TGV genome in Trinity assembly	110
Table 4.3 Totiviridae genomes used for the	112
Table 4.4 Outcomes from paired end sequencing of cDNA libraries	114

List of Figures

Fig.1.1 Morphology of <i>Trichomonas gallinae</i>	11
Fig. 1.2. Morphology of the greenfinch trichomonad parasite. Scanning electron micrograph	11
Fig.1.3. Oral lesions (Adapted from Robinson et al., 2010).	16
Fig.1.4. Necrotic ingluvitis lesions and trichomonad parasite morphology.	16
Fig. 1.5. Hypotheses on various effects of the virus on the parasite-host relationship.	19
Fig. 2.1 Direct immunofluorescence	32
Fig. 2.2 Amplification of signal with polyclonal secondary antibodies labelled with a fluorophore	32
Fig. 2.3 Amplification of signal with polyclonal secondary antibodies conjugated with multiple fluorophore–protein complexes	33
Fig. 2.4 Schematic representation of blotting and detection procedure	34
Fig. 2.5 The growth of <i>T. gallinae</i> sub-types (1-10 sub-types) from day 1 to day 5	47
Fig. 2.6 The growth of <i>T. gallinae</i> sub-types (11-21 sub-types) from day 1 to day 5	48
Fig. 2.7 The growth of <i>T. gallinae</i> sub-types C10, C4, C3 and A1.	49
Fig. 2.8 Agarose gel electrophoresis of the extracted RNA from 21 isolates of <i>T. gallinae</i> .	50
Fig. 2.9 Agarose gel electrophoresis of the extracted RNA of <i>T. gallinae</i>	50
Fig. 2.10 Sub-types (A1, C3, C4, and C10) stained with Giemsa stain	52
Fig. 2.11 Cell area of <i>T.gallinae</i> Sub-types (A1, C3, C4, and C10 stained with Giemsa stain	52
Fig. 2.12.1 to Fig. 2.12.8. Using monoclonal ant-dsRNA (J2) antibody by immunofluorescence microscopy in sub-type A1.	53
Fig. 2.13.1. to Fig.2.13.8. Using monoclonal ant-dsRNA (J2) antibody by immunofluorescence microscopy in sub-type C3.	54
Fig.2.14.1. to Fig.2.14.8 Using monoclonal ant-dsRNA (J2) antibody by immunofluorescence microscopy in sub-type C4.	55
Fig.2.15.1. to Fig.2.15.8. Immunofluorescence detection of dsRNA (J2) antibody in <i>T. gallinae</i> possibly infected cells in sub-type C10.	56
Fig. 2.16 Blotting bands for the four isolates of <i>T. gallinae</i>	75
Fig. 2.17 Sub-types C10, C3 with increase dsRNA, C4, A1 are negative samples, the last dot is positive control	58
Fig. 3.1 Negative staining of supernatants: (Protocol 1.)	76

Fig. 3.2 Negative staining of potentially infected supernatants: (Protocol 1.)	77
Fig. 3.3 Negative staining of supernatants: (Protocol 2.)	78
Fig. 3.4 Negative staining of infected supernatants: (Protocol 2.) Ex: Exosomes	78-79
Fig. 3.5 TEM N: nucleus, G: Golgi apparatus, V: vacuole VIP: virus -like particles, AF: anterior flagellum, (H) hydrogenosome, RF recurrent flagellum, C costa.	80
Fig. 3.6. TEM deformation of the golgi apparatus in C10.	81
Fig. 3.7. STEM using grids (Protocol 1.) AF: anterior flagellum, PF: posterior flagellum, UM: undulating membrane	82
Fig. 3.8. SEM using glasses coverslips (Protocol 2.) PF: Posterior flagellum, AS: Axostyle, UM: undulating membrane	83
Fig. 3.9. SEM (Protocol 3.) AF: anterior flagellum, PF: posterior flagellum, UM: undulating membrane	83
Fig. 3.10. Using Osmium tetroxide and Poly-I-lysine coverslip (Protocol 4)	85
Fig. 3.11. SEM (Protocol 4.)	85
Fig. 3.12. Viral shedding in C10	86
Fig. 3.13. A. SEM B. TEM	86
Fig. 3.14. Cell area comparison of the two subtypes C10 and C4.	87
Fig. 4.1 An overview of the steps in a typical gene expression microarray or RNA-Seq experiment	100
Figure 4.2 Indirect and direct approaches to RNA-seq.	102
Fig. 4.3 RNA-Seq workflow	103
Figure 4.4. The complete cDNA sequence of the genome of TVV1.	116
Figure 4.5 Phylograms of the protein sequences encoded by TGV1 compared with other related viruses of the Totiviridae	118
Figure 4.6 The 678 amino-acid sequence for the capsid protein of TGV1	120
Figure 4.7 alignment of the protein sequences encoded by TGV1 capsid compared with TVV1 A) B)	121
Figure 4.8A A) epitope predictions and B) conserved peptide with multiple epitopes	121
Figure 4.8 complete CDs of the TGV capsid protein gene	122

Figure 4.9 A) and B) Two conserved target regions (>70% identity) of the capsid gene in the TGV genome against which primers will be made for RT-PCR based detection.	123
---	-----

List of Abbreviations

2D	two-dimensional
3D	three-dimensional
BLAST	Basic local alignment search tool
CSpV1	Cryptosporidium parvum virus 1
DAPI	6-diamidino-2-phenylindole
dH ₂ O	Distilled water
DIC	Differential Interference Contrast
DMSO	Dimethyl sulfoxide coronavirus disease 2019 (COVID-19
DNA	Deoxyribonucleic acid
dsRNA	double-stranded RNA
EIDs	Emerging Infectious Diseases
FeHyd	Fe-hydrogenase
FE-SEM	Modern field-emission scanning electron microscopy
Fig	Figure
FITC	Fluorescein-5-isothiocyanate
GF1c	UK finch epidemic strain
GRV	Giardia RNA Virus
H5N1	Influenza A virus subtype H5N1
HIV	Human Immunodeficiency Virus
IF	Immunofluorescence
ITS	Internal Transcribed Spacer
IWT	IWT—the illicit movement or exchange of wildlife
lncRNAs	long non-coding RNAs
LRV	Leishmania RNA Virus
MEGA	Molecular Evolutionary Genetics Analysis
miRNAs	MicroRNAs
ML	Maximum Likelihood
MLST	Multilocus sequence typing
MP	Maximum Parsimony
MPER	Mammalian Protein Extraction Reagent lysis
MW	Molecular weight
NCBI	National Center for Biotechnology Information
ncRNAs	noncoding RNAs
NGS	Next Generation Sequencing
NJ	Neighbor-Joining
PacBio	Pacific Biosciences
PBS	Phosphate-buffered saline

PCR	Polymerase Chain Reaction
PFA	paraformaldehyde
PME	post-mortem examination
PVDF	Polyvinylidene fluoride
RAPD	Random Amplified Polymorphic DNA
REIDs	re-emerging infectious diseases
RNA-seq	RNA sequencing
RNP	Ribonucleoprotein
rpm	Revolutions per minute
rRNA	ribosomal RNA
RT-PCR	Reverse Transcription Polymerase Chain Reaction
SARS-CoV-2	The novel severe acute respiratory syndrome coronavirus 2
SDS – PAGE	sodium dodecyl sulfate–polyacrylamide gel electrophoresis
SEM	Scanning Electron Microscopy
sEVs	small exosomal vesicles
sEVs	extracellular environment via
SNPs	Single Nucleotide Polymorphisms
SPB	sodium phosphate buffer
ssRNA	single stranded RNA
TBE	Tris borate-EDTA
TBST	Tris-buffered saline Tween 20 solution
TEM	Transmission Electron Microscopy
TGV	Trichomonas gallinae virus
TLR3	Toll-like receptor 3
tRNA	Transfer RNA
TRV	Trichomonas RNA Virus, TRV
TVV	Trichomonas vaginalis virus
TYM	Trypticase-yeast extract-maltose
UrV1	Umbelopsis ramanniana virus 1
UV	Ultra-violet
VDPVs	vaccine-derived polioviruses
VLPs	virus-like particles

List of Appendices

Appendix 2.1 The growth of <i>T. gallinae</i> over the five days for samples from 1-10	140
Appendix 2.2. The growth of <i>T. gallinae</i> in the five days for samples from 11-2110 9-C3 12-A1 13-C420	140

Chapter 1

1.General introduction

1.1. Emerging infectious diseases (EIDs)

Emerging infectious diseases (EIDs) are diseases that are newly recognized, newly introduced, or newly evolved, or that have recently and rapidly changed in incidence or expanded their geographic, host, or vector range (McArthur, 2019). They also include diseases that have affected a given region in the past, declined over time, or were controlled, but again resurfaced in growing numbers (WHO, 2018). The SARS-CoV2 global pandemic (Atzrodt *et al.*, 2020) and the recent outbreaks of Zika virus (ZIKAV) and Ebola virus (EboV) in different regions remind us that the world is still largely unprepared to fight promptly and efficiently with these EIDs (Noorbakhsh *et al.*, 2019).

A study revealed that 60.3% of EIDs infecting humans between 1940 and 2004 were zoonotic in nature (i.e., transmitted from animals to humans) and one in five was transmitted by invertebrate vectors such as mosquitoes, ticks, and midges (Jones *et al.*, 2008).

Pathogens such as avian influenzas emerging in domestic poultry occasionally jump to wild birds and human hosts, causing considerable loss of life and disruption to global commerce. Evidence suggests that climate change and human movements and commerce may have played a role in the recent range expansions of avian pathogens (Fuller *et al.*, 2012; CDC, 2022).

Emerging diseases have been categorized as newly emerging, re-emerging, or “deliberately emerging,” that is, associated with bioterrorism (Table 1.1) (Morens, Folkers and Fauci, 2008; Morens and Fauci, 2013). To these we add “accidentally emerging” human-generated diseases, such as repeated emergences of vaccine-derived polioviruses (VDPVs) resulting from naturally occurring back-mutations of live virus vaccines, as well as a live human-engineered vaccine that escaped to cause a new epizootic disease: naturally transmitted vaccinia (Trejos *et al.*, 1967).

In humans emerging infectious diseases (EIDs) and re-emerging infectious diseases (REIDs) are responsible for a significant proportion of the infectious disease outbreaks that have plagued humanity over the ages, have occurred previously in humans but affected only small populations in isolated areas, or have occurred in the past but were only recently recognized as distinct diseases caused by infectious agents (Tabish, 2009). REIDs are infectious diseases that constituted significant health problems in a particular geographic area or globally during a previous time period, then declined significantly, but are now again becoming health problems of major importance (Tabish, 2009). Most human EIDs and REIDs have a zoonotic origin, meaning that the disease has emerged within an animal and crossed the species barrier to infect humans (WHO, 2021). The majority of these zoonoses come from wild animals, while others originate from domesticated animals and intensive animal farming (Wolfe *et al.*, 2007; Jones *et al.*, 2008; Stephens *et al.*, 2021). They are transmitted from animals to humans through direct contact, droplets, water, food, vectors, or fomites (Rahman *et al.*, 2020). However, as mentioned, not all EIDs and REIDs are zoonotic. Infections due to several multi-drug resistant organisms such as vancomycin-resistant *Staphylococcus aureus* and *Candida auris*, are considered non-zoonotic EIDs that are related to antibiotic overuse and misuse. Irrespective of the origin of an EID or REID, in order for a pathogen to be established in the community, it must be introduced into a susceptible population and have the ability to spread from human to human and cause disease (McArthur, 2019).

1.2 Emerging infectious pathogens in wildlife

As mentioned earlier an infectious pathogen recently introduced or reintroduced to a population with an increased incidence or range is defined as an emerging infectious pathogen (Morse, 2004). Changing environments, globalization, human and animal movements, and other drivers contribute to the evolution of infectious agents, allowing them into new ecological niches (Aguirre and Tabor, 2008). Recent EID events attributed to anthropogenic factors include the

legal and illegal wildlife trade (IWT—the illicit movement or exchange of wildlife), species overexploitation, habitat loss and degradation, exotic species introduction, pollution and climate change (Bell, Robertson and Hunter, 2004; Karesh *et al.*, 2005). Because IWT poses many threats to public health, wildlife, and the integrity of ecosystems (Bell *et al.*, 2004; Gomez and Aguirre, 2008), it is a primary driver of EIDs. IWT opens new disease transmission mechanisms that lead to zoonotic and epizootic outbreaks (Karesh *et al.*, 2005). This risk increases with the sale and transport of wildlife away from their endemic regions (Swift *et al.*, 2019).

EIDs threaten economic stability, biodiversity conservation, and environmental security. Over half of known human pathogens are zoonotic (Cleaveland *et al.*, 2007). Many recent zoonotic EID outbreaks, including the emergence of highly pathogenic influenza H5N1, swine influenza H1N1, SARS, Ebola, Marburg, and MERS, originated from wildlife (Bell *et al.*, 2004; Tu *et al.*, 2004; Kan *et al.*, 2005).

1.3 SARS-CoV2 and other significant emerging infectious diseases

The novel severe acute respiratory syndrome coronavirus 2 (SARS-CoV-2) responsible for the coronavirus disease 2019 (COVID-19) pandemic engulfed the entire world in less than 6 months, with high mortality in the elderly and those with associated comorbidities. The pandemic has severely affected the world economy where shortage of lockdowns, self-distancing, wearing masks, travel restrictions and avoiding gatherings were imperfect constraining measures. Now with more than 546,357,444 confirmed cases and more than 6 million deaths it seems that the addition of vaccine(s) to existing countermeasures holds the best hope for pandemic control (Wang *et al.*, 2020; Wu *et al.*, 2020; Zhu *et al.*, 2020; WHO, 2022). Pandemics such as COVID-19 are not new phenomena (Table 1.1.).

Table 1.1. Significant Emerging Infectious Diseases in History

Year	Name	Deaths	Comments
430 BCE	‘Plague of Athens’	~ 100,000	First identified trans-regional pandemic
541	Justinian plague (<i>Yersinia pestis</i>)	30-50 million	Pandemic; killed half of world population
1340s	‘Black Death’ (<i>Yersinia pestis</i>)	~50 million	Pandemic; killed at least a quarter of world population
C.1500	Tuberculosis	High millions	Ancient diseases; became pandemic in middle ages
1520	Hueyatzuatl (<i>Variola major</i>)	3.5 million	Pandemic brought to New World by Europeans
1793-1798	‘The American plague’	~25,000	Yellow fever affected colonial America
1832	2 nd Cholera pandemic (Paris)	18,402	Spread from India to Europe/Western Hemisphere
1918	‘Spanish’ influenza	~50 million	Led to additional pandemics in 1957, 1968, 2009
1976-2020	Ebola	15,200	First recognized in 1976; 29 regional epidemics to 2020
1981	Acute haemorrhagic conjunctivitis	Rare deaths	First recognized in 1969; Pandemic in 1981
1981	HIV/AIDS	~37 million	First recognized in 1981; ongoing pandemic
2002	SARS	813	Near-pandemic
2009	H1N1 ‘swine flu’	280\$,000	5 th Influenza pandemic of century
2104	Chikungunya	Uncommon	Pandemic, mosquito-borne
2015	Zika	~1,000?	Pandemic, mosquito-borne
2103	H7N9	19%	Case-fatality rate (Yu <i>et al.</i> , 2013)
2022	Covid-19 in 1 July 2022	6,334,728 deaths as of 1 July 2022	(WHO, 2022)
(Adapted from (Morens and Fauci, 2020))			

Newly emerging (and re-emerging) infectious diseases have been threatening humans since the Neolithic period, 12,000 years ago, when human hunter-gatherers settled into villages to domesticate animals and cultivate crops (Morens *et al.*, 2008; Morens and Fauci, 2020). These

beginnings of domestication were the earliest steps in man's systematic, widespread manipulation of nature. Ancient emerging zoonotic diseases with deadly consequences include smallpox, falciparum malaria, measles, and bubonic/ pneumonic plague. Some, e.g., the Justinian plague (541 AD) and the Black Death (1348 AD), killed substantial proportions of humans in the "known" world, i.e., the world known to those whose recordings of it survive, predominantly in Asia, the Middle East, and Europe. Only a century ago, the 1918 influenza pandemic killed 50 million or more people, apparently the deadliest event in recorded human history (Taubenberger and Morens, 2020).

The 1918 Spanish influenza, which infected more than one-third of the world's population and killed approximately 50 million people, is the best known example. There have been several influenza pandemics since 1918—in 1957 and 1968, as well as H1N1 in 2009 (Grennan, 2019). A number of emerging infectious diseases are caused by microbes that originate in nonhuman vertebrates. Hantavirus pulmonary syndrome was first noted in the Four Corners area of New Mexico in 1993 (Steere *et al.*, 2004). The disease is caused by Sin Nombre virus, which is endemic in the deer mouse *Peromyscus maniculatus*. Why humans first became infected with this rodent virus is not known, but an increase in the deer mouse population might have been a factor. In 1992–93, abundant rainfall produced a large crop of piñon nuts, which are food for both humans and the deer mouse. As the mouse population rose, contact with humans increased. The virus is excreted in mouse droppings, and contaminated blankets or dust from floors provided opportunities for human infection. The emergence of Lyme disease, discussed in the review by Steere, Coburn, and Glickstein (2), followed a similar course (Steere *et al.*, 2004). Protozoan parasites are responsible for severe diseases in humans worldwide. Apart from disease transmission via insect vectors and contaminated soil, food, or water, transmission may occur congenitally or by way of blood transfusion and organ transplantation (Sutrave and Richter, 2021).

Infections caused by intestinal protozoan parasites (IPPs) are among the most prevalent human pathogens that typically affect low-income communities particularly in developing countries (Castellanos-Gonzalez *et al.*, 2018; Tegen *et al.*, 2020). They have been recognised as significant causes of gastrointestinal illnesses, malnutrition and mortality. Several pathogenic protozoan parasites are responsible for the above health issues including *Entamoeba*, *Giardia lamblia* (also known as *Giardia intestinalis* and *Giardia duodenalis*), *Cryptosporidium* spp. and *Balantidium coli*, which are the most common species associated with significant illnesses (Castellanos-Gonzalez *et al.*, 2018; (Tegen *et al.*, 2020). Infection by *E. histolytica* is considered the third most common cause of death after malaria and schistosomiasis (Ouattara *et al.*, 2010). In addition, *Cryptosporidium* spp. and *G. lamblia* are important nonviral causes of diarrhoeal diseases in humans (Squire and Ryan, 2017), while other species of intestinal protozoa are either not widely prevalent or non-pathogenic parasites.

1.4 *Trichomonas gallinae*

1.4.1 *T. gallinae* Morphology/History

Avian trichomonosis, caused by the flagellated protozoan parasite *T. gallinae*, is an infectious disease affecting avian communities worldwide (Tompkins *et al.*, 2015). *T. gallinae* belongs to the flagellate protozoa of the family *Trichomonadidae*, within the order *Trichomonadida*, which are amitochondriate, possessing a highly evolved organelle, the hydrogenosome (Brugerolle, 2000). The hydrogenosome is a membrane-bound organelle which is able to release molecular hydrogen as a result of anaerobic energy production in the cell. *T. gallinae* and *Tetratrichomonas gallinarum*, are the two common trichomonad species described in birds. *T. gallinae*, present in lesions of the upper digestive tract of pigeons, was firstly reported by Rivolta (1878), who named it *Cercomonas gallinae*. Because some flagellates were also found in a pigeon liver in connection with caseous hepatitis the pathogen was also called *Cercomonas hepaticum*. Later, Stabler (1956) introduced the name *T. gallinae* for trichomonads that

colonize the crop of pigeons. *T. gallinae* is the only trichomonad species with a non-ambiguous, proven pathogenic potential for birds (Bondurant and Honigberg, 1994).

Colonization of the caecum of chickens by *T. gallinarum* has been known for more than 100 years (Martin and Robertson, 1911). The flagellate is a common inhabitant in the caecum of gallinaceous birds (Hess and McDougald, 2013).

The parasite *T. gallinae* is of veterinary and economic importance as it causes avian trichomonosis, a disease with important medical and commercial implications. Avian trichomonosis has been reported from several continents and is considered a major the disease of numerous avian species, especially columbiformes and falconiformes (Stabler, 1954). In pigeons, the disease is also called canker. The rock pigeon (*Columba livia*) is the primary host of *T. gallinae* and has been considered responsible for the worldwide distribution of this protozoal infection (Stabler, 1954; Harmon *et al.*, 1987). Similarly, other species within the Columbidae, like doves (e.g. *Streptopelia decaocto*) and feral or wood pigeons (e.g. *Columba palumbus*) are also important hosts (Bondurant and Honigberg, 1994).

Raptors, like hawks, eagles and falcons, are also susceptible to infection by *T. gallinae* (Krone *et al.*, 2005), and may develop trichomonosis, which is also termed ‘frounce’ in these birds after they prey on infected columbids (McDougald, 2013). In the UK avian trichomonosis has been identified as an emerging infectious disease of wild finches (Robinson *et al.*, 2010), which spread to continental Europe as a consequence of bird migration (Lawson *et al.*, 2011).

Trichomonosis, characterized by morbidity and mortality was also reported in wild free-ranging house finches *Carpodacus mexicanus*, mockingbirds *Mimus polyglottos* and corvids (scrub jay: *Aphelocoma californica*; crow: *Corvus brachyrhynchos*; raven: *Corvus corax*) in northern California (Anderson *et al.*, 2009). In comparison to the species of birds mentioned before only a few natural occurrences of trichomonosis have been reported in gallinaceous birds like turkeys (Hawn, 1937) and chickens (Levine and Brandly, 1939). However, the

disease has also been found to be a major cause of mortality in endangered columbids such as the Mauritian Pink pigeon (Bunbury *et al.*, 2007).

In adult columbid the infection can occur during courtship or parental feeding of crop milk while raptors can be infected from prey animals carrying the parasite. The infection of turkeys and chickens happens mainly via drinking water contaminated by pigeons (Bondurant and Honigberg, 1994).

It seems that the severity of the disease depends on the susceptibility of the infected birds together with the pathogenic potential of the incriminated strain and the stage of infection (Cooper and Petty, 1988; Cole and Friend, 1999). It was also thought that variations in virulence are related to the antigenic composition of the parasite (Stepkowski and Honigberg, 1972; Dwyer, 1974; Maiden, 2006).

Different studies have been conducted on *T. gallinae* using staining, culture and molecular techniques targeting the prevalence and strains in varied wild birds are summarized in Table 1.2.

Table 1.2. Examples of species studies reporting *T. gallinae*

No.	Country	Type of sample/bird	Number of samples	Detection method	<i>Trichomoniasis</i> %	Reference
1	Egypt	Pigeons	3315	PCR	1.9%	(El-Khatam <i>et al.</i> , 2016)
2	USA	Wild Birds (Raptor)	188	Culture and PCR	0.53	(Spriggs <i>et al.</i> , 2020)
3	USA	Finches	NA	Wet mount and PCR	1.7% in house finches	Anderson <i>et al.</i> , 2009)
4	Iran	Pigeons	100/62	Oropharyngeal swabs and blood samples (PCR)	57%, 62%	(Nematollahi <i>et al.</i> , 2012)
5	USA	Golden Eagle nestlings	96	PCR	13% in of eagle nestlings across 10 western states 41% of nestlings in southwestern Idaho	(Dudek <i>et al.</i> , 2018)
6	China	Pigeons	569	Culture+PCR	The overall prevalence was 28.30%. nestling pigeons (33.16%), adolescent pigeons (30.05%) and breeding pigeons (20.59%)	(Feng <i>et al.</i> , 2018)
7	Spain	wild and domestic pigeons (<i>Columba livia</i>) and birds of prey from 15 different species	612, 102	PCR	44.8%	(Sansano-Maestre <i>et al.</i> , 2009)
8	Saudi Arabia	captive falcons	158	PCR	26.58%	(Alrefaei, 2020)
9	Bangladesh	Pigeons	300	Giemsa's method	67.3%	(Begum, 2008)
10	Germany	Birds	440	Trichomonas-selective culture medium, PCR	35.6% Owls (58%) and columbids (50%), 36% in Accipitriformes, 28% in	(Quillfeldt <i>et al.</i> , 2018)

					Falconiformes and 28% in Passeriformes	
11	Ireland	Wild birds	60	Culture	15	(Doyle, 2022)
12		Columbidae Mourning Doves White-winged Doves			5.6 34.2 95	(Schulz <i>et al.</i> , 2005)

Representatives of the order Trichomonadida are unicellular organisms with a single nucleus. These flagellates are characterized by the presence of a single karyomastigont, five to six flagella, undulating membrane of lamelliform-type and the B-type costa (Cepicka *et al.*, 2010). Trichomonads lack classic of mitochondria as sites of oxidative fermentation, Trichomonads have specialized organelles called hydrogenosomes (Muller, 1993). These energy-generating organelles use a fermentative pathway for pyruvate metabolism and not the Krebs cycle as classical mitochondria. The presence or absence of a protruding flagellum behind the posterior end of the body is the main morphological feature for differentiation between *T. gallinae* and *T. gallinarum*. The trophozoite (stage of development in *T. gallinae*) of *T. gallinae* measures from 7–11 µm and possess four free anterior flagellae and a fifth recurrent one, (Tasca and De Carli, 2003; Mehlhorn *et al.*, 2009). The nucleus is ovoid with a size of 2·5–3 µm (Fig.1.1).

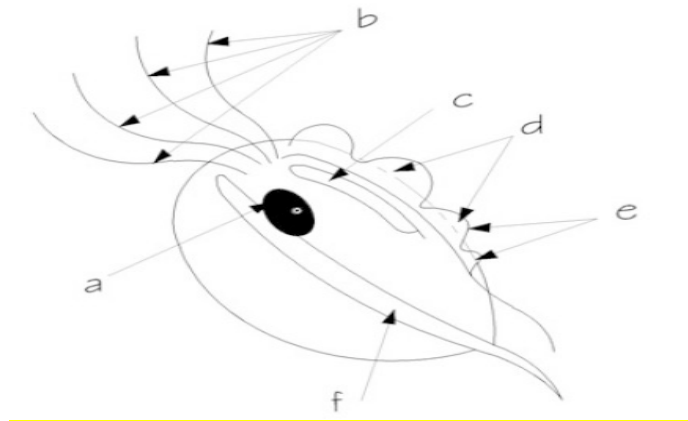


Fig.1.1. Morphology of *Trichomonas gallinae*, a. Nucleus b. anterior flagella c. parabasal body d. undulating membrane e. posterior flagella f. axostyle (Adapted from Samanta et al., 2017)

However, *T. gallinae* does not have a posterior flagellum, an important diagnostic feature that separates the organism from *Tetratrichomonas gallinarum*, which is often found in avian species, especially those in the order Galliformes (Tasca and De Carli, 2003; Mehlhorn *et al.*, 2009). Giemsa-stained parasite culture preparations revealed a variable morphology (body dimensions range 8–11mm) typical of a trichomonad parasite with a single nucleus and axostyle, anterior flagella and an undulating membrane. Scanning and transmission electron microscopy (Fig. 1.2.) confirmed the presence of a parasite with plastic pyriform morphology and four anterior flagella that typically exited the body together in pairs. A prominent undulating membrane, with no free posterior trailing flagellum, was present (Robinson *et al.*, 2010).

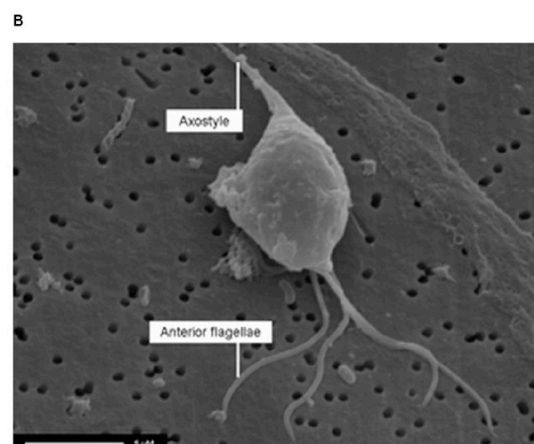


Fig. 1.2. Morphology of the greenfinch trichomonad parasite. Scanning electron micrograph. Arrows indicate anterior flagella and axostyle (Adapted from Samanta et al., 2017).

It was reported that 15 novel genotypes of *Trichomonas gallinae* were discovered with moderate to high host-specificity, with only two genotypes found in more than one host species (Chou *et al.*, 2022). *Trichomonas* genotypes were phylogenetically clustered into four well-supported clades and the genus exhibited moderate genetic diversity. The most basal of these consisted of three *Trichomonas* genotypes detected by PCR in *Ptilinopus regina* and *Ptilinopus ornatus*. Other Australasian lineages formed an entirely Australasian clade or were part of an ‘Old World’ clade with Eurasian and African genotypes. A fourth, ‘New World’, clade consisted predominantly of North American genotypes but also included the cosmopolitan human pathogen *T. vaginalis*. Concatenated and partitioned 18S and ITS1/5.8S/ITS2 rRNA gene phylogenies for a subset of genotypes provided support for the ‘Old World’ clade as sister to the ‘New World’ clade. Ancestral state reconstruction provided strong posterior support (90%) for columbids as the host of the most recent common ancestor of all extant *Trichomonas* lineages, and even higher support (97–99%) for columbids as the ancestral host of each of the four major clades. There was moderate posterior support (51%) for an Australasian origin for the genus (Peters *et al.*, 2020). It was reported that the finch trichomonosis epidemic is caused by a clonal strain of *T. gallinae* (Lawson *et al.*, 2011). ITS region sequences obtained from 11 species of affected British passerines showed that they had 100% identity to each other and to ITS region type A isolates from the USA (Anderson *et al.*, 2009; Gerhold *et al.*, 2009), Mauritius (Gaspar da Silva *et al.*, 2007), Brazil (Kleina *et al.*, 2004), Spain (Sansano-Maestre *et al.*, 2009).

Sequence typing from cultured *T. gallinae* at the ITS1/5.8S rRNA/ITS2 region resolved three distinct ITS region types circulating in free-ranging British birds. Subtyping by sequence analyses at the Fe-hydrogenase gene demonstrated further strain variation within these ITS region types (Chi *et al.*, 2013).

Several methods to cultivate trichomonads using a growth medium for trichomonads detection was found to be effective (Bunbury *et al.*, 2005). In addition, cultivation has been the gold standard for detection of trichomonads as it is easy to interpret and gives valid results, even in birds with asymptomatic infections. *T. gallinae* grows in a variety of media (Forrester and Foster, 2008).

InPouch™ TF Kits has been used by many studies as commercial product originally developed to culture *Tritrichomonas foetus* from cattle, which was shown to be very convenient and effective for use in the field (Schulz *et al.*, 2005; Bunbury *et al.*, 2007).

Polymerase chain reaction (PCR) was also used to identify flagellated protozoan in wood pigeons (*Columba palumbus*) (Hofle *et al.*, 2004). Molecular methods used to discriminate strains of *T. gallinae* include sequence data from the 5.8S ribosomal RNA (rRNA) and surrounding internal transcribed spacer regions 1 and 2 (ITS1, ITS2) have been increasingly used to detect *T. gallinae* infection (Gaspar da Silva *et al.*, 2007) and to identify genetic heterogeneities in the parasite (Gerhold *et al.*, 2008; Anderson *et al.*, 2009; Grabensteiner *et al.*, 2010). Sequence analyses of the ITS1/5.8S/ITS2 region (hereafter called ITS region) have identified marked variation amongst isolates obtained from a wide geographical region and from different host taxa, with some 15 distinct ITS region sequences identified as discrete ITS ribotypes (Gerhold *et al.*, 2008; Anderson *et al.*, 2009).

Multilocus sequence typing (MLST) is a nucleotide sequence-based method that is used to characterize the genetic relationships between microbial species. It has been successfully applied to study populations of bacterial and eukaryotic organisms (Maiden *et al.*, 1998; Hanage WP, 2005; Subileau *et al.*, 2009). Selected loci are normally single copy housekeeping genes so that the variation within these genes is nearly neutral but less prone to homoplasy than using an alternative approach such as multilocus microsatellite typing, and thus they are better able to serve as robust markers of ancient and modern ancestry.

Multilocus sequence typing (MLST) has proven to be an effective and widely used method for characterizing bacterial Isolates. MLST indexes the diversity of nucleotide sequences of fragments of housekeeping genes (loci), with most bacterial MLST schemes employing seven loci of approximately 400–500 bp each, a length initially chosen as achievable with dideoxy sequencing technology (Maiden *et al.*, 1998).

Another advantage to using MLST as a genotyping approach is that the DNA sequences can be determined using automated technology and therefore require minimal subjective interpretation of the data (Maiden *et al.*, 1998).

MLST has since been applied to a number of different bacteria and eukaryotic organisms as a tool for the epidemiological analysis and surveillance of pathogens as well as to investigate their population structure and evolution. MLST has also been deployed in studies of the population structure of nonpathogenic bacteria (Maiden, 2006).

MLST provides a number of advantages over other typing approaches. First, it uses sequence data and can therefore detect changes at the DNA level that are not apparent by phenotypic approaches, such as serotyping, and by MLEE that uses the migration rate of proteins in starch gels. Second, it is a generic technique that can be readily reproduced and does not require access to specialized reagents or training. Third, modern methods of direct nucleotide sequencing, based on the polymerase chain reaction (PCR), do not require direct access to live bacterial isolates or high-quality genomic DNA. These techniques can be performed on killed cell suspensions, avoiding all the difficulties associated with the transport and manipulation of pathogens, or on clinical samples, such as the cerebrospinal fluid or blood of a patient undergoing antibiotic therapy, from which a live bacterial isolate might be difficult to obtain. Fourth, the data generated are fully portable among laboratories and can be shared through-out the world via the Internet. Finally, the Internet can also be used to disseminate MLST methods, providing standardization of approaches (Maiden, 2006).

Traditionally, MLST starts with a PCR amplification step using primers that are specific for the loci of the MLST scheme, followed by Sanger sequencing. The procedure is both costly and time-consuming. In this new era of high-throughput sequencing, it may be more rational to use whole-genome sequence (WGS) data for typing. The cost of DNA sequencing has steadily gone down roughly 10-fold every 5 years (Service, 2006).

1.4.2 Pathogenesis/Pathology of *T. gallinae*

The preferred site for *T. gallinae* infection is the upper digestive tract including the mouth, pharynx, oesophagus and crop, with the parasite rarely found posterior to the proventriculus . (CAUTHEN, 1936). *T. gallinae* can cause the development of caseous lesions in the oropharynx that can lead to significant loss of weight and muscle mass and, ultimately, death (Hawn, 1937). Trichomonosis is characterised by caseated, necrotic lesions of the respiratory and upper digestive tracts and may cause difficulty breathing and swallowing, leading to significant loss of weight and muscle mass, starvation or suffocation and, ultimately, death (Hawn, 1937; Amin *et al.*, 2014).

T. gallinae strains of moderate virulence are often associated with caseous abscesses in the upper digestive tract and oropharyngeal region, whereas no visible lesions are produced by avirulent strains of *T. gallinae* (Cole and Friend, 1999).

Trichomonosis can cause swelling of the neck that may be visible from a distance, and the disease may progress over several days or even weeks. The oral lesions shown in Fig.1.3. preclude feeding and impede normal breathing by obstructing the upper digestive and respiratory tracts.



Fig.1.3. Oral lesions (Adapted from (Robinson *et al.*, 2010)).

Necrotic ingluvitis, typically extending through the full thickness of the oesophageal wall and often involving adjacent connective tissue has been found through post-mortem examination of (Fig. 1.4) (Robinson *et al.*, 2010).

A

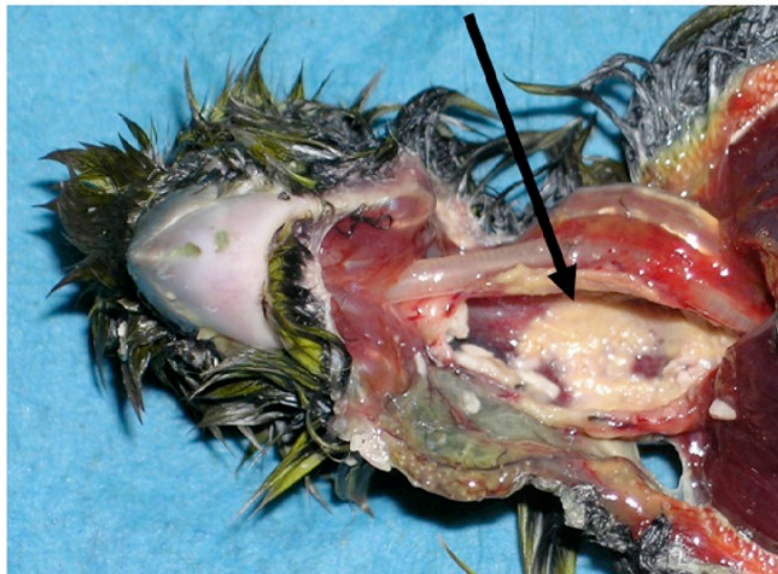


Fig.1.4. Necrotic ingluvitis lesions and trichomonad parasite morphology. Necrotic ingluvitis lesions (arrow) with a characteristic yellow caseous appearance in a greenfinch caused by *T. gallinae* infection (Robinson *et al.*, 2010).

1.5 *T. gallinae*/virulence/viruses

Protozoan Parasites are known to be “parasitized” by viruses although a detrimental effect on the parasite is not always clearly visible (Gomez-Olive *et al.*, 2017). The first reports of viruses in parasites were based on electron microscopy studies. They revealed the presence of virus-

like particles (VLPs) in several parasitic protozoa such as *Entamoeba histolytica* (Diamond *et al.*, 1972) and *Leishmania hertigi* (Molyneux, 1974).

Several viruses of a broad range group of parasites have since been described at the molecular level. A virus infecting *T. vaginalis*, which causes trichomoniasis in humans, was first characterized biochemically and identified as a double-stranded RNA (dsRNA)-containing virus (Wang and Wang, 1985).

As in *T. vaginalis*, many parasitic protozoa investigated from diverse groups also contain viruses with dsRNA genomes which are summarized in (Table 1.3) (Wang and Wang, 1986). Such is the case of the *Giardia lamblia* the causative agent of giardiasis, and of *Leishmania* spp. (Tarr *et al.*, 1988; Widmer *et al.*, 1989), the cause of leishmaniasis. Several of these viruses, Trichomonas virus (*Trichomonas* RNA Virus, TRV), *Giardiavirus* (*Giardia* RNA Virus, GRV) and *Leishmanivirus* (*Leishmania* RNA Virus, LRV) harbour closely-related monopartite dsRNA genomes and are classified in the *Totiviridae* family; their genomes are packaged in isometric particles with no lipid or carbohydrate content reviewed (Hartley M-A, 2012).

The symbiotic relationship between *T. vaginalis* and its endobiont viruses and intracellular mycoplasmas could represent an interesting model to study basic biological mechanisms both of the evolutionary origin of intracellular organelles and the role of protozoa as reservoirs or vectors in the transmission of infections to human hosts. The ability of Mycoplasma species to invade, resist and multiply in the *T. vaginalis* cytoplasm demonstrates that the bacteria have evolved effective strategies to resist and adapt to intracellular hostile environments (Fichorova *et al.*, 2017).

Other opinions reported that following purification, virus-like particles were not observed by transmission electron microscopy, nor were dsRNA segments visualized in agarose gels after electrophoresis of extracted RNA from any of the 12 *T. gallinae* isolates in USA (Gerhold *et al.*, 2009).

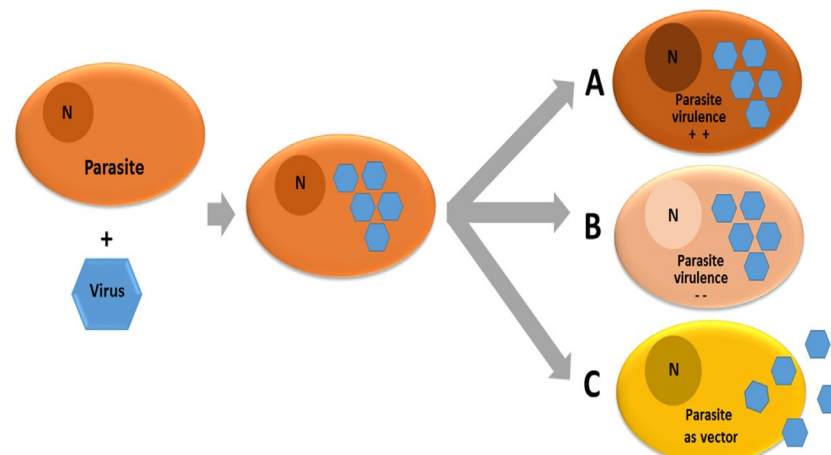
Table 3. Types of viruses of protozoan parasites. (Adapted from (Gomez-Olive *et al.*, 2017))

Parasite Genus	Supergroup/order	Virus		Reference
		Genome	Family	
<i>Leishmania</i>	<i>Excavata/ Trypanosomatida</i>	dsRNA	<i>Totiviridae</i>	(Tarr <i>et al.</i> , 1988).
<i>Trichomonas</i>	<i>Excavata/ Trichomonadida</i>	dsRNA	<i>Totiviridae</i>	(Flegr <i>et al.</i> , 1987); (Goodman <i>et al.</i> , 2011)
<i>Cryptosporidium</i>	<i>Alveolata/ Eucoccidiorida</i>	dsRNA	<i>Partitiviridae</i>	(Khramtsov <i>et al.</i> , 1997) (Nibert <i>et al.</i> , 2009)
<i>Giardia</i>	<i>Excavata/ Diplomonadida</i>	dsRNA	<i>Totiviridae</i>	(Wang and Wang, 1986); (Janssen <i>et al.</i> , 2015)
<i>Trypanosoma</i>	<i>Excavata/ Trypanosomatida</i>	dsRNA	Unknown	Molyneux and Heywood (1984)
<i>Plasmodium</i>	<i>Alveolata/ Haemosporida</i>	Unknown	Unknown	(Garnham <i>et al.</i> , 1962)
<i>Entamoeba</i>	<i>Amoebozoa/ Amoebida</i>	ssRNA	<i>Rhabdoviridae</i>	(Bird and McCaul, 1976)

Certain viruses when residing in parasites might modulate the interaction of the parasites with their host and might have consequences for infection and virulence of the parasites. Several scenarios proposed are presented in (Fig.1.5.). Certain viruses might function as an additional weapon of the parasites and in cases in which increased infectivity or persistence of the parasite in its own host is observed, this effect could be triggered by the virus of the parasite and result in possible hypervirulence (Fig. 1.5 A). In other cases, the presence of the virus in the parasite might attenuate the disease caused by the infected parasite on its host, leading to hypovirulence (Fig. 1.5 B). This capacity presents the virus as an ally of the parasite's host (e.g. symbiont viruses of fungi). Another possibility is when the virus uses the parasite as vector or Trojan horse to enter into the host of the parasite

(Fig. 5 C). This kind of parasite can accommodate several microorganisms including viruses, and act as reservoir for viruses, protecting them from unfavourable environmental conditions; in this case they might affect the dissemination or transmission of the virus.

Fig. 1.5. Hypotheses on various effects of the virus on the parasite-host relationship. (A) Viruses possibly can increase the virulence of the parasite (++) exacerbating the disease in the parasite host by hypervirulence. (B)



Viruses possibly can decrease the virulence of parasites (– –) producing hypovirulence. (C) Viruses might use the parasite as vector to enter into the parasite host. N: nucleus of the parasite (Adapted from Gómez-Arreaza et al., 2017).

Kartali's group detected four double-stranded RNA (dsRNA) bands in the *Umbelopsis ramanniana* fungus NRRL 1296 strain by gel electrophoresis. Also they described the molecular characterization of its dsRNA elements as well as the discovery of four novel dsRNA viruses: *U. ramanniana* virus 1 (UrV1), (UrV2), (UrV3), and (UrV4) (Kartali *et al.*, 2019).

It was suggested that the presence of a parasite dsRNA virus could contribute to the severity of the disease in strains of *Lieshmania guyanensis* (Ronet *et al.*, 2011; Hartley M-A, 2012) This *Leishmania* dsRNA virus (LRV) has been found in various *L. viannia* species as well as in one *L. major* strain (Scheffter *et al.*, 1995).

Furfine and Wang (1990) (Furfine and Wang, 1990) successfully isolated a double-stranded RNA (dsRNA) virus from the protozoan *G. lamblia* (GLV) and subsequently infected virus-free *G. lamblia* with a single stranded RNA (ssRNA) intermediate of GLV (Gerhold *et al.*, 2009). Virus-like particles were detected in *T. fetus* by electron microscopy only after the

trichomonads were treated with cytoskeleton-affecting chemicals including colchicine, vinblastine, taxol, nocodazole, and griseofulvin (Gomes Vancini and Benchimol, 2005).

MicroRNAs (miRNAs) are a set of small non-coding RNAs that are now considered as a key mechanism of gene regulation and are essential for the complex life cycles of different parasites (Wang *et al.*, 2010; Wang *et al.*, 2012; Xu *et al.*, 2013) regulating gene expression at the post-transcriptional level and resulting in post-transcriptional repression (Blahna and Hata, 2012). MiRNAs are conserved in metazoans and have been reported in diverse organisms from viruses to mammals (Zhang *et al.*, 2007).

Double-stranded RNA virus particles, detected in *T. vaginalis*, were assumed to be a virulence factor by Wang *et al.* (Wang *et al.*, 1987). However, these particles were not detected by transmission electron microscope and dsRNA segments were not visualized in agarose gel electrophoresis of extracted RNA from 12 *T. gallinae* isolates recovered from wild birds (Gerhold *et al.*, 2009).

1.6 The aims of this thesis

The general aim of the current thesis is provided to determine whether the viruses effect and modulate *T. gallinae* pathology.

The specific aims are:

1. To screen an archive of genetically diverse *T. gallinae* isolates from the UK.
2. To use Transmission Electron Microscopy and negative staining of supernatants to validate the presence of virus in the isolates identified in the screen
3. To evaluate phenotypic differences between infected and closely related uninfected isolates using Scanning Electron Microscopy and Transmission Electron Microscopy.
4. To determine the genomic sequences of any novel viruses identified.

1.7 References:

- Aguirre, A. A. and Tabor, G. M. (2008) 'Global Factors Driving Emerging Infectious Diseases', *Annals of the New York Academy of Sciences*, 1149(1), pp. 1–3. doi: 10.1196/annals.1428.052.
- Alrefaei, A. F. (2020) 'Molecular detection and genetic characterization of *Trichomonas gallinae* in falcons in Saudi Arabia', *PLOS ONE*. Edited by M. A. Pacheco, 15(10), p. e0241411. doi: 10.1371/journal.pone.0241411.
- AMIN, A. *et al.* (2014) 'Trichomonads in birds – a review', *Parasitology*, 141(6), pp. 733–747. doi: 10.1017/S0031182013002096.
- Anderson, N. L. *et al.* (2009) 'Studies of trichomonad protozoa in free ranging songbirds: Prevalence of *Trichomonas gallinae* in house finches (*Carpodacus mexicanus*) and corvids and a novel trichomonad in mockingbirds (*Mimus polyglottos*)', *Veterinary Parasitology*, 161(3–4), pp. 178–186. doi: 10.1016/j.vetpar.2009.01.023.
- Atzrodt, C. L. *et al.* (2020) 'A Guide to COVID-19 : a global pandemic caused by the novel coronavirus SARS-CoV-2', 287, pp. 3633–3650. doi: 10.1111/febs.15375.
- Begum, N. M., S.A, M. A. A. R. and Bari, A. S. M. (2008) 'Epidemiology and pathology of *Trichomonas gallinae* in the common pigeon (*Columba livia*)'.
- Bell, D., Robertson, S. and Hunter, P. R. (2004) 'Animal origins of SARS coronavirus: possible links with the international trade in small carnivores', *Philosophical Transactions of the Royal Society of London. Series B: Biological Sciences*. Edited by R. M. May *et al.*, 359(1447), pp. 1107–1114. doi: 10.1098/rstb.2004.1492.
- Bird, R. G. and McCaul, T. F. (1976) 'The rhabdoviruses of *Entamoeba histolytica* and *Entamoeba invadens*', *Annals of Tropical Medicine & Parasitology*, 70(1), pp. 81–93. doi: 10.1080/00034983.1976.11687098.
- Blahna, M. T. and Hata, A. (2012) 'Smad-mediated regulation of microRNA biosynthesis', *FEBS Letters*, 586(14), pp. 1906–1912. doi: 10.1016/j.febslet.2012.01.041.
- BonDurant, R. H. and Honigberg, B. M. (1994) 'Trichomonads of Veterinary Importance', in Protozoa, P. (ed.) *Parasitic Protozoa*. New York, NY, USA: Elsevier, pp. 111–188. doi: 10.1016/B978-0-12-426019-1.50007-6.
- Brugerolle, G. and Muller, M. (2000) 'Amitochondriate flagellates', *SYSTEMATICS ASSOCIATION SPECIAL VOLUME*. SYSTEMATICS ASSOCIATION SPECIAL VOLUME, 59, pp. 166–189.
- Bunbury, N. *et al.* (2005) 'Comparison of the InPouch TF Culture System and Wet-Mount Microscopy for Diagnosis of *Trichomonas gallinae* Infections in the Pink Pigeon *Columba mayeri*', *Journal of Clinical Microbiology*, 43(2), pp. 1005–1006. doi: 10.1128/JCM.43.2.1005-1006.2005.
- Bunbury, N. *et al.* (2007) 'TRICHOMONAS GALLINAE IN MAURITIAN COLUMBIDS: IMPLICATIONS FOR AN ENDANGERED ENDEMIC', *Journal of Wildlife Diseases*, 43(3), pp. 399–407. doi: 10.7589/0090-3558-43.3.399.
- Castellanos-Gonzalez, A. *et al.* (2018) 'Molecular diagnosis of protozoan parasites by Recombinase Polymerase Amplification', *Acta Tropica*, 182, pp. 4–11. doi: 10.1016/j.actatropica.2018.02.002.

- CAUTHEN, G. (1936) 'STUDIES ON TRICHOMONAS COLUMBAE, A FLAGELLATE PARASITIC IN PIGEONS AND DOVES^{1,2}', *American Journal of Epidemiology*, 23(1), pp. 132–142. doi: 10.1093/oxfordjournals.aje.a118201.
- CDC (2022) *Avian Influenza in Birds*. Available at: <https://www.cdc.gov/flu/avianflu/avian-in-birds.htm> (Accessed: 3 March 2020).
- Cepicka, I., Hampl, V. and Kulda, J. (2010) 'Critical Taxonomic Revision of Parabasalids with Description of one New Genus and three New Species', *Protist*, 161(3), pp. 400–433. doi: 10.1016/j.protis.2009.11.005.
- CHI, J. F. *et al.* (2013) 'The finch epidemic strain of *Trichomonas gallinae* is predominant in British non-passerines', *Parasitology*, 140(10), pp. 1234–1245. doi: 10.1017/S0031182013000930.
- Chou, S. *et al.* (2022) 'Genetic characterization of *Trichomonas gallinae* (Rivolta, 1878) in companion birds in Japan and the genotypical relationship in the Asia region', *Journal of Microbiology, Immunology and Infection*, 55(3), pp. 527–534. doi: 10.1016/j.jmii.2021.05.010.
- Church, G. (2006) 'The race for the \$1000 genome', *Science*, 311, pp. 1544–1546.
- Cleaveland, S., Haydon, D. T. and Taylor, L. (2007) 'Overviews of Pathogen Emergence: Which Pathogens Emerge, When and Why?', in *Curr Top Microbiol Immunol*, pp. 85–111. doi: 10.1007/978-3-540-70962-6_5.
- Cole, R. and Friend, M. (1999) 'Trichomoniasis', in Friend, M. and Franson, J. C. . (eds) *Field Manual of Wildlife Diseases*. Washington, DC, USA: USGS-National Wildlife Health Cente.
- Cooper, J. E. and Petty, S. J. (1988) 'TRICHOMONIASIS IN FREE-LIVING GOSHAWKS (*ACCIPITER GENTILIS GENTILIS*) FROM GREAT BRITAIN', *Journal of Wildlife Diseases*, 24(1), pp. 80–87. doi: 10.7589/0090-3558-24.1.80.
- Diamond, L. S., Mattern, C. F. T. and Bartgis, I. L. (1972) 'Viruses of *Entamoeba histolytica* I. Identification of Transmissible Virus-Like Agents', *Journal of Virology*, 9(2), pp. 326–341. doi: 10.1128/jvi.9.2.326-341.1972.
- Doyle, S. *et al.* (2022) 'Confirmation of avian trichomonosis among wild birds in Ireland', *European Journal of Wildlife Research*, 68(1), p. 10. doi: 10.1007/s10344-021-01558-3.
- Dudek, B. M. *et al.* (2018) 'PREVALENCE AND RISK FACTORS OF TRICHOMONAS GALLINAE AND TRICHOMONOSIS IN GOLDEN EAGLE (*AQUILA CHRYSAETOS*) NESTLINGS IN WESTERN NORTH AMERICA', *Journal of Wildlife Diseases*, 54(4), pp. 755–764. doi: 10.7589/2017-11-271.
- DWYER, D. M. (1974) 'Analysis of the Antigenic Relationships Among *Trichomonas*, *Histomonas*, *Dientamoeba* and *Entamoeba* III. Immunoelectrophoresis Technics*', *The Journal of Protozoology*, 21(1), pp. 139–145. doi: 10.1111/j.1550-7408.1974.tb03628.x.
- El-Khatam, A. O. *et al.* (2016) 'Trichomonas gallinae : Prevalence and molecular characterization from pigeons in Minoufiya governorate, Egypt', *Experimental Parasitology*, 170, pp. 161–167. doi: 10.1016/j.exppara.2016.09.016.
- Feng, S.-Y. *et al.* (2018) 'Prevalence and molecular characterization of *Trichomonas gallinae* from domestic pigeons in Beijing, China', *Infection, Genetics and Evolution*, 65, pp. 369–372. doi:

10.1016/j.meegid.2018.08.021.

- Fichorova, R. *et al.* (2017) 'Trichomonas vaginalis infection in symbiosis with Trichomonasvirus and Mycoplasma', *Research in Microbiology*, 168(9–10), pp. 882–891. doi: 10.1016/j.resmic.2017.03.005.
- Flegr, J. *et al.* (1987) 'The dsRNA of Trichomonas vaginalis is associated with virus-like particles and does not correlate with metronidazole resistance', *Folia Microbiologica*, 32(4), pp. 345–348. doi: 10.1007/BF02877224.
- Forrester, D. J. and Foster, G. W. (2008) 'Trichomonosis', in Atkinson, C. T., Thomas, N. J., and Hunter, D. B. (eds) *Parasitic Diseases of Wild Birds*. USA: Wiley-Blackwell.
- Fuller, T. *et al.* (2012) 'The Ecology of Emerging Infectious Diseases in Migratory Birds: An Assessment of the Role of Climate Change and Priorities for Future Research', *EcoHealth*, 9(1), pp. 80–88. doi: 10.1007/s10393-012-0750-1.
- Furfine, E. S. and Wang, C. C. (1990) 'Transfection of the Giardia lamblia Double-Stranded RNA Virus into Giardia lamblia by Electroporation of a Single-Stranded RNA Copy of the Viral Genome', *Molecular and Cellular Biology*, 10(7), pp. 3659–3663. doi: 10.1128/mcb.10.7.3659-3662.1990.
- Garnham, P. C. C., Bird, R. G. and Baker, J. R. (1962) 'Electron microscope studies of motile stages of malaria parasites', *Transactions of the Royal Society of Tropical Medicine and Hygiene*, 56(2), pp. 116–120. doi: 10.1016/0035-9203(62)90137-2.
- Gaspar da Silva, D. *et al.* (2007) 'Molecular identity and heterogeneity of trichomonad parasites in a closed avian population', *Infection, Genetics and Evolution*, 7(4), pp. 433–440. doi: 10.1016/j.meegid.2007.01.002.
- Gerhold, R. W. *et al.* (2008) 'Molecular Characterization of the Trichomonas gallinae Morphologic Complex in the United States', *Journal of Parasitology*, 94(6), pp. 1335–1341. doi: 10.1645/GE-1585.1.
- Gerhold, R. W. *et al.* (2009) 'Examination for double-stranded RNA viruses in Trichomonas gallinae and identification of a novel sequence of a Trichomonas vaginalis virus', *Parasitology Research*, 105(3), pp. 775–779. doi: 10.1007/s00436-009-1454-5.
- Gomes Vancini, R. and Benchimol, M. (2005) 'Appearance of virus-like particles in Tritrichomonas foetus after drug treatment', *Tissue and Cell*, 37(4), pp. 317–323. doi: 10.1016/j.tice.2005.03.009.
- Gomez-Olive, F. X. *et al.* (2017) 'Variations in disability and quality of life with age and sex between eight lower income and middle-income countries: data from the INDEPTH WHO-SAGE collaboration', *BMJ Global Health*, 2(4), p. e000508. doi: 10.1136/bmjgh-2017-000508.
- Gómez, A. and Aguirre, A. A. (2008) 'Infectious Diseases and the Illegal Wildlife Trade', *Annals of the New York Academy of Sciences*, 1149(1), pp. 16–19. doi: 10.1196/annals.1428.046.
- Goodman, R. P. *et al.* (2011) 'Trichomonasvirus: a new genus of protozoan viruses in the family Totiviridae', *Archives of Virology*, 156(1), pp. 171–179. doi: 10.1007/s00705-010-0832-8.
- Grabensteiner, E. *et al.* (2010) 'Molecular analysis of clonal trichomonad isolates indicate the

- existence of heterogenic species present in different birds and within the same host', *Veterinary Parasitology*, 172(1–2), pp. 53–64. doi: 10.1016/j.vetpar.2010.04.015.
- Grennan, D. (2019) 'What Is a Pandemic?', *JAMA*, 321(9), p. 910. doi: 10.1001/jama.2019.0700.
- Hanage, William P. *et al.* (2005) 'Using Multilocus Sequence Data To Define the Pneumococcus', *Journal of Bacteriology*. Edited by W P Hanage and a, 187(17), pp. 6223–6230. doi: 10.1128/JB.187.17.6223-6230.2005.
- Harmon, W. M. *et al.* (1987) 'Trichomonas gallinae in Columbiform Birds from the Galapagos Islands', *Journal of Wildlife Diseases*, 23(3), pp. 492–494. doi: 10.7589/0090-3558-23.3.492.
- Hartley, M.-A. *et al.* (2012) 'Leishmania RNA virus: when the host pays the toll', *Frontiers in Cellular and Infection Microbiology*, 2, pp. 99–102. doi: 10.3389/fcimb.2012.00099.
- Hawn, M. C. (1937) 'Trichomoniasis of Turkeys', *Journal of Infectious Diseases*, 61(2), pp. 184–197. doi: 10.1093/infdis/61.2.184.
- Hess, M. and McDougald, L. R. (2013) 'Protozoal Infections', in Swayne, D. E. *et al.* (eds) *Diseases of Poultry*. Wiley, pp. 1147–1201. doi: 10.1002/9781119421481.ch28.
- Hofle, U. *et al.* (2004) 'Outbreak of trichomoniasis in a woodpigeon (*Columba palumbus*) wintering roost', *European Journal of Wildlife Research*, 50(2). doi: 10.1007/s10344-004-0043-2.
- Janssen, M. E. W. *et al.* (2015) 'Three-Dimensional Structure of a Protozoal Double-Stranded RNA Virus That Infects the Enteric Pathogen *Giardia lamblia*', *Journal of Virology*. Edited by S. López, 89(2), pp. 1182–1194. doi: 10.1128/JVI.02745-14.
- Jones, K. E. *et al.* (2008) 'Global trends in emerging infectious diseases', *Nature*, 451(7181), pp. 990–993. doi: 10.1038/nature06536.
- Kan, B. *et al.* (2005) 'Molecular Evolution Analysis and Geographic Investigation of Severe Acute Respiratory Syndrome Coronavirus-Like Virus in Palm Civets at an Animal Market and on Farms', *Journal of Virology*, 79(18), pp. 11892–11900. doi: 10.1128/JVI.79.18.11892-11900.2005.
- Karesh, W. B. *et al.* (2005) 'Wildlife Trade and Global Disease Emergence', *Emerging Infectious Diseases*, 11(7), pp. 1000–1002. doi: 10.3201/eid1107.050194.
- Kartali, T. *et al.* (2019) 'Detection and Molecular Characterization of Novel dsRNA Viruses Related to the Totiviridae Family in *Umbelopsis ramanniana*', *Frontiers in Cellular and Infection Microbiology*, 9, p. 249. doi: 10.3389/fcimb.2019.00249.
- Khramtsov, N. V *et al.* (1997) 'Virus-like, double-stranded RNAs in the parasitic protozoan *Cryptosporidium parvum*', *Molecular Microbiology*, 26(2), pp. 289–300. doi: 10.1046/j.1365-2958.1997.5721933.x.
- Kleina, P. *et al.* (2004) 'Molecular phylogeny of Trichomonadidae family inferred from ITS-1, 5.8S rRNA and ITS-2 sequences', *International Journal for Parasitology*, 34(8), pp. 963–970. doi: 10.1016/j.ijpara.2004.04.004.
- Krone, O., Altenkamp, R. and Kenntner, N. (2005) 'PREVALENCE OF TRICHOMONAS GALLINAE IN NORTHERN GOSHAWKS FROM THE BERLIN AREA OF NORTHEASTERN GERMANY', *Journal of*

- Wildlife Diseases*, 41(2), pp. 304–309. doi: 10.7589/0090-3558-41.2.304.
- Lawson, B. *et al.* (2011) 'Evidence of Spread of the Emerging Infectious Disease, Finch Trichomonosis, by Migrating birds', *EcoHealth*, 8(2), pp. 143–153. doi: 10.1007/s10393-011-0696-8.
- Levine, D and Brandly, A. (1939) 'A pathogenic Trichomonas from the upper digestive tract of chickens', *J Am Vet Med Assoc*, 95(8), p. 77.
- Maiden, M. C. J. *et al.* (1998) 'Multilocus sequence typing: A portable approach to the identification of clones within populations of pathogenic microorganisms', *Proceedings of the National Academy of Sciences*, 95(6), pp. 3140–3145. doi: 10.1073/pnas.95.6.3140.
- Maiden, M. C. J. (2006) 'Multilocus Sequence Typing of Bacteria', *Annual Review of Microbiology*, 60(1), pp. 561–588. doi: 10.1146/annurev.micro.59.030804.121325.
- MARTIN, C. H. and ROBERSON, M. (1911) 'Memoirs: Further Observations on the Cæcal Parasites of Fowls, With some Reference to the Rectal Fauna of other Vertebrates', *Journal of Cell Science*, s2-57(225), pp. 53–81. doi: 10.1242/jcs.s2-57.225.53.
- McArthur, D. B. (2019) 'Emerging Infectious Diseases', *Nursing Clinics of North America*, 54(2), pp. 297–311. doi: 10.1016/j.cnur.2019.02.006.
- McDougald, L. R. (2013) 'Protozoal Infections', in Saif, Y. M. *et al.* (eds) *Diseases of Poultry*. USA: Wiley, pp. 1147–1201. doi: 10.1002/9781119421481.ch28.
- Mehlhorn, H. *et al.* (2009) 'Fine structure of the bird parasites Trichomonas gallinae and Tetratrichomonas gallinarum from cultures', *Parasitology Research*, 105(3), pp. 751–756. doi: 10.1007/s00436-009-1451-8.
- MOLYNEUX, D. H. (1974) 'Virus-like particles in Leishmania parasites', *Nature*, 249(5457), pp. 588–589. doi: 10.1038/249588a0.
- Molyneux, D. H. and Heywood, P. (1984) 'Evidence for the incorporation of virus-like particles into Trypanosoma', *Zeitschrift für Parasitenkunde Parasitology Research*, 70(4), pp. 553–556. doi: 10.1007/BF00926697.
- Morens, D. M. and Fauci, A. S. (2013) 'Emerging Infectious Diseases: Threats to Human Health and Global Stability', *PLoS Pathogens*. Edited by J. Heitman, 9(7), p. e1003467. doi: 10.1371/journal.ppat.1003467.
- Morens, D. M. and Fauci, A. S. (2020) 'Emerging Pandemic Diseases: How We Got to COVID-19', *Cell*, 182(5), pp. 1077–1092. doi: 10.1016/j.cell.2020.08.021.
- Morens, D. M., Folkers, G. K. and Fauci, A. S. (2008) 'Emerging infections: a perpetual challenge', *The Lancet Infectious Diseases*, 8(11), pp. 710–719. doi: 10.1016/S1473-3099(08)70256-1.
- MORSE, S. S. (2004) 'Factors and determinants of disease emergence', *Revue Scientifique et Technique de l'OIE*, 23(2), pp. 443–451. doi: 10.20506/rst.23.2.1494.
- Muller, M. (1993) 'Review Article: The hydrogenosome', *Journal of General Microbiology*, 139(12), pp. 2879–2889. doi: 10.1099/00221287-139-12-2879.
- Nematollahi, A. *et al.* (2012) 'Prevalence of Haemoproteus columbae and Trichomonas gallinae in

- pigeons (*Columba domestica*) in Isfahan, Iran', *Journal of Parasitic Diseases*, 36(1), pp. 141–142. doi: 10.1007/s12639-011-0082-z.
- Nibert, M. L. *et al.* (2009) 'Cryspovirus: a new genus of protozoan viruses in the family Partitiviridae', *Archives of Virology*, 154(12), pp. 1959–1965. doi: 10.1007/s00705-009-0513-7.
- Noorbakhsh, F., Abdolmohammadi, K. and Fatahi, Y. (2019) 'Zika Virus Infection , Basic and Clinical Aspects : A Review Article', *A review article. Iranian journal of public health*, 48(1), pp. 20–31.
- Quattara, M. *et al.* (2010) 'Prevalence and Spatial Distribution of *Entamoeba histolytica*/dispar and *Giardia lamblia* among Schoolchildren in Agboville Area (Côte d'Ivoire)', *PLoS Neglected Tropical Diseases*. Edited by D. Eichinger, 4(1), p. e574. doi: 10.1371/journal.pntd.0000574.
- Peters, A., Das, S. and Raidal, S. R. (2020) 'Molecular Phylogenetics and Evolution Diverse *Trichomonas* lineages in Australasian pigeons and doves support a columbid origin for the genus *Trichomonas*', *Molecular Phylogenetics and Evolution*. Elsevier, 143(October 2019), p. 106674. doi: 10.1016/j.ympev.2019.106674.
- Quillfeldt, P. *et al.* (2018) 'Prevalence and genotyping of *Trichomonas* infections in wild birds in central Germany', *PLOS ONE*. Edited by J. Waldenström, 13(8), p. e0200798. doi: 10.1371/journal.pone.0200798.
- Rahman, M. T. *et al.* (2020) 'Zoonotic Diseases: Etiology, Impact, and Control', *Microorganisms*, 8(9), p. 1405. doi: 10.3390/microorganisms8091405.
- Rivolta, S. (1878) *Una forma di croup prodotta da un infusorio, nei polli*. G Anatom Fisiol e Patol Animal.
- Robinson, R. A. *et al.* (2010) 'Emerging Infectious Disease Leads to Rapid Population Declines of Common British Birds', *PLoS ONE*. Edited by S. Rands, 5(8), p. e12215. doi: 10.1371/journal.pone.0012215.
- Ronet, C., Beverley, S. M. and Fasel, N. (2011) 'Muco-cutaneous leishmaniasis in the New World', *Virulence*, 2(6), pp. 547–552. doi: 10.4161/viru.2.6.17839.
- Samanta, I. and Bandyopadhyay, S. (2017) 'Toxicity', in *Pet bird diseases and care*. Singapore: Springer Singapore, pp. 253–262. doi: 10.1007/978-981-10-3674-3_4.
- Sansano-Maestre, J., Garijo-Toledo, M. M. and Gómez-Muñoz, M. T. (2009) 'Prevalence and genotyping of *Trichomonas gallinae* in pigeons and birds of prey', *Avian Pathology*, 38(3), pp. 201–207. doi: 10.1080/03079450902912135.
- Scheffter, S. M. *et al.* (1995) 'The Complete Sequence of *Leishmania* RNA Virus LRV2-1, a Virus of an Old World Parasite Strain', *Virology*, 212(1), pp. 84–90. doi: 10.1006/viro.1995.1456.
- Schulz, J. H., Bermudez, A. J. and Millspaugh, J. J. (2005) 'Monitoring Presence and Annual Variation of *Trichomoniasis* in Mourning Doves', *Avian Diseases*, 49(3), pp. 387–389. doi: 10.1637/7333-012505R.1.
- Service, R. F. (2006) 'The Race for the \$1000 Genome', *Science*, 311(5767), pp. 1544–1546. doi: 10.1126/science.311.5767.1544.

- Spriggs, M. C., Purple, K. E. and Gerhold, R. W. (2020) 'Detection of *Trichomonas gallinae* in Wild Birds Admitted to a Rehabilitation Center, Florida, USA', *Journal of Wildlife Diseases*, 56(3), p. 733. doi: 10.7589/2019-05-127.
- Squire, S. A. and Ryan, U. (2017) 'Cryptosporidium and Giardia in Africa: current and future challenges', *Parasites & Vectors*, 10(1), p. 195. doi: 10.1186/s13071-017-2111-y.
- Stabler, R. M. (1954) 'Trichomonas gallinae: A review', *Experimental Parasitology*, 3(4), pp. 368–402. doi: 10.1016/0014-4894(54)90035-1.
- Steere, A. C., Coburn, J. and Glickstein, L. (2004) 'The emergence of Lyme disease', *Journal of Clinical Investigation*, 113(8), pp. 1093–1101. doi: 10.1172/JCI21681.
- Stephens, P. R. *et al.* (2021) 'Characteristics of the 100 largest modern zoonotic disease outbreaks', *Philosophical Transactions of the Royal Society B: Biological Sciences*, 376(1837), p. 20200535. doi: 10.1098/rstb.2020.0535.
- STEPKOWSKI, S. and HONIGBERG, B. M. (1972) 'Antigenic Analysis of Virulent and Avirulent Strains of *Trichomonas gallinae* by Gel Diffusion Methods*', *The Journal of Protozoology*, 19(2), pp. 306–315. doi: 10.1111/j.1550-7408.1972.tb03465.x.
- Subileau, M. *et al.* (2009) 'Trypanosoma cruzi: New insights on ecophylogeny and hybridization by multigene sequencing of three nuclear and one maxicircle genes', *Experimental Parasitology*, 122(4), pp. 328–337. doi: 10.1016/j.exppara.2009.04.008.
- Sutrave, S. and Richter, M. H. (2021) 'The Truman Show for protozoan parasites: A review of in vitro cultivation platforms', *PLOS Neglected Tropical Diseases*. Edited by C. I. Brodskyn, 15(8), p. e0009668. doi: 10.1371/journal.pntd.0009668.
- Swift, B. M. C. *et al.* (2019) 'Anthropogenic environmental drivers of antimicrobial resistance in wildlife', *Science of The Total Environment*, 649, pp. 12–20. doi: 10.1016/j.scitotenv.2018.08.180.
- Tabish, S. A. (no date) 'Recent trends in emerging infectious diseases', *Int J Health Sci (Qassim)*, 3(2), p. Available at: <https://www.ncbi.nlm.nih.gov/pubmed/21475529>.
- Tarr, P. I. *et al.* (1988) 'LR1: a candidate RNA virus of Leishmania.', *Proceedings of the National Academy of Sciences*, 85(24), pp. 9572–9575. doi: 10.1073/pnas.85.24.9572.
- Tasca, T. and De Carli, G. A. (2003) 'Scanning electron microscopy study of *Trichomonas gallinae*', *Veterinary Parasitology*, 118(1–2), pp. 37–42. doi: 10.1016/j.vetpar.2003.09.009.
- Taubenberger, J. K. and Morens, D. M. (2020) 'The 1918 Influenza Pandemic and Its Legacy', *Cold Spring Harbor Perspectives in Medicine*, 10(10), p. a038695. doi: 10.1101/cshperspect.a038695.
- Tegen, D., Damtie, D. and Hailegebriel, T. (2020) 'Prevalence and Associated Risk Factors of Human Intestinal Protozoan Parasitic Infections in Ethiopia: A Systematic Review and Meta-Analysis', *Journal of Parasitology Research*, 2020, pp. 1–15. doi: 10.1155/2020/8884064.
- Tompkins, D. M. *et al.* (2015) 'Emerging infectious diseases of wildlife: a critical perspective', *Trends in Parasitology*, 31(4), pp. 149–159. doi: 10.1016/j.pt.2015.01.007.

- Trejos, A. *et al.* (1967) 'Vaccinia Epidemic and Epizootic in El Salvador', *The American Journal of Tropical Medicine and Hygiene*, 16(3), pp. 332–338. doi: 10.4269/ajtmh.1967.16.332.
- Tu, C. *et al.* (2004) 'Antibodies to SARS Coronavirus in Civets', *Emerging Infectious Diseases*, 10(12), pp. 2244–2248. doi: 10.3201/eid1012.040520.
- Wang, A. L. and Wang, C. C. (1985) 'A linear double-stranded RNA in *Trichomonas vaginalis*.' *Journal of Biological Chemistry*, 260(6), pp. 3697–3702. doi: 10.1016/S0021-9258(19)83679-7.
- Wang, A. L. and Wang, C. C. (1986) 'The double-stranded RNA in *Trichomonas vaginalis* may originate from virus-like particles.' *Proceedings of the National Academy of Sciences*, 83(20), pp. 7956–7960. doi: 10.1073/pnas.83.20.7956.
- Wang, A., Wang, C. C. and Alderete, J. F. (1987) 'Trichomonas vaginalis phenotypic variation occurs only among trichomonads infected with the double-stranded RNA virus.' *Journal of Experimental Medicine*, 166(1), pp. 142–150. doi: 10.1084/jem.166.1.142.
- Wang, D. *et al.* (2020) 'Clinical Characteristics of 138 Hospitalized Patients With 2019 Novel Coronavirus–Infected Pneumonia in Wuhan, China', *JAMA*, 323(11), p. 1061. doi: 10.1001/jama.2020.1585.
- Wang, J. *et al.* (2012) 'A comparative study of small RNAs in *Toxoplasma gondii* of distinct genotypes', *Parasites & Vectors*, 5(1), p. 186. doi: 10.1186/1756-3305-5-186.
- Wang, Z. *et al.* (2010) 'An "In-Depth" Description of the Small Non-coding RNA Population of *Schistosoma japonicum* Schistosomulum', *PLoS Neglected Tropical Diseases*. Edited by E. Ghedin, 4(2), p. e596. doi: 10.1371/journal.pntd.0000596.
- WHO (2018) *Influenza fact sheet*. Available at: [https://www.who.int/en/news-room/fact-sheets/detail/influenza-\(avian-and-other-zoonotic\)](https://www.who.int/en/news-room/fact-sheets/detail/influenza-(avian-and-other-zoonotic)) (Accessed: 15 January 2021).
- WHO (2021) *A Brief Guide to Emerging Infectious Diseases and Zoonoses*.
- WHO (2022) *WHO Coronavirus WHO Coronavirus, Who website*. Available at: <https://covid19.who.int/>.
- Widmer, G. *et al.* (1989) 'Characterization of a RNA virus from the parasite *Leishmania*.' *Proceedings of the National Academy of Sciences*, 86(15), pp. 5979–5982. doi: 10.1073/pnas.86.15.5979.
- Wolfe, N. D., Dunavan, C. P. and Diamond, J. (2007) 'Origins of major human infectious diseases', *Nature*, 447(7142), pp. 279–283. doi: 10.1038/nature05775.
- Wu, J. *et al.* (2020) 'Clinical Features of Maintenance Hemodialysis Patients with 2019 Novel Coronavirus–Infected Pneumonia in Wuhan, China', *Clinical Journal of the American Society of Nephrology*, 15(8), pp. 1139–1145. doi: 10.2215/CJN.04160320.
- Xu, M.-J. *et al.* (2013) 'Identification and characterization of microRNAs in the pancreatic fluke *Eurytrema pancreaticum*', *Parasites & Vectors*, 6(1), p. 25. doi: 10.1186/1756-3305-6-25.
- Yu, H. *et al.* (2013) 'Human infection with avian influenza A H7N9 virus: an assessment of clinical severity', *The Lancet*, 382(9887), pp. 138–145. doi: 10.1016/S0140-6736(13)61207-6.
- Zhang, W. *et al.* (2007) 'Prevalence of virulence genes in *Escherichia coli* strains recently isolated

from young pigs with diarrhea in the US', *Veterinary Microbiology*, 123(1–3), pp. 145–152. doi: 10.1016/j.vetmic.2007.02.018.

Zhu, N. *et al.* (2020) 'A Novel Coronavirus from Patients with Pneumonia in China, 2019', *New England Journal of Medicine*, 382(8), pp. 727–733. doi: 10.1056/NEJMoa2001017.

Chapter 2

A dsRNA screen of *Trichomonas gallinae* isolates for potential viral infection

Abstract

Since the onset of the Finch epidemic in the UK (Alrefaei Abdulwahed, 2017; Robinson *et al.*, 2010) UEA and ZSL have collaborated to collect a curated genotyped library of predominantly UK derived isolates of *Trichomonas gallinae* from columbids, raptors, passerines and strigiformes. For most of these isolates' metadata was also collected relating to the source species and the health of the host and substantial variation in the virulence of different strains has been demonstrated (Alrefaei, 2020). In the closely related and morphologically indistinguishable parasite *Trichomonas vaginalis*, the presence of dsRNA viruses of the class *Totiviridae* have been positively associated with isolate specific virulence. Consequently, I set out to determine whether the variation in virulence observed in *T.gallinae* subtypes might be correlated with the presence of viruses. I began by culturing 21 of *T. gallinae* isolates from 15 species of birds in axenic culture using Diamond's Modified Medium (TYM). Cultures were maintained for five days during which the samples were examined daily under the microscope to monitor growth status. The results of *T. gallinae* cultivation showed that 72 hr was the optimum duration of the growth period after which growth declined. Both *T. gallinae* lineages putatively infected with virus-RNA and those free of viral-RNA showed highest growth peak at day three. Consequently total RNA was extracted from all 21 isolates at this time point.

By using agarose gel electrophoresis an RNA band was found in two samples at close to the expected 4.5kb suggesting these could be virus-infected sample of *T. gallinae*. Both these samples (from subtypes C10 and C3) were derived from routine surveillance of exotic UK zoo kept columbid species neither of which showed any evidence of associated pathology and were thus considered asymptomatic infections by avirulent isolates. For further investigation these two samples and two additional more virulent samples were examined as a panel. UK finch

epidemic strain A1 (GF1c) a clone of the highly virulent epidemic finch isolate for which the genome is available and C4 a subtype to the two subtypes C10, C3 which displayed additional bands of RNA and which is known to be able to cause symptomatic infection. This panel of four isolates was then examined for variation in rate of growth, morphological variation using Giemsa staining and light microscopy, and for the presence of dsRNA using north and dot blotting and immunofluorescence microscopy using dsRNA specific antibody. By north and dot blotting the C10 lineage showed a clear increase in dsRNA compared with the other lineages and the C3 sample subtype also appeared to be associated with a somewhat elevated amount of dsRNA on the dot blot I conducted. In terms of phenotypic analysis. I found some evidence of a reduction in growth rate for the C10 lineage and the cells appeared smaller showing a significant reduction in the surface area occupied on examination of the Giemsa stained slides. By immunofluorescence microscopy the C10 isolate alone showed a punctate peripheral staining characteristic of viral infection. In conclusion it appears based on preliminary, standard analyses that the C10 lineage may be host to an active viral infection. The C3 lineage also seems to show elevated levels of dsRNA but it is not clear that is the results of an active dsRNA virus infection.

2.1 Introduction

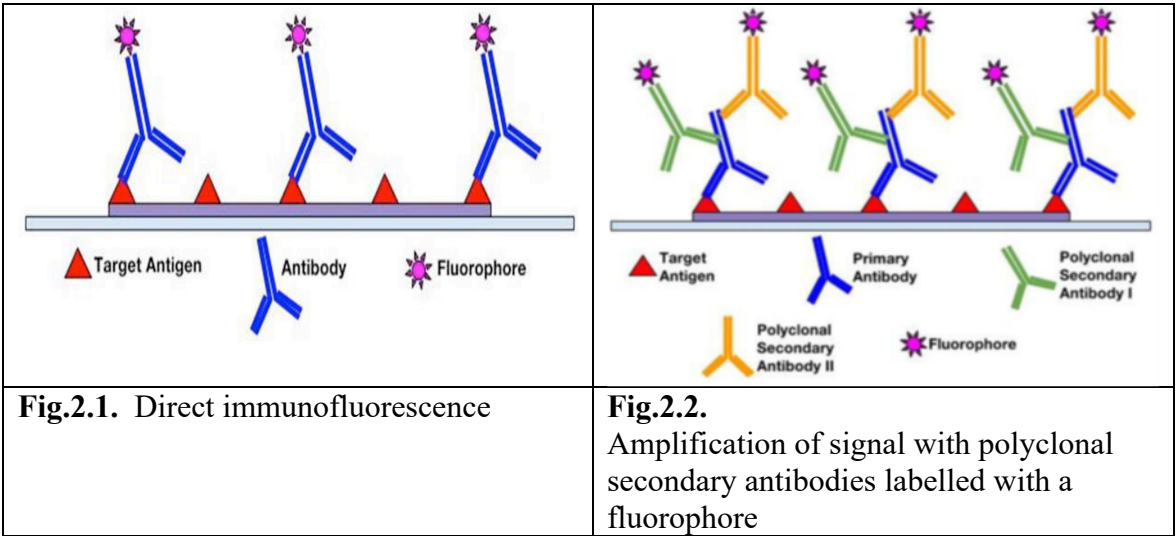
Trichomonas gallinae causes trichomoniasis in a variety of avian host orders. This protozoan occurs in various morphological forms such as round, stalked amoeboid, bell-shaped amoeboid and pyriform (Tasca and De Carli, 2003) and measures about 7–11 μm (Mehlhorn *et al.*, 2009). The structure of *T. gallinae* includes four anterior flagella and an axostyle. It is accepted in the literature that *T. gallinae* does not form true cysts (Levine, 1961). (Kietzmann, 1993) showed that the bell-shaped amoeboid has the potential to cause cell damage to avian palatal-esophageal epithelium during disease onset and progression. As the main host of *T. gallinae*,

the domestic pigeon *Columba livia* plays an important role in the spread of this parasite among other members of the order causing morbidity and mortality.

Identification of *T. gallinae* can be done by making wet mounts of swabbed mucosal samples taken from the crop and oesophagus of birds followed by a) applying the Wright-Giemsa staining method and microscopic examination (Stabler, 1954; Coles, 1980; Kietzmann, 1993; Anderson *et al.*, 2009) or b) by the inoculation of such material culture into Diamond’s medium (KOCAN and KNISLEY, 1970; MCKEON, DUNSMORE and RAIDAL, 1997; Amin *et al.*, 2010; S. B. Qiu, 2012) and c) inoculation of InPouch TF kits produced by BioMed Diagnostics, California (Honigberg, 1978; Bunbury *et al.*, 2005, 2007).

2.2 Detection of dsRNA in *T.gallinae* using monoclonal anti –ds RNA(J2) antibody

Immunofluorescence (IF) is one of the important immunochemical techniques that permits the detection and localization of a wide variety of antigens in different types of tissues or cultures cells. IF is characterized by excellent sensitivity and amplification of signal in comparison to immunohistochemistry, employing various microscopy techniques. There is a method available, depending on the scope of the experiment or the specific antibodies in use: Direct (Primary) and (Secondary) shown in Figs.2.1 to Fig.2.3. (Im *et al.*, 2019).



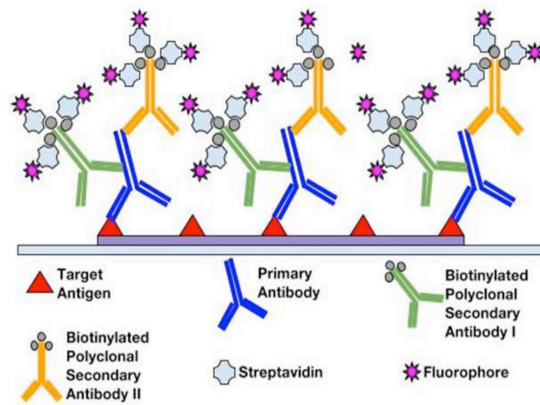


Fig.2.3. Amplification of signal with polyclonal secondary antibodies conjugated with multiple fluorophore-protein complexes

Fig.2.1 to Fig.2.3 are adapted from (Im *et al.*, 2019).

Western blotting is an important technique used in cell and molecular biology. By using a western blot, researchers are able to identify specific proteins from a complex mixture of proteins extracted from cells. The technique uses three elements to accomplish this task: (1) separation by size, (2) transfer to a solid support, and (3) marking target protein using a proper primary and secondary antibody to visualize (Yang and Mahmood, 2012). This is summarized in Fig.2.4.

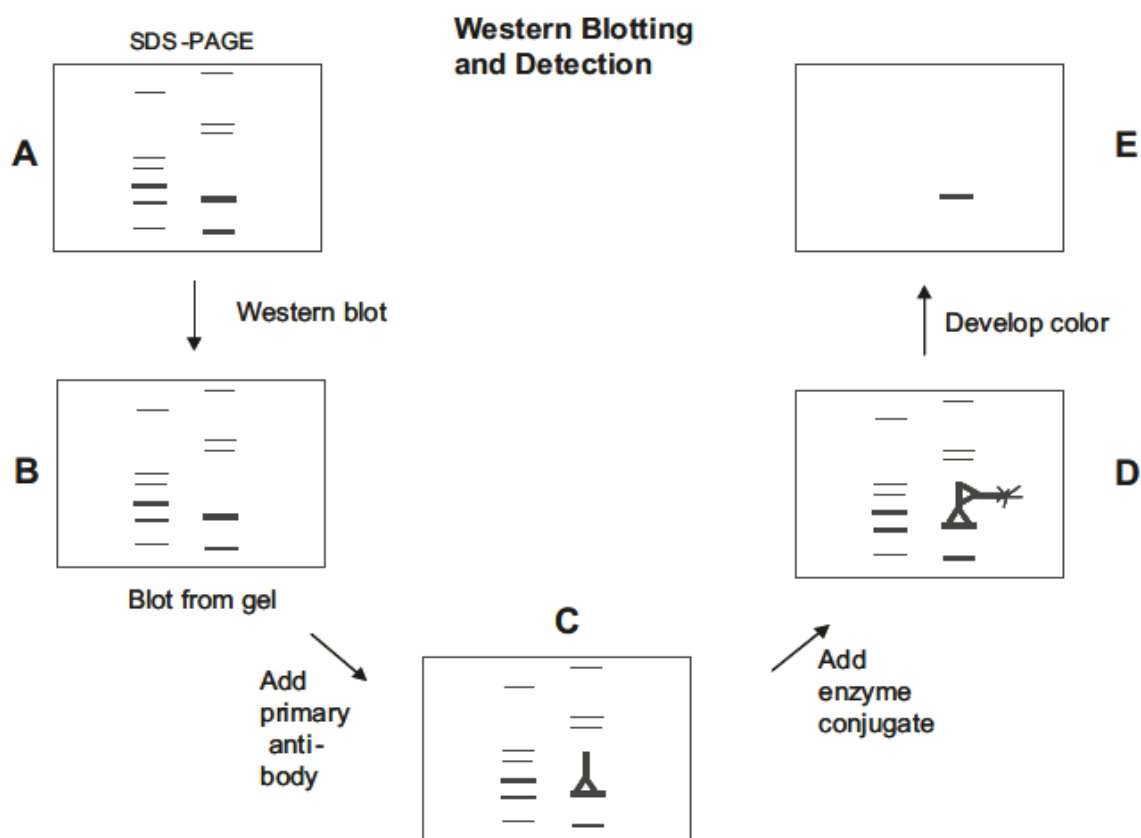


Figure 2.4. Schematic representation of blotting and detection procedure. (a) Unstained (sodium dodecyl sulfate–polyacrylamide gel electrophoresis (SDS-PAGE) gel prior to blot. The bands shown are hypothetical. (b) An exact replica of SDS-PAGE gel was obtained as a blot following transfer the sample. (c) Primary antibody binding to a specific band on the blot. (d) Secondary antibody conjugated to an enzyme (alkaline phosphatase or horseradish peroxidase) binding to the primary antibody. Adapted from (Kurien, 2021).

Northern assays (Grunenwald *et al.*, 2018) function is detecting a direct binding of a given RNA molecule to a protein immobilized on a nitrocellulose membrane. Also, north assays can identify whether the protein of interest can directly and independently bind RNA even in the presence of contaminating bacterial proteins or degradation products that at times may prevent interpretation of results obtained from gel mobility shift or Ribonucleoprotein (Nonaka, 2008) immunoprecipitation assays (Zang and Lin, 2016).

It was suggested that the presence of a parasitic dsRNA virus could contribute to the severity of the disease in strains of *Lieshmania guyanensis* (Ives *et al.*, 2011; Ronet, Beverley and

Fasel, 2011; Hartley *et al.*, 2012). This *Leishmania* dsRNA virus (LRV) has been found in various *L. (Viannia)* species as well as in one *L. major* strain (Scheffter *et al.*, 1995).

Leishmania is present as a motile extracellular promastigote form in the midgut of a female sand fly, and a nonmotile intracellular amastigote form in the mammalian host macrophage. One of the models proposes that the innate recognition of LRV takes place in the first few hours of infection. Here, some fraction of parasites die, releasing viral dsRNA that then binds to Toll-like receptor 3 (TLR3) triggering the subsequent Interferons(IFN) -type I driven inflammatory cascade that worsens disease (Ives *et al.*, 2011; Ronet, Beverley and Fasel, 2011). A high LRV burden in infecting parasites could therefore be a major determinant of disease severity and pathology.

The aim of the present research

To investigate the presence of dsRNA in *T. gallinae* using immunofluorescence monoclonal antibodies J2 specific to dsRNA viruses.

Initial research aims which are reported in this chapter were to:

1. To screen the UEA based archive of cryostabilates of *Trichomonas* for the presence of possible viruses using agarose electrophoresis of total RNAs extracted from cultures of the isolates to visualize any potential bands of viral dsRNA.
2. To confirm any bands visible as dsRNA using RNase III treatment and the use of the dsRNA specific monoclonal antibody J2
3. To investigate any obvious variation in growth characteristics or morphology using classical microbiological methods (cell counts and giemsa staining).

2.3 Methods

2.3.1 Selection of *Trichomonas gallinae* isolates from the cryobank

A total of 21 samples of *T. gallinae* were obtained from the sample CryoBank held at the University of East Anglia (Table 2.1.) where Tyler's group has a collection of hundreds of isolates of *T. gallinae* previously preserved. The isolates are collected from a diverse array of birds across a wide geographical range. These 21 isolates were obtained from a range of avian species including greenfinch *Chloris chloris*, chaffinch *Fringilla coelebs*, goldfinch *Carduelis carduelis*, bullfinch *Pyrrhula pyrrhula*, siskin *Carduelis spinus*, wood pigeon *Columba palumbus*, feral pigeon *Columba livia domestica*, tawny owl *Strix aluco*, common buzzard *Buteo buteo*, black-naped fruit dove *Ptilinopus melanospilus*, pink pigeon *Nesoenas mayeri*, collared dove *Streptopelia decaocto*, Socorro dove *Zenaida graysoni* and brambling *Fringilla montifringilla*.

Nine of the 21 isolates were from the birds showing characteristic lesions of necrotic stomatitis and ingluvitis. The samples were derived from different locations to maintain geographic diversity. Table 2.1. indicates species, year found, geographical location, evidence of lesions, culture extract, and subtype designated using Fe-hydrogenase.

Table 2.1. A 21 Isolates of *T. gallinae* obtained from of birds and preserved in cryobank at the University of East Anglia(Alrefaei Abdulwahed, 2017)

S.No.	Host species	Year found	Location	Lesions	FeHyd subtype
1	Greenfinch	2013	Wiltshire	Yes	A1
2	Chaffinch	2008	Norfolk	Yes	A1
3	Goldfinch	2016	Somerset	Yes	A1
4	Bullfinch	2011	Hampshire	Yes	A1
5	Siskin	2016	Tyne & Wear	No	A1
6	Wood pigeon	2013	Hampshire	Yes	N1
7	Feral pigeon	2014	Devon	No	A1
8	Tawny owl	2015	Hampshire	Yes	A1
9	Common Buzzard	2014	Northamptonshire	Yes	C4
10	Wood pigeon	2013	Norfolk	No	A1
11	Wood pigeon	2014	Norfolk	No	C4
12	Pink pigeon	2017	UK Zoological collection	No	C3
13	Black naped fruit dove	2013	UK Zoological collection	No	A1
14	Feral pigeon	2015	Norfolk	No	A1
15	Feral pigeon	2015	Norfolk	No	C8
16	Wood pigeon	2015	Norfolk	No	C4
17	Pink pigeon	2015	Norfolk	No	C4
18	Collared dove	2014	Norfolk	Yes	A1
19	Feral pigeon	2015	Norfolk	No	C4
20	Brambling	2015	West Midlands	Yes	A1
21	Socorro dove	2015	UK Zoological Collection	Yes	A1

2.3.2 Medium preparation

A medium first developed by Diamond (1957) for the culture of *Trichomonads*, Medium TYM was used, modified to optimize *Trichomonas gallinae* growth (<https://www.atcc.org/~media/18E35E9518EF438B836CB69ACF7FD227.ashx>) This contained the following: 20.0 g of BBL Trypticase™ Peptone (Becton Dickinson, France), 10.0 g of yeast extract (Sigma-Aldrich, St. Louis, USA), 5.0 g general purpose grade maltose (Thermo Fisher Scientific, Loughborough, UK), 1.0 g of L-cysteine-HCl (Sigma-Aldrich, St. Louis, USA), 0.2 g of ascorbic acid (Sigma-Aldrich, St. Louis, USA), 0.8 g dipotassium hydrogen orthophosphate, anhydrous (K₂HPO₄) (Sigma-Aldrich, St. Louis, USA), 0.8 g Potassium dihydrogen phosphate, anhydrous (KH₂PO₄) (Sigma-Aldrich, St. Louis, USA), 1.0 ml ferric ammonium citrate (22.8 mg/ml) (Sigma-Aldrich, St. Louis, USA) and 0.5 g of *Bacto*® Agar (Becton Dickinson, USA).

The ingredients listed were mixed in 990 ml of distilled water. The pH was then adjusted to 7.2, after which 30 minutes of sterilization was undertaken, using an autoclave at a temperature of 121 °C, then 10 ml of heat-inactivated horse serum was added.

Bacterial contamination of the medium was avoided by using penicillin and streptomycin (10,000units/ml; Life Technologies, Paisley, UK). The medium was stored at -20°C and returned to room temperature before use (Diamond, 1962).

2.3.3 Giemsa-staining *T. gallinae*

After successfully culturing all of 21 of *T. gallinae*, we used Giemsa-staining of cells potentially infected and non-infected with RNA-virus to investigate potential morphological differences in those samples of four sub-types (A1, C3, C4 and C10) (Fig. 2.9)

Each cultured sample of *T. gallinae* was transferred to 1.5 ml Eppendorf tube and centrifuged to remove the media. The pellets were washed with phosphate buffered saline (PBS) buffer pH 7.4 and the cells were counted so that 10⁶ parasites were present in 900 microlitres of

Phosphate-buffered saline buffer (PBS). A total of 400uL of 4% ice cold methanol was added to Eppendorf to fix the cells. This was left to allow the methanol to evaporate before continuing. Using tweezers, one sterile round coverslip was placed at the bottom of a well in a 24 well plate. This was then washed gently with about 500uL of sterile PBS. Each well was washed three times, and 500 phosphate buffered saline (PBS) was added to the pellet and mixed and then 200 microliters was added to each coverslip. The Giemsa stain was diluted to a 1:20 dilution using tap water. After 20 minutes, or when the methanol had evaporated, the wells were washed twice with PBS. The PBS was then removed and 400uL of Giemsa was added to each well and left for 15 minutes. All but a few microlitres of Giemsa was left in the wells to prevent the cells from drying out. Tweezers were used with a pipette tip, and the cover slip removed carefully from the well. The next step was dipping the coverslip in the following solutions (in this order), and leaving coverslip in the vials for about 10 seconds for each solution:

1. Pure Acetone
2. Pure Acetone 2
3. 7:3 Acetone:Xilol
4. 3:7 Acetone:Xilol
5. 7:3 Xilol:Acetone
6. Pure Xilol

The coverslips were left to dry cell slide up on some tissue paper. When dry, a pipette tip was used to put one drop of mounting fluid (Entellan) onto the cell of the coverslip. The tweezers were used to flip the coverslip over and 'stick' it to a microscope slide. The slide was labelled, and clear nail varnish was used to seal the edges of the coverslip to the slide. Cells were viewed using an Axioplan upright digital imaging microscope.

2.3.4 Optimization of growth conditions for RNA extraction

The 21 isolates listed in Table 2.1 were grown using Diamond medium as explained above with the growth of *T. gallinae* further promoted using Trypticase-yeast extract-maltose. The samples were examined everyday under the microscope to monitor their growth and to find appropriate time for RNA extraction.

2.3.5 Monitoring of *T. gallinae* culture and counting cells

Microscopic observations were made using a double chamber haemocytometer and counting was conducted of motile *T. gallinae* parasites at $10\times$ magnification. Both grids of the haemocytometer were used to count motile *T. gallinae* parasites. Only the centre square and the four outer corner squares of the ruled grid were examined for counting purposes in *T. gallinae* cells from culture.

2.3.6 Growth curve for four panel of *T. gallinae*

For each isolate the number of parasite/ml was counted using a haemocytometer. Then 10^4 trophozoites of each isolate were inoculated into falcon tubes containing 10 ml of sterile Diamond medium. The growth for each isolate was followed by counting the *T. gallinae* cells every 24 hours over five days. Triplicate counts of cells were done. This was undertaken to record the duration of parasite log growth and the time at which cells reach their maximum population, this information was used for future experiments.

2.4 Extraction of RNA from *Trichomonas gallinae* isolates for detection of dsRNA

A total of 21 isolates listed in Table 2.1 were grown and RNA was extracted using the TRIZOL Thermo Fisher protocol (Graves *et al.*, 2019). Here a total of 1 mL of TrizolTM Reagent was added to every 50–100 mg of cultured cells for all samples. This was then homogenized using a homogenizer. A centrifuge was used to pellet the cells, after which the supernatant was discarded. 0.75 mL of TrizolTM Reagent per 0.25 mL of sample at a concentration of 1×10^7

cell was then added to the pellet. The cells were not washed prior to the addition of TrizolTM Reagent to avoid mRNA degradation. The lysate was then pipetted up and down several times in order to homogenize it. A volume of 0.2 mL of chloroform per 1 mL of TrizolTM Reagent used for lysis, was added to the cultures. The tubes were then securely capped and incubated for 2–3 minutes. The samples were then centrifuged for 15 minutes at $12,000 \times g$ at 4°C. The mixture separated into a lower red phenol-chloroform, an interphase, and a colourless upper aqueous phase. The aqueous phase was then transferred to a new tube. This was carried out by angling the tube at 45° and pipetting out the solution. 0.5 mL of isopropanol was added to the aqueous phase, for every 1 mL of the TrizolTM Reagent used for lysis. Incubation took place for a period of 10 minutes. Centrifuging was then conducted for 10 minutes at $12,000 \times g$ at 4°C. The total RNA precipitate formed a white gel-like pellet at the bottom of the tube. The supernatant was discarded using a micropipette. The next step was to wash the RNA pellet once with 75% ice-cold ethanol. A mix of 1 mL of 75% cold ethanol per 1 mL of TRIZOL reagent was used., after which the pellet was resuspended in 1 mL of 75% ethanol per 1 mL of TRIZOLTM Reagent used for lysis. Some of the samples were required to be kept in storage. For this, 75% ethanol was used at a temperature of –20°C. This allows samples to be retained for one year. For short term storage of one week, a temperature of 4°C is adequate. The sample was then vortexed briefly, then centrifuged for 5 minutes at $7500 \times g$ at 4°C. The supernatant was then discarded using a micropipette. Any RNA pellet was left on the bench to air dry for 5–10 minutes. 30 µl of RNase-free water was added to the pellet of the RNA. The RNA samples were examined using agarose gel electrophoresis (1.5. gm agarose/100m; TAE and 5 µl ethidium bromide) Firstly, 3.5 µl nuclease-free water was added to 4 µL of the extracted RNA plus 1.5 µL DNA and loading dye. Previously, I had added 1 µL of the extracted RNA and 1.5 µL of loading dye, along with 4 µL nuclease-free water (Graves *et al.*, 2019).

RNaseIII treatment and disappearance of dsRNA bands.

To confirm that the dsRNA band visible around 4.5 kb in isolates from sample number 12 (subtype C3) pink pigeon and Sample number 21(sub type C10) Socorro dove Table 2.1 is of dsRNA, I added Ambion recombinant RNase III to the total RNA and incubated sample for one hour. This RNase is capable of cleaving dsRNA. Upon running agarose gel of the RNase treated sample, the RNA band had disappeared completely, confirming that the band we see in agarose gel prior to treatment with RNase III was of dsRNA (Figure 2.14). This experiment was repeated three times with same results.

2.5 Material of Immunofluorescence Microscopy Assay:

A total of 4 % Paraformaldehyde (PFA): Phosphate-buffered saline PBS - 16 g of PFA was added to 200 ml of freshly boiled water. Then NaOH was added until the liquid lost turbidity. Then 100 ml of the previously prepared solution was added to 80 ml of H₂O and 20 ml of 10X Phosphate-buffered saline (PBS) and the pH was adjusted to pH 7.8. The solution was aliquoted and frozen at -20 ° C. The 0.5 % bovine serum albumin (BSA): consists of 0.5 mg BSA in 100 ml 1x PBS and stored at -20 ° C. The blocking buffer: (5% normal goat sera, 0.1% Triton-X100, 1× PBS) was prepared.

2.5.1 Immunofluorescence assay procedure

In this protocol 10⁶ *T. gallinae* parasites were fixed with 2% paraformaldehyde in PBS for 2 min. Cells were washed once in PBS and adhered to glass coverslips ((Merck, Gillingham, UK) by centrifugation (500 g for 2 min). The blocking buffer was used to remove more cellular membrane lipids (5% normal goat sera, 0.1% Triton-X100, 1× PBS) for 30 min at room temperature then incubated with mouse anti-dsRNA J2 antibody (1:1000) for one hour. Cells were washed 3× in PBS and incubated with goat anti-mouse IgG AlexaFluor 488 (1:1000, Invitrogen) for one hour. After washing again in PBS (3×), cells were then incubated with 30 to 100 µl of 4',6-diamidino-2-phenylindole [DAPI] for three min. The nuclei of cells were

stained by DAPI, cover slips were hydromounted (Hydromount, National Diagnostics inc , USA) on microscope slides and left to dry for 24 hours at + 4 ° C.

2.5.2 Microscopic images analysis

All cell images were obtained on a Zeiss Axpotome 2 microscope at either x400 or x630 magnification. Images were taken using the Axiovision software 4.8.1 and analysed using both Axiovision software and ImageJ (doi : 10.1038 / nmeth.2019) Fig. 3.7.

Working dilutions for antibodies used for immunofluorescence were as follows: The Primary antibody J2 working dilution was 1:1000, while the secondary antibody Goat anti - mouse 680 nm was 1:1000.

2.6 Northwestern Blotting

Preparation of *T. gallinae* samples for sodium dodecyl sulfate–polyacrylamide gel electrophoresis SDS - PAGE / North blot assays and Protein extraction:

The Diamond culture (TYM) was used for sample growth, then transferred to 4ml tubes and centrifuged for 5min at 10 ,000 rpm; the media was then removed. Pellets were resuspended in 500 µl PBS to be washed twice and centrifuged at 10,000 rpm for 5min then the liquid was removed.

The number of *T. gallinae* cells approximately was 10⁶. A total of 70 micromiter (Campero *et al.*) Mammalian Protein Extraction Reagent lysis was added, incubated in ice for 30 min and centrifuged at 10,000 rpm for 5min. Supernatants were collected into 0.5 ml Eppendorf tubes; protein concentrations were assessed by Protein Assay Kit (BCA), and tubes were stored at - 20 ° C until use for north blot analysis.

2.7 Protein concentration assessment.

Samples were prepared accordingly to their protein concentration in order to load 10 µg of proteins.

2.7.1 SDS - electrophoresis

Proteins were mixed with loading buffer (3:1 ratio) and boiled for 5 min at 100 ° C (Laemmli et al., 1970). The vertical gel tank system was loaded with precast gels and 500 ml of 1x NuPAGE® MES SDS 2-(N-morpholino) ethane sulfonic acid running buffer were placed between them until it overflowed into the surrounding tank. Gels were loaded with 15µl of samples alongside a protein standard molecular weight marker (Precision Plus Dual Colour Protein Standard, BioRad, UK) and run at 150 V for approximately 1 hour at room temperature, or until the protein standard indicated good separation.

2.7.2 Protein blotting

After SDS - electrophoresis, Polyvinylidene fluoride (PVDF) membranes were activated in methanol and gels were semi - dry blotted for 30 minutes at 15 V for one gel or 25 V for two gels. Membranes were washed and blocked buffer (Blocking buffer 5% (w/v) milk. 5% milk, 5 g milk powder in 100 mL wash buffer Tris-buffered saline Tween 20 solution (1x TBST (Tris Buffered Saline-Tween (20X, with 1% Tween-20, pH 7.4). Primary antibody mix: 1:1000 dilution of antibody in blocking buffer), for one hour. Primary antibodies were prepared in blocking buffer and left overnight at + 4 ° C on a rotary shaker. Membranes were washed four times in TBST, 5 minutes per wash. Secondary antibodies were also prepared in blocking buffer and left at room temperature for 1.5 hours. Membranes were washed in TBST stands for four times for 5 minutes and once in PBS for 5 minutes. Images were performed on the Odyssey machine (Li-Cor, UK) and associated imaging software.

2.8 Antibodies and fluorescent dyes

For northwester-dot blot and immunofluorescence assay the same primary antibody was Anti-rsRNA monoclonal antibody J2 was purchased (Scicons, Hősök, Hungary)

The secondary antibody for Immunofluorescence Alexafluor 488nm was purchased from Molecular Probes (Invitrogen, Paisley, UK). While the secondary antibody for blot, north- blot

was Goat anti-mouse 680 nm and purchased from Li-Cor (Lincoln, USA). DAPI was purchased from Sigma (St Louis, USA). Working dilutions for antibodies used for north blot were as follows: The Primary antibody J2 working dilution was 1:1000 and the same dilution was used for the secondary antibody Alexafluor 488nm.

2.9 DotBlot

Dot blot used to determine if antibodies detect the protein or the system are effective.

A total of 15 µl of proteins from each *T. gallinae* sample sub-types of C3, C4, C10, A1 into nitrocellulose membrane, then the labeled membrane was placed on a filter paper and the membrane edges were secured with tape to prevent the edge curling. The membrane was blocked in 5% milk, 1X TBST for 1 hour on a rotating shaker. During blocking the primary antibody was diluted in 1:1000 in 5% milk, 1X TBST, where we prepared enough diluted antibody to cover the blot during shaking incubation. In the next step the blocking solution was decanted and the membrane was rinsed in 1X TBST, then the membrane was washed 2-3 times at 15 minutes each occasion with 1X TBST buffer with shaking on a rotating shaker.

The membrane was incubated with the diluted primary antibody 2 µl+ 10 ml milk. The diluted primary antibody was discarded and washed with 5% milk, 1X TBST three times for 15 minutes each. The secondary antibody was diluted in 5% milk, 1X TBST. After washing, the membrane was incubated with the diluted secondary antibody 1 µl with 68RDL red +10 ml milk and incubated for 30 minutes on a rotating shaker. Then the membrane PVDF was washed three times 10 minutes each. Images were performed on the Odyssey machine (Li - Cor, U) and associated imaging software.

2.10 Statistical Analysis:

All statistical analysis was conducted using GraphPad Prism 9.4.1. One-Way ANOVA was carried out to test differences between experimental groups. Paired T-tests were used to compare between two groups.

2.11 Results

2.11.1 Optimization of growth conditions for RNA extraction

In the present study we cultured 21 isolates of *T. gallinae* cells using Medium TYM where all the cells were grown successfully. During the culture it is obvious that the growth of cells varied over time. The examination of *T. gallinae* cells revealed that 72 hours was the optimum length of cell growth time and after that growth starts to decline (Figure 2.5). Based on these data, it was decided to harvest the samples after 3 days for extraction of possible RNA present and analysis. The 21 samples were divided into two lists alongside accompanying Figs 2.5 & 2.8. and Appendix 2.1. and Appendix 2.2.

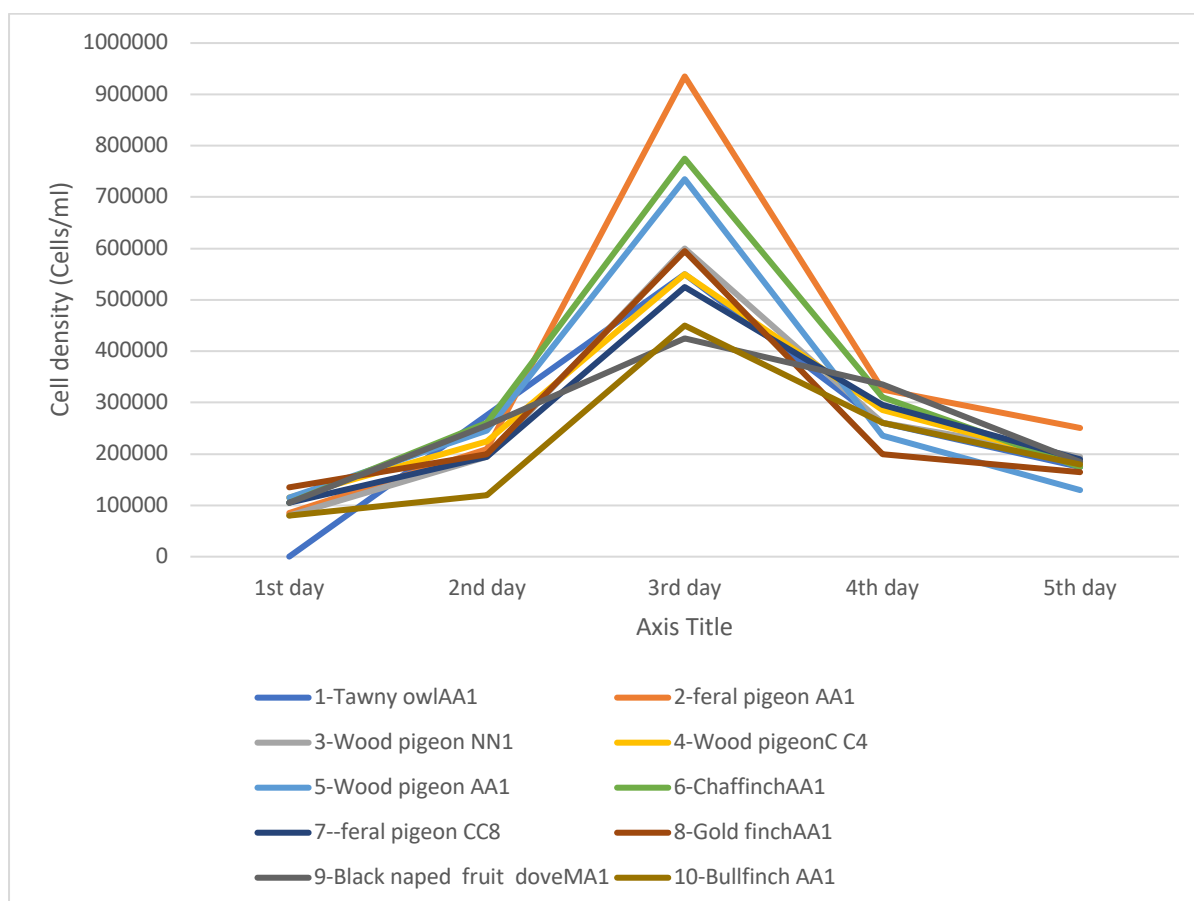


Fig. 2.5 The growth of *T. gallinae* sub-types (1-10 sub-types) from day 1 to day 5

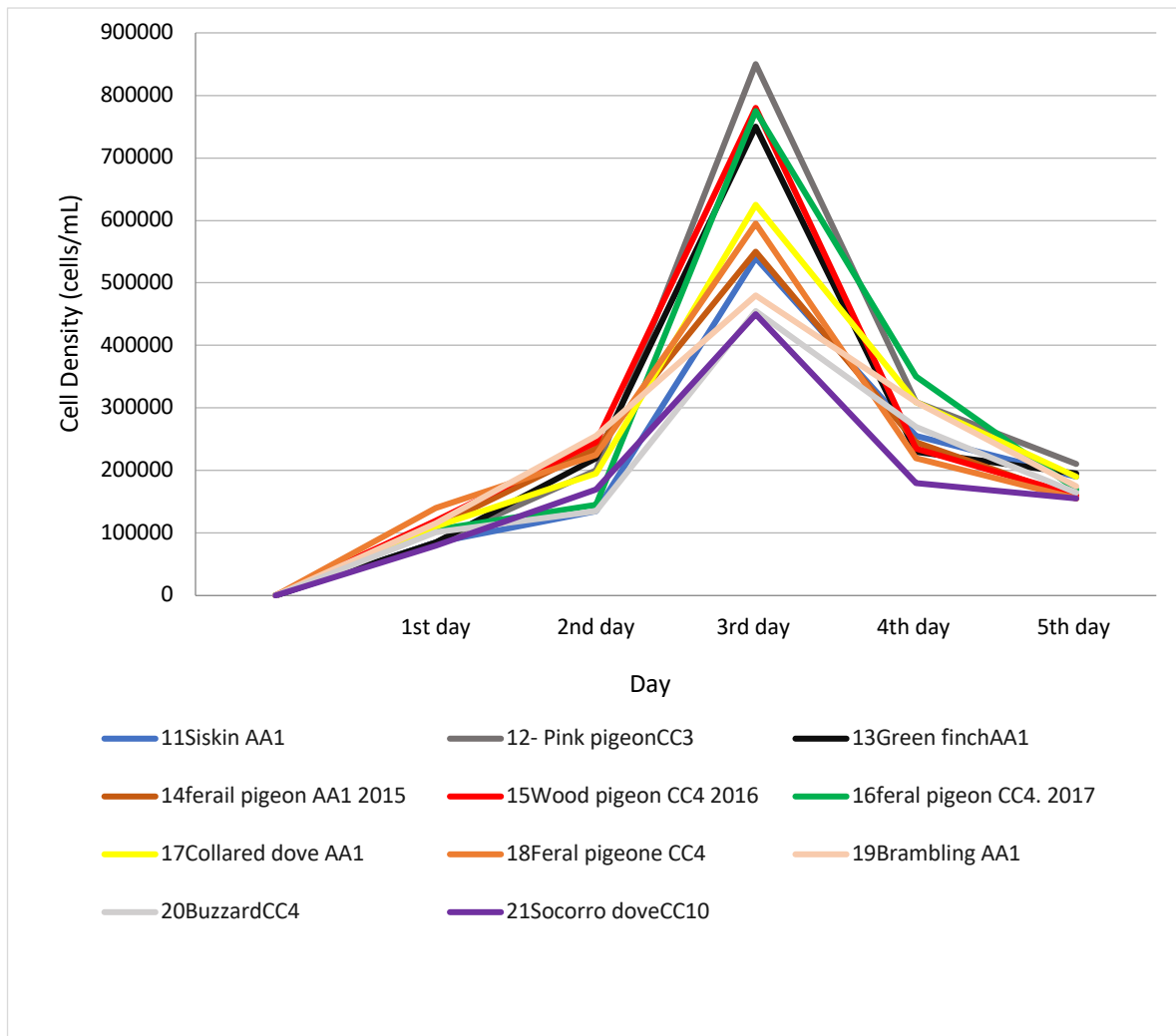


Fig. 2.6 The growth of *T. gallinae* sub-types (11-21 sub-types) from day 1 to day 5

The highest growth for isolates shown in Figs. 2.5 and 2.6 respectively were for samples 2. and 12 respectively namely from a feral pigeon A1 sub-type and a Pink pigeon C3 sub-type, both on day three.

Growth of trophozoites from the four panel in TYM medium reached the maximum value at 72 hours. Although a lower growth was observed after 120 hours, no significant differences

were observed between the groups by one way ANOVA. ($P < 0.05$, $n=4$, $r^2= 0.09351$) (Fig.2.7).

The growth of *T. gallinae* sub-types C10,C4,C3and A1.

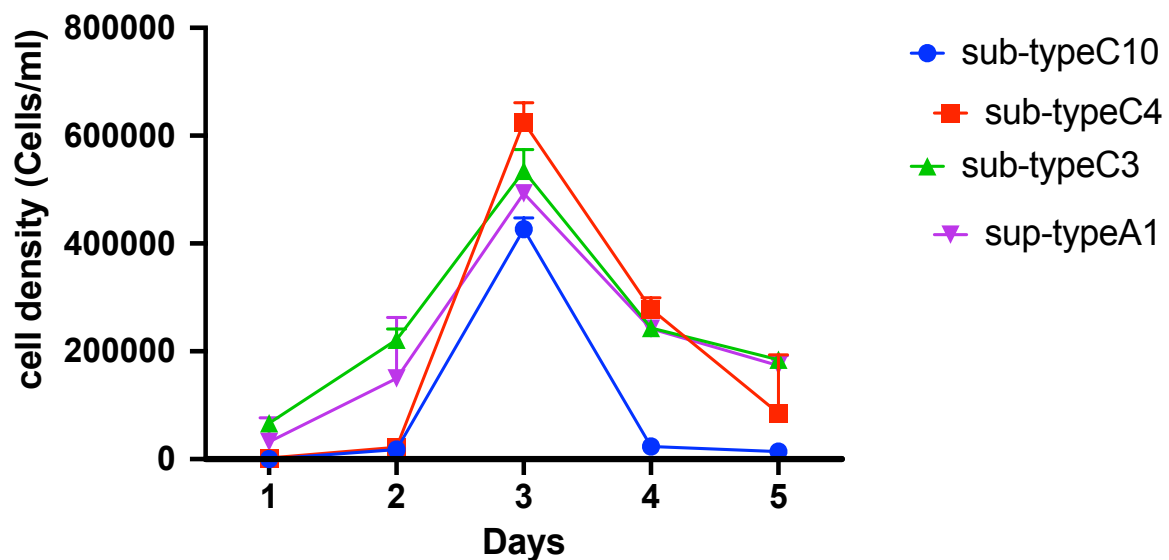


Fig. 2.7 The growth of *T. gallinae* sub-types C10, C4, C3 and A1.

2.11.2 Appearance of sub-types of *T. gallinae* with potential virus

T. gallinae sample number 12 (subtype C3) pink pigeon Table 2.1, sample number 21(subtype C10) Socorro dove (Table 2.1) appeared to be positive for RNA-virus on the basis of evidence from the agarose gel electrophoresis: this constituted 2 of the total 21 samples examined (9.5%). We noticed that sub-type C10 represents the Socorro dove has the lowest growth rate compared to the C3 sub-type from a pink pigeon.

2.11.3 The agarose gel electrophoresis

The initial Agarose gel-based screen of extracted RNA from the 21 different isolates of *T. gallinae* revealed an extra band of dsRNA in the range of 4.5 kb in two isolates consistent with the size of viral dsRNA and indicative of viral infection in *T. gallinae*. These results were confirmed by three biological replications. This band was present in sample number 12 (subtype C3) pink pigeon (Table 2.1) and sample number 21(subtype C10) Socorro dove Table

2.1. The agarose gel electrophoresis revealed the presence of RNA traces at around 4.5 kb. (Figure 2.8 and Fig. 2.9.).

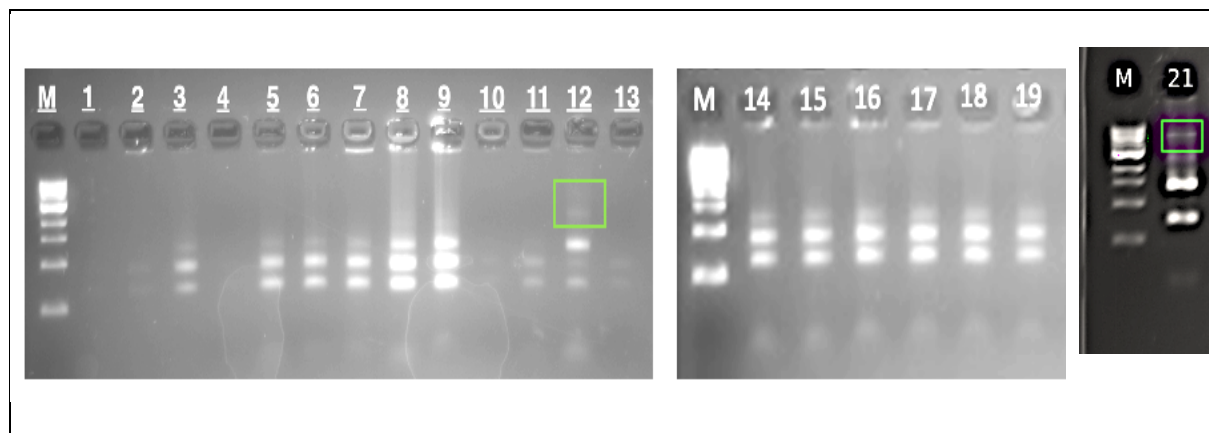


Figure 2.8 Agarose gel electrophoresis of the extracted RNA from 21 isolates of *T. gallinae*. M denotes 1 kb DNA ladder. A band around 4kb is visible in lanes 12 and 21 (green boxes). These two lanes represent isolates 12 (subtype C3) pink pigeon (Table 2.1.) and sample number 21(sub type C10) Socorro dove listed in Table 2.1. This dsRNA band is absent in other isolates. The sub-type C10 revealed clear band as indicated in Fig. 2.9

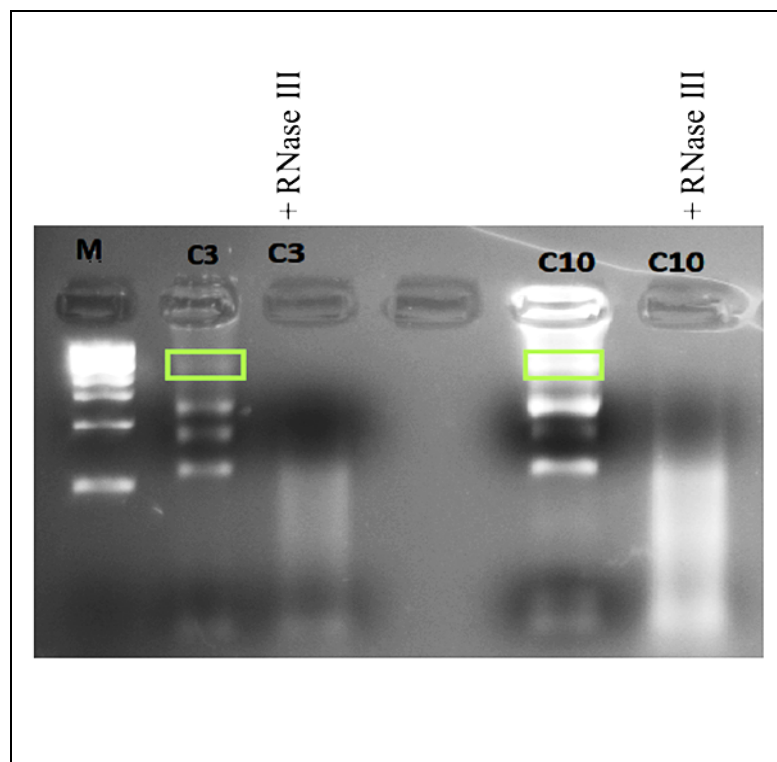


Figure 2.9 Agarose gel electrophoresis of the extracted RNA of *T. gallinae* treated with RNase III from isolate sample number 12 (subtype C3) pink pigeon (Table 2.1) and sample number 21(subtype C10) Socorro dove M denotes 1 kb DNA ladder. RNA was extracted from sample number 12 (subtype C3) pink pigeon and sample number 21(subtype C10) Socorro dove and run on agarose gel with and without RNase III added. Green boxes indicate the band of dsRNA and after RNase treatment the band of RNA had disappeared.

2.11.4 Giemsa-staining for the study of morphology *T. gallinae*:

Giemsa-stained cytoplasm with light purple. The nucleus is clearly shown as a much darker purple and the flagella are very well defined. When using Giemsa stain C 10 sub-type was smaller with comparing with other cells (Fig.2.10).

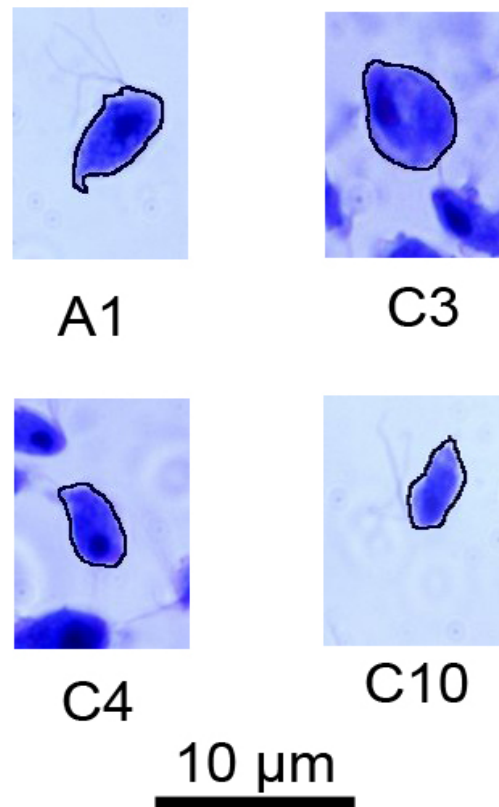


Fig. 2.10 Sub-types (A1, C3, C4, and C10) stained with Giemsa stain

ImageJ was used to measure the area of *T. gallinae*. Cells were outlined (black line) and ImageJ was used to quantify the area in cm^2 . 100 cells were measured for each sub-type, the average was taken and used for further analysis.

2.11.5 Using cell area of *T. gallinae* subtypes to compare

The cell area was measured by Image J of 100 cells per the four sub-types to investigate any difference. There was clear difference in the cell area between subtypes, in particular between

C10, C3 and C4. Subtype C10 has a cell area one third smaller than subtype C3, while C10 is only two thirds the size of C4, as shown in Fig. 2.11.

Cell area of *T. gallinae* sub-types .

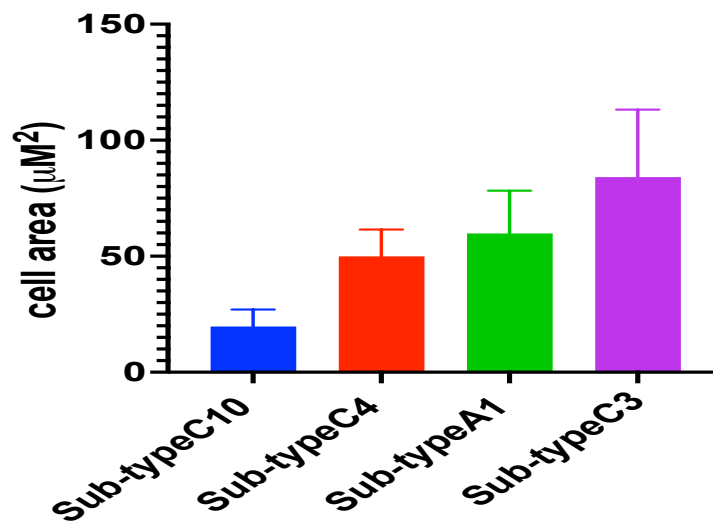


Fig. 2.11 Cell area of *T.gallinae* Sub-types (A1, C3, C4, and C10 stained with Giemsa stain

Significant differences were observed between the groups by one way ANOVA. ($P < 0.0001$, $n=400$, $r^2 = 0.6100$). Means for each sub-type are as follows: C10=19.70, C4=49.91, A1=59.84, C3=84.07

2.11.6 Immunofluorescence microscopy assay

The antibodies used in this technique will allow its binding to fluorescent molecules and fluorescent microscopy allowed us to track the fluorescent molecules revealing any dsRNA inside *T. gallinae* cells. The results showed that the samples from sub-types C3, C4, A1 of *T.gallinae* showed no evidence of dsRNA using monoclonal antibodies J2 as shown in Figs. 2.12.1 to Fig. 2.12.8. J2 antibody preferentially binds to the ends of dsRNA molecules.

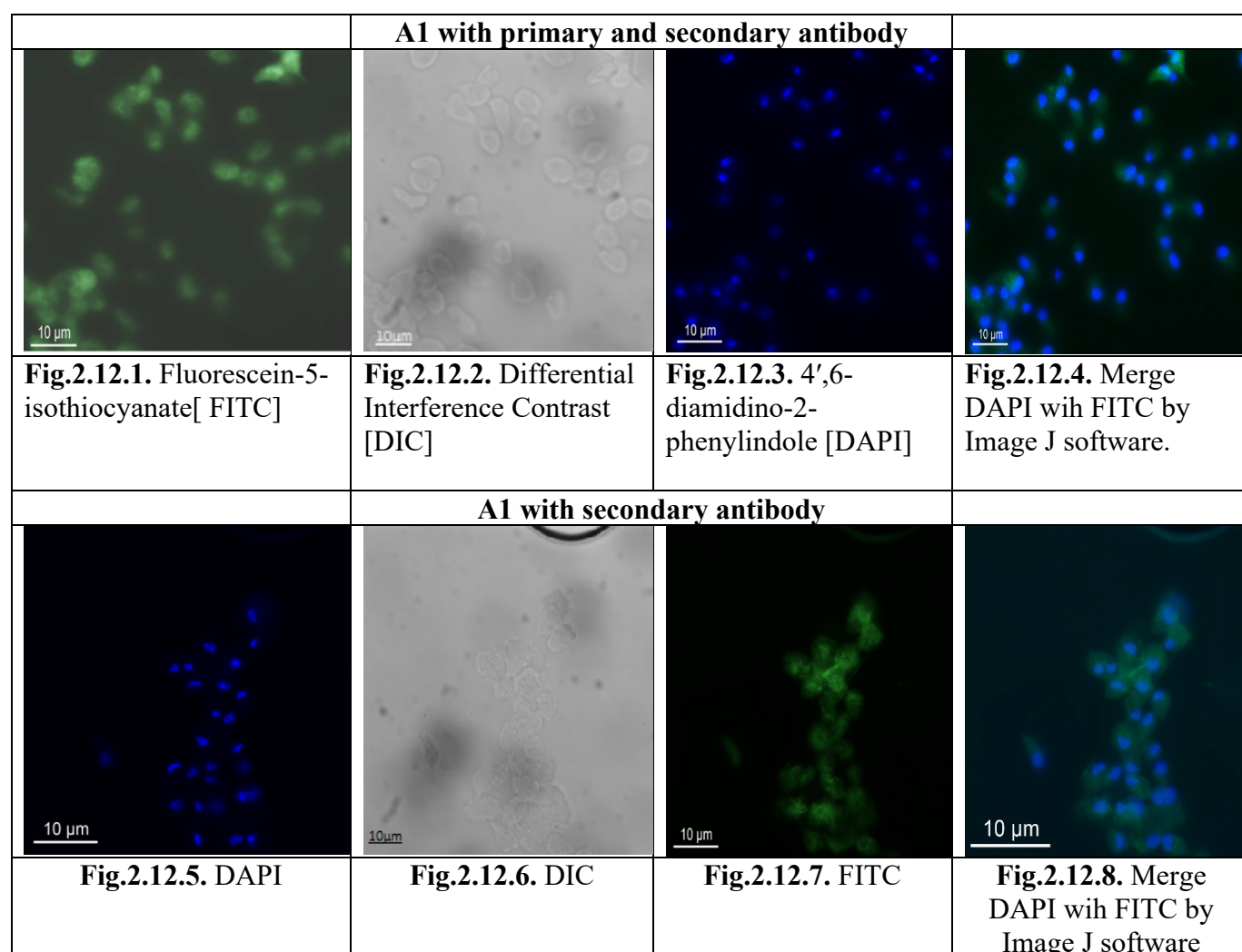


Fig. 2.12.1 to Fig. 2.12.8. Using monoclonal ant-dsRNA (J2) antibody by immunofluorescence microscopy in sub-type A1.

The results indicated that *T. gallinae* with monoclonal anti-dsRNA (J2) antibody by immunofluorescence microscopy in sub-type C3 was free from any dsRNA Fig. 2.13.1. to Fig.2.13.8.

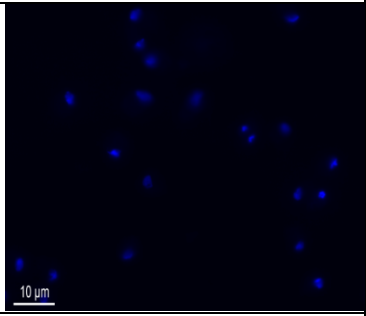
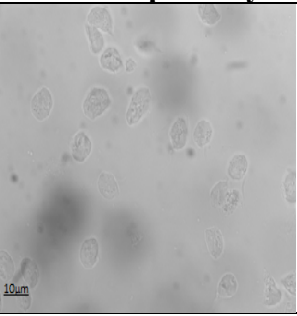
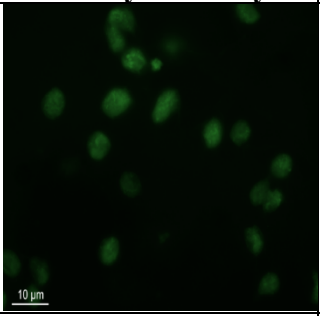
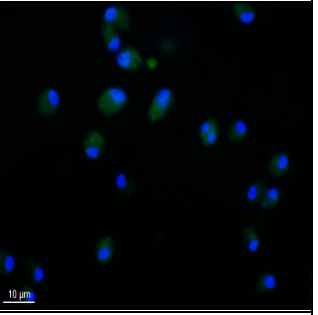
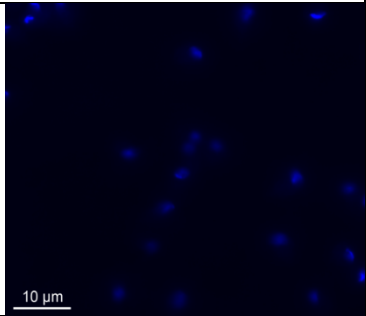
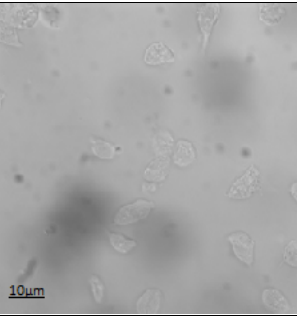
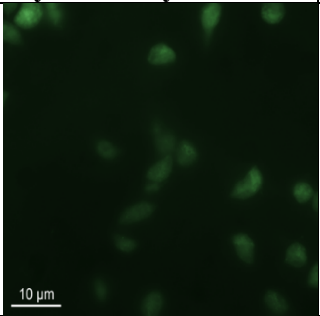
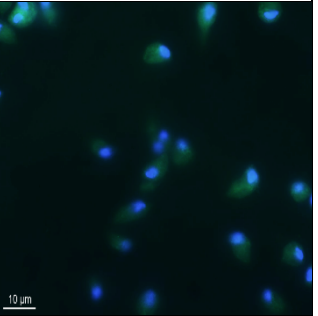
C3 with primary and secondary antibody			
			
Fig.2.13.1. [DAPI]	Fig.2.13.2 [DIC]	Fig.2.13.3. [FITC]	Fig.2.13.4. Merge DAPI wih FITC by Image J software.
C3 with secondary antibody			
			
Fig.2.13.5. [DAPI]	Fig.2.13.6. [DIC]	Fig.2.13.7. [FITC]	Fig.2.13.8. Merge DAPI wih FITC by Image J software

Fig. 2.13.1. to Fig.2.13.8. Using monoclonal ant-dsRNA (J2) antibody by immunofluorescence microscopy in sub-type C3.

The results showed that *T. gallinae* when using monoclonal ant-dsRNA (J2) antibody by immunofluorescence microscopy in sub-type C4 was free from any dsRNA Fig.2.14.1. to Fig.2.14.8.

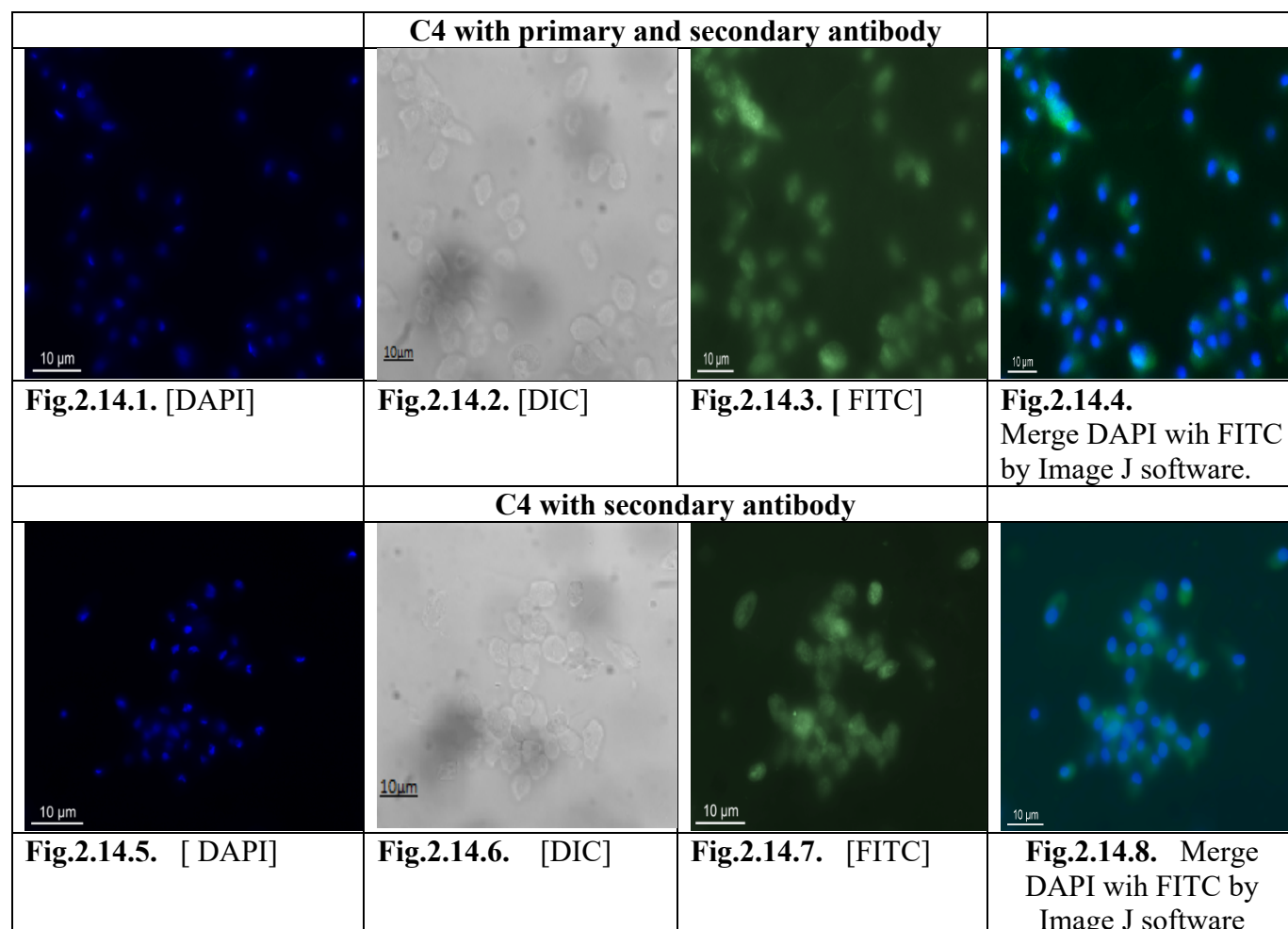


Fig.2.14.1. to Fig.2.14.8 Using monoclonal ant-dsRNA (J2) antibody by immunofluorescence microscopy in sub-type C4.

However, the results indicated that *T. gallinae* with monoclonal anti-dsRNA (J2) antibody by immunofluorescence microscopy in sub-type C10 was positive for dsRNA where *T. gallinae* are surrounded with the fluorescent spots where it is surrounding the cytoplasm of the cells as in Fig.2.15.3. and Fig.2.15.4.

In addition, when secondary antibody was used no signal for dsRNA was noticed shown in Fig.3.15.7.

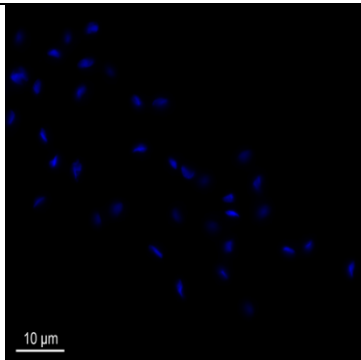
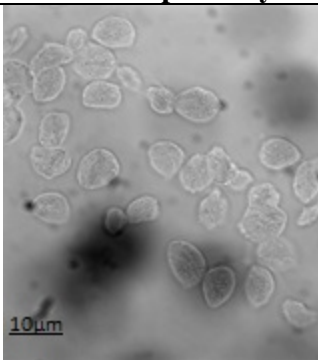
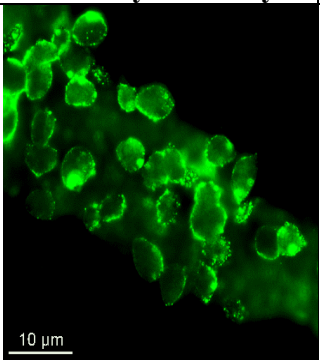
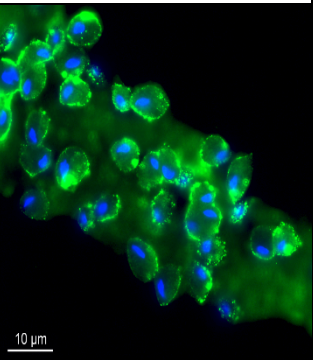
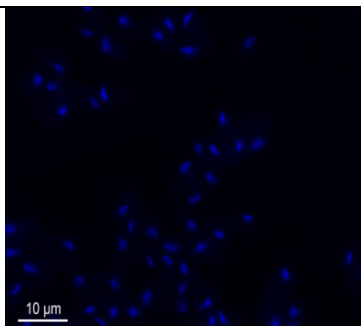
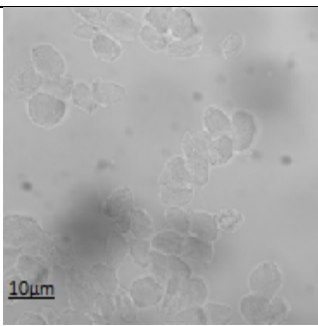
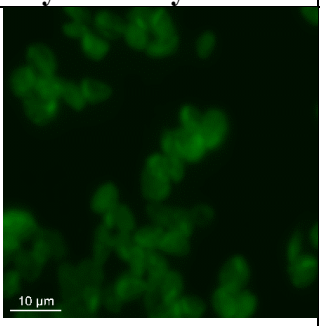
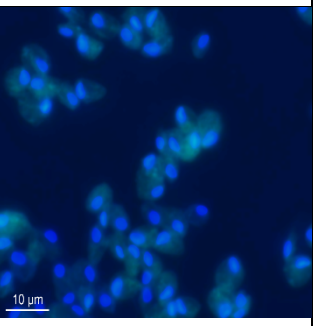
C10 with primary and secondary antibody			
			
Fig.2.15.1. [DAPI]	Fig.2.15.2. [DIC]	Fig.2.15.3. [FITC]	Fig.2.15.4. Merge DAPI with FITC by Image J software.
C10 with secondary antibody			
			
Fig.2.15.5. [DAPI]	Fig.2.15.6. [DIC]	Fig.2.15.7. [FITC]	Fig.2.15.8. Merge DAPI with FITC by Image J software

Fig.2.15.1. to Fig.2.15.8. Immunofluorescence detection of dsRNA (J2) antibody in *T. gallinae* possibly infected cells in sub-type C10.

2.12 Northwestern blot.

The results obtained were difficult to analyze where it showed unexpected sizes and multiple bands (Fig. 2.16). We used the marker protein kDa and the sizing is not clear on SDS gel and the nucleic acids may not migrating.

Using north blot in the four sub-types of *T. gallinae* sub-types C10, C3, C4 and A1 where I repeated this experiment six times. This means that no evidence of the presence of dsRNA-virus was found in these samples using this technique.

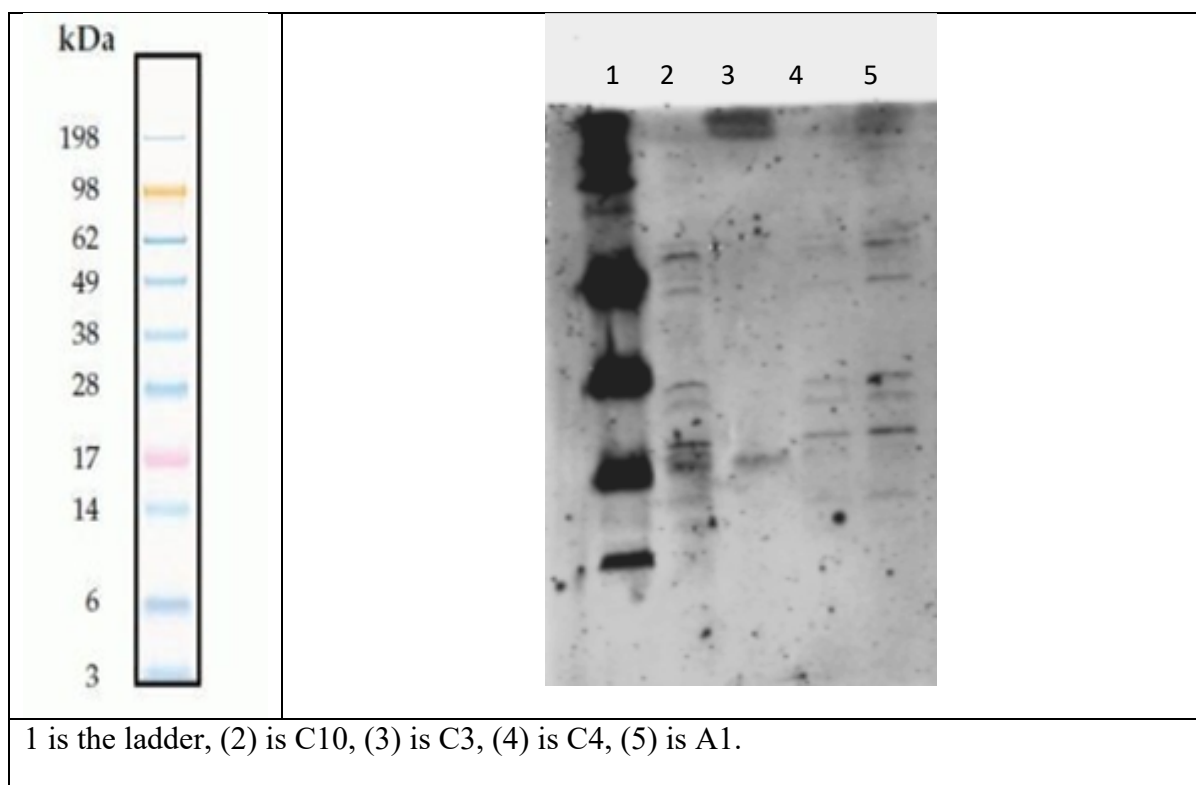


Fig. 2.16 Blotting bands for the four isolates of *T. gallinae*

2.13 Dot blot

The current experiment optimized dot blot by using monoclonal antibodies J2 and revealed it's presence a clear increase in dsRNA in the samples from C10 and C3 *T.gallinae* sub-types but absence in other strains samples from C4 and A1 *T.gallinae* sub-types as shown in Fig.2.17.

The dsRNA positive control was used for confirmation.

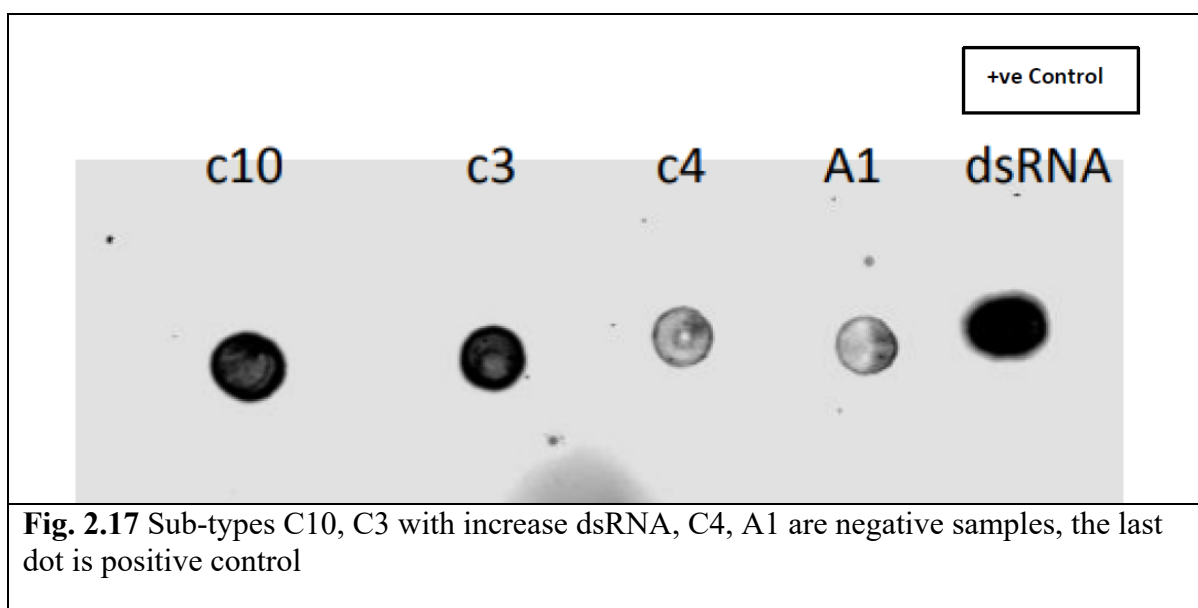


Fig. 2.17 Sub-types C10, C3 with increase dsRNA, C4, A1 are negative samples, the last dot is positive control

2.14 Discussion.

We optimized the growth and culturing of 21 sub-types of *T. gallinae* cells using TYM medium, and found that optimum length of growth was three days. Both *T. gallinae* sub-types infected with the potential virus-RNA and those free of viral-RNA showed highest growth peak at day three.

By using Giemsa stain the morphology of *T. gallinae* cells was clear, with defined pear shape, and very well defined flagella, in addition the cytoplasm gave light purple, while the nucleus was dark purple. The sub-type C10 grew slowly and was smaller than others sub-types in Giemsa. Dot blotting indicated some evidence for increased dsRNA in the C10 and C3 strains. However, fluorescence staining for dsRNA showed a clear punctate peripheral staining pattern consistent with a viral infection only in the C10 strain and this was consistent with identification of appropriate dsRNA banding on a Northwestern blot for only C10.

The present research found evidence of dsRNA bands indicating viral presence in *T.gallinae* samples cultured from sub-types C10 and C3 using dot blot technique. One potential field of application of Northwestern blot method is the discrimination between subclinical infections

and disease (Inieta *et al.*, 2007). Our study indicated that immunofluorescence techniques using monoclonal antibodies J2 were useful in finding dsRNA in sub-type C10.

Avian trichomonosis, caused by the protozoan *T. gallinae*, has been reported from several continents and is considered a major disease within avian species in the orders Columbiformes and Falconiformes and more recently passeriformes, specifically finches (Stabler, 1954; Forrester, D.J. and Spalding, 2003; VILLANÚA *et al.*, 2006; Gerhold *et al.*, 2007). Isolation of a double-stranded RNA (dsRNA) virus from the protozoan *Giardia lamblia* (GLV) and subsequently infected virus-free *G. lamblia* with a single stranded RNA (ssRNA) intermediate of GLV was reported early (Furfine and Wang, 1990).

We optimized the growth of *T. gallinae* cells in TYM medium with a 72 hr length growth time. The agarose gel electrophoresis indicated the presence of ds RNA traces in two sub-types. While our results showed that the highest level of growth reached its peak at 550,000 cell/mls, in the 3rd day then decreased in both the 4th and fifth days.

The nutritional requirements and energy metabolism of trichomonads differ from those of the majority of eukaryotic cells. Trichomonad flagellates depend mainly on pre-formed metabolites as nutrients which indicates the absence of essential biosynthetic pathways (Muller, 1993).

Regarding the clinical environment of the parasites in our study the peak count number of *T. gallinae* was reached at 37 °C. The number of live cells for *T. gallinae* was higher at 37 °C in comparison to 40 °C of incubation (Amin *et al.*, 2010).

The surface area of the measures cells of *T. gallinae* ranged from 20-80 μM^2 and is consistent with the findings reported for *Trichomonas stableri* (Girard *et al.*, 2014). Double-stranded RNA (dsRNA) virus particles, detected in *T. vaginalis*, were assumed to be a virulence factor (Wang *et al.*, 1987).

C3 sub-type gave band, this is consistent with the size of double stranded RNA found in *T. vaginalis* isolates. In other samples band for dsRNA was not detected which means either these samples do not have viruses or viral RNA cannot be extracted under the experimental conditions employed in the current study. Interestingly, sub-type C3 is phylogenetically closely related to sub-type C10 so, we included another isolate of *T. gallinae* belonging to C10 sub-type in our list and extracted RNA from this.

The first reports of viruses in parasites were based on electron microscopy studies. They revealed the presence of virus-like particles (VLPs) in several parasitic protozoa such as *Entamoeba histolytica* (Diamond *et al.*, 1972) and *Leishmania hertigi* (Molyneux, 1974). The presence of ds RNA in the cell of *T. gallinae* in our isolates and isolates from different studies, may display a point of debate toward this. It was reported that the presence of dsRNA viruses infecting the parasite *T. vaginalis* is perceived by its human host, and might have an effect on disease. *T. vaginalis* is the most common non-viral sexually transmitted parasite; it causes inflammatory diseases in the mucosal epithelium of the human genitourinary tract, and is commonly found carrying one or several *T. vaginalis*-specific, dsRNA viruses of the genus *Trichomonas vaginalis* virus, (TVV), family *Totiviridae* (Flegr *et al.*, 1987); (Goodman *et al.*, 2011). It was demonstrated, using a human epithelial culture model, that the cytokines produced by epithelial cells exposed to *T. vaginalis* and TVV (Fichorova *et al.*, 2012). Through the participation of TLR3 signaling, the presence of the virus in the protozoa triggers activation of the nuclear factor "B, of the chemokine interleukin (IL)-8, and of interferon (IFN) a specific cytokine for anti-viral response, thereby amplifying the inflammatory response in the host (Fichorova *et al.*, 2012). The presence of the virus can also affect the pattern of proteins expressed by the parasite. Notorious is defined as the increase in the case of infected parasites, of the number and amount of cysteine proteinases that are established virulence factors

(Provenzano *et al.*, 1997). These results provide a link between the presence of TVVs in *T. vaginalis* and the increase in pathogenicity.

In the parasitic protozoa of the genera *Leishmania*, *Trichomonas* and *Cryptosporidium*, viral infection might also exacerbate virulence of the protozoa (hypervirulence). These cases would represent an example, at least for the parasite, of a virus as mutual symbiont or “good virus” (Roossinck, 2011).

In the present study three techniques, northwestern blot, dot blot (Gomez-Olive *et al.*, 2017) and immunofluorescence assay (IFA) were employed.

Double-stranded RNA (dsRNA) viruses from the genus *Trichomonasvirus* of the *Totiviridae* family was found hosting cells like *T. vaginalis* (Weber *et al.*, 2003). Overall, dsRNA virus was detected in 21 (75%) of 28 *T. vaginalis* isolates (95% confidence interval [CI], 55%-89%) in USA (Wendel *et al.*, 2002). *T. vaginalis* viruses (TVVs) first identified by Wang (Wang *et al.*, 1987). The virus-like particles (VLPs) were found in the cytoplasm closely associated with the Golgi complex, with some VLPs budding from the Golgi, and other VLPs were detected adjacent to the plasma membrane (Benchimol *et al.*, 2002). *T. vaginalis* can be infected with up to four distinct TVVs (Goodman *et al.*, 2011). High rates of double-stranded RNA viruses and *Mycoplasma hominis* in *T. vaginalis* clinical isolates were also recorded in South Brazil (da Luz Becker *et al.*, 2015).

Within the *Totiviridae* family, 5 genera, *Giardiavirus*, *Trichomonasvirus*, *Leishmanivirus*, *Totivirus*, and *Victorivirus*, are currently recognised which share common characteristics. Their genomes are linear uncapped dsRNA encoding for two partially overlapping proteins; the capsid protein (Schantz *et al.*, 1995) and the RNA-dependent RNA polymerase (RdRp). The RdRp is generally expressed as a CP/RdRp fusion protein by means of a –1 or, more rarely, a+1/–2 ribosomal frameshift or by ribosomal hopping (Hillman and Cohen, 2021).

In similar flagellates (to our *Trichomonas*), the double-stranded RNA (dsRNA) virus from the protozoan *Giardia lamblia* (GLV) was isolated and subsequently infected virus-free *G. lamblia* with a single stranded RNA (ssRNA) intermediate of GLV. The researchers disclosed that the ssRNA was a competent replicative intermediate for the GLV dsRNA virus, demonstrating that transfection of RNA from virus-positive to virus-free protozoans could initiate a productive infection (Gerhold *et al.*, 2009).

Immunofluorescence (IF) is a technique that allows visualization of virtually many components in any given tissue or cell type. This can be happened through combinations of specific antibodies tagged with fluorophores (Im *et al.*, 2019). In our study IF was performed on cultured cells of the avian parasite *T. gallinae* and this was evident in detection of ds RNA using monoclonal antibodies J2 in sub-type C10 .

Using the antibody J2, the first dot blot assay for a *Totivirus* in *Leishmania* was reported by researchers who used J2 for immunofluorescence, ELISA, and dot and slot blot assays for various strains of *Leishmania guyanensis* of known infection status (Zangger *et al.*, 2013).

Anti-dsRNA antibodies like J2 has practical importance such use in cell biology, especially the unravelling of the various intermediate steps in viral replication. Also, dsRNA intermediates were discovered in the replication of positive-strand ssRNA viruses as well as ssDNA and dsDNA viruses. However, dsRNA intermediates in the replication of negative-sense ssRNA viruses were beyond detection at that time (Weber *et al.*, 2006).

Studies showed that *T. vaginalis* virus (TVV) which is a member of the *Totiviridae* family under the distinct genus *Trichomonasvirus* and is considered mono-segmented dsRNA viruses has the potential to infect *T. vaginalis* (Goodman *et al.*, 2011; Fraga *et al.*, 2012).

As our results showed two out of four *T. gallinae* isolates may be infected with ds RNA-virus using different techniques. A total of 35 dsRNA viruses were identified from 18 (19%) *T. vaginalis* isolates (Rivera *et al.*, 2017).

In Italy the researchers isolated 48 strains of *T. vaginalis* and tested these strains of the presence of double-stranded RNA *Trichomonasvirus* (TVV), (TVV1, TVV2, TVV3, and TVV4). The most prevalent virus was TVV2 (79.17% of positive *T. vaginalis* strains) followed by TVV1 (70.83%) and by TVV3 (54.17%) (Margarita *et al.*, 2019).

It was reported that four of the known dsRNA viruses infecting *T. vaginalis* were detected in vaginal swab specimens through RT-PCR in Philippines (Rivera *et al.*, 2017). This finding confirms/supports our results for the active of RNA-virus in the isolates of *T. gallinae* as both *Trichomonas* are belonging to the same genus.

Many RNA viruses are found in protozoan parasites. They can be responsible for more serious pathology or treatment failure (Isorce and Fasel, 2020). Moreover, these viruses have been described as potential virulence factors (Fichorova *et al.*, 2013; El-Gayar, Mokhtar and Hassan, 2016; Rath *et al.*, 2019). So detection of dsRNA in parasitic protozoa of importance.

Some studies detected the viral Double-Stranded RNA by DNase I and Nuclease S1 digestions in *Leishmania* parasites as an additional tool supports other methods and recommended to detect other viral dsRNA in other parasites (Isorce and Fasel, 2020).

In the current study using dot blot enabled us to confirm of increase for RNA-virus in two subtypes C10 and C3.

In Japan the researchers demonstrated that *Cryptosporidium parvum* virus 1 (CSpV1), a symbiotic virus of *C.parvum*, can be a high-resolution tool to trace *C. parvum* (MURAKOSHI *et al.*, 2020).

Dot blot showed high sensitivity in the detection of dsRNA in *T. gallinae* where 2 out of samples were found containing dot of dsRNA this mean 50% of samples was positive, compared to the results of Margarita *et al.*, TVV2 (79.17% of positive *T. vaginalis* strains) followed by TVV1 (70.83%) and by TVV3 (54.17%) (Margarita *et al.*, 2019). The global MicroRNAs miRNAs of the protozoan *T. gallinae* was studied and 4 miRNA candidates were

identified (Xu *et al.*, 2014). The number of miRNAs of *T. gallinae* was similar to the miRNAs described by Lin *et al.* (Lin *et al.*, 2009) who revealed 9 novel miRNAs from *T. vaginalis*, a closely related parasite. The three novel miRNAs described is did not possess homologues in miRNAs from *T. vaginalis*, and therefore, the three miRNA candidates identified in the present study may be *T. gallinae* specific (Lin *et al.*, 2009).

2.15 References

- Abdulwahed Alrefaei (2017) *Impact of the genetic heterogeneity of Trichomonas gallinae on the molecular ecology of avian trichomonosis*. University of East Anglia.
- Alrefaei, A. F. (2020) 'Molecular detection and genetic characterization of Trichomonas gallinae in falcons in Saudi Arabia', *PLOS ONE*. Edited by M. A. Pacheco, 15(10), p. e0241411. doi: 10.1371/journal.pone.0241411.
- Amin, A. *et al.* (2010) 'Axenization and optimization of in vitro growth of clonal cultures of Tetratrichomonas gallinarum and Trichomonas gallinae', *Experimental Parasitology*, 124(2), pp. 202–208. doi: 10.1016/j.exppara.2009.09.014.
- Anderson, N. L. *et al.* (2009) 'Studies of trichomonad protozoa in free ranging songbirds: Prevalence of Trichomonas gallinae in house finches (Carpodacus mexicanus) and corvids and a novel trichomonad in mockingbirds (Mimus polyglottos)', *Veterinary Parasitology*, 161(3–4), pp. 178–186. doi: 10.1016/j.vetpar.2009.01.023.
- Benchimol, M., Chang, T.-H. and Alderete, J. F. (2002) 'Visualization of new virus-like-particles in Trichomonas vaginalis', *Tissue and Cell*, 34(6), pp. 406–415. doi: 10.1016/S0040816602000757.
- Bunbury, N. *et al.* (2005) 'Comparison of the InPouch TF Culture System and Wet-Mount Microscopy for Diagnosis of Trichomonas gallinae Infections in the Pink Pigeon Columba mayeri', *Journal of Clinical Microbiology*, 43(2), pp. 1005–1006. doi: 10.1128/JCM.43.2.1005-1006.2005.
- Bunbury, N. (2011) 'Trichomonad Infection in Endemic and Introduced Columbids in the Seychelles', *Journal of Wildlife Diseases*, 47(3), pp. 730–733. doi: 10.7589/0090-3558-47.3.730.
- Coles, E. (1980) 'Coles eh'. Philadelphia: Sounder's Company.
- Diamond, L. S. (1957) 'The Establishment of Various Trichomonads of Animals and Man in Axenic Cultures', *The Journal of Parasitology*, 43(4), p. 488. doi: 10.2307/3274682.
- DIAMOND, L. S. and Bartgis, I. L. (1962) 'Axenic Cultivation of Trichomonas tenax, the Oral Flagellate of Man I. Establishment of Cultures', *The Journal of Protozoology*, 9(4), pp. 442–444. doi: 10.1111/j.1550-7408.1962.tb02650.x.
- Diamond, L. S., Mattern, C. F. T. and Bartgis, I. L. (1972) 'Viruses of Entamoeba histolytica I. Identification of Transmissible Virus-Like Agents', *Journal of Virology*, 9(2), pp. 326–341. doi: 10.1128/jvi.9.2.326-341.1972.
- El-Gayar, E. K., Mokhtar, A. B. and Hassan, W. A. (2016) 'Molecular characterization of double-stranded RNA virus in Trichomonas vaginalis Egyptian isolates and its association with pathogenicity', *Parasitology Research*, 115(10), pp. 4027–4036. doi: 10.1007/s00436-016-5174-3.
- Fichorova, R. N. *et al.* (2012) 'Endobiont Viruses Sensed by the Human Host - Beyond Conventional Antiparasitic Therapy', *PLoS ONE*, 7(11). doi: 10.1371/journal.pone.0048418.
- Fichorova, R. N. *et al.* (2013) 'The Villain Team-Up or how Trichomonas vaginalis and bacterial vaginosis alter innate immunity in concert', *Sexually Transmitted Infections*, 89(6), pp. 460–

466. doi: 10.1136/sextrans-2013-051052.

- Flegel, J. *et al.* (1987) 'The dsRNA of *Trichomonas vaginalis* is associated with virus-like particles and does not correlate with metronidazole resistance', *Folia Microbiologica*, 32(4), pp. 345–348. doi: 10.1007/BF02877224.
- Forrester, D.J. and Spalding, M. G. (2003) 'Parasites and diseases of wild birds in Florida', *University Press of Florida*.
- Fraga, J. *et al.* (2012) 'Genetic characterization of three Cuban *Trichomonas vaginalis* virus. Phylogeny of Totiviridae family', *Infection, Genetics and Evolution*, 12(1), pp. 113–120. doi: 10.1016/j.meegid.2011.10.020.
- Furine, E. S. and Wang, C. C. (1990) 'Transfection of the *Giardia lamblia* Double-Stranded RNA Virus into *Giardia lamblia* by Electroporation of a Single-Stranded RNA Copy of the Viral Genome', *Molecular and Cellular Biology*, 10(7), pp. 3659–3663. doi: 10.1128/mcb.10.7.3659-3662.1990.
- Gerhold, R. W. *et al.* (2007) 'Necropsy Findings and Arbovirus Surveillance in Mourning Doves from the Southeastern United States', *Journal of Wildlife Diseases*, 43(1), pp. 129–135. doi: 10.7589/0090-3558-43.1.129.
- Gerhold, R. W. *et al.* (2009) 'Examination for double-stranded RNA viruses in *Trichomonas gallinae* and identification of a novel sequence of a *Trichomonas vaginalis* virus', *Parasitology Research*, 105(3), pp. 775–779. doi: 10.1007/s00436-009-1454-5.
- Girard, Y. A. *et al.* (2014) '*Trichomonas stableri* n. sp., an agent of trichomonosis in Pacific Coast band-tailed pigeons (*Patagioenas fasciata monilis*)', *International Journal for Parasitology: Parasites and Wildlife*, 3(1), pp. 32–40. doi: 10.1016/j.ijppaw.2013.12.002.
- Gomez-Olive, F. X. *et al.* (2017) 'Variations in disability and quality of life with age and sex between eight lower income and middle-income countries: data from the INDEPTH WHO-SAGE collaboration', *BMJ Global Health*, 2(4), p. e000508. doi: 10.1136/bmjgh-2017-000508.
- Goodman, R. P. *et al.* (2011) '*Trichomonasvirus*: a new genus of protozoan viruses in the family Totiviridae', *Archives of Virology*, 156(1), pp. 171–179. doi: 10.1007/s00705-010-0832-8.
- Graves, K. J. *et al.* (2019) '*Trichomonas vaginalis* Virus Among Women With Trichomoniasis and Associations With Demographics, Clinical Outcomes, and Metronidazole Resistance', *Clinical Infectious Diseases*, 69(12), pp. 2170–2176. doi: 10.1093/cid/ciz146.
- Grunenwald, C. *et al.* (2018) '*Tetratrichomonas* and *Trichomonas* spp.-Associated Disease in Free-Ranging Common Eiders (*Somateria mollissima*) from Wellfleet Bay, MA and Description of ITS1 Region Genotypes', *Avian Diseases*, 62(1), pp. 117–123. doi: 10.1637/11742-080817-Reg.1.
- Hartley, M.-A. *et al.* (2012) '*Leishmania* RNA virus: when the host pays the toll', *Frontiers in Cellular and Infection Microbiology*, 2, pp. 99–102. doi: 10.3389/fcimb.2012.00099.
- Hillman, B. I. and Cohen, A. B. (2021) 'Totiviruses (totiviridae', in *Encyclopedia of Virology*, pp. 648–657.
- Honigberg, B. M. (1978) '*Trichomonads* of importance in human medicine', in *Parasitic Protozoa*, pp.

- Im, K. *et al.* (2019) 'An Introduction to Performing Immunofluorescence Staining', in *Methods Mol Biol*, pp. 299–311. doi: 10.1007/978-1-4939-8935-5_26.
- Iniesta, L., Gállego, M. and Portús, M. (2007) 'Idiotypic expression of IgG1 and IgG2 in dogs naturally infected with *Leishmania infantum*', *Veterinary Immunology and Immunopathology*, 119(3–4), pp. 189–197. doi: 10.1016/j.vetimm.2007.05.006.
- Isorce, N. and Fasel, N. (2020) 'Viral Double-Stranded RNA Detection by DNase I and Nuclease S1 digestions in *Leishmania* parasites', *BIO-PROTOCOL*, 10(9), p. 3598. doi: 10.21769/BioProtoc.3598.
- Ives, A. *et al.* (2011) 'Leishmania RNA Virus Controls the Severity of Mucocutaneous Leishmaniasis', *Science*, 331(6018), pp. 775–778. doi: 10.1126/science.1199326.
- Kietzmann, G. E. (1993) 'Relationships of *Trichomonas gallinae* to the Palatal-Esophageal Junction of Ring Doves (*Streptopelia risoria*) as Revealed by Scanning Electron Microscopy', *The Journal of Parasitology*, 79(3), p. 408. doi: 10.2307/3283578.
- KOCAN, R. M. and KNISLEY, J. O. (1970) 'Challenge Infection as a Means of Determining the Rate of Disease Resistant *Trichomonas Gallinae*-Free Birds in a Population', *Journal of Wildlife Diseases*, 6(1), pp. 13–15. doi: 10.7589/0090-3558-6.1.13.
- Kurien, B. T. (no date) *blotting for the non-expert*. Springer.
- Laemmli, U. K., Beguin, F. and Gujer-Kellenberger, G. (1970) 'A factor preventing the major head protein of bacteriophage T4 from random aggregation', *Journal of Molecular Biology*, 47(1), pp. 69–85. doi: 10.1016/0022-2836(70)90402-X.
- Levine, N. D. (1961) *Protozoan parasites of domestic animals and of man*. Minneapolis: Burgess Pub. Co. doi: 10.5962/bhl.title.7000.
- Lin, Wei-Chen *et al.* (2009) 'Identification of microRNA in the protist *Trichomonas vaginalis*', *Genomics*, 93(5), pp. 487–493. doi: 10.1016/j.ygeno.2009.01.004.
- da Luz Becker, D. *et al.* (2015) 'High rates of double-stranded RNA viruses and *Mycoplasma hominis* in *Trichomonas vaginalis* clinical isolates in South Brazil', *Infection, Genetics and Evolution*, 34, pp. 181–187. doi: 10.1016/j.meegid.2015.07.005.
- Margarita, V. *et al.* (2019) 'Prevalence of double-stranded RNA virus in *Trichomonas vaginalis* isolated in Italy and association with the symbiont *Mycoplasma hominis*', *Parasitology Research*, 118(12), pp. 3565–3570. doi: 10.1007/s00436-019-06469-6.
- MCKEON, T., DUNSMORE, J. and RAIDAL, S. (1997) '*Trichomonas gallinae* in budgerigars and columbid birds in Perth, Western Australia', *Australian Veterinary Journal*, 75(9), pp. 652–655. doi: 10.1111/j.1751-0813.1997.tb15363.x.
- Mehlhorn, H. *et al.* (2009) 'Fine structure of the bird parasites *Trichomonas gallinae* and *Tetratrichomonas gallinarum* from cultures', *Parasitology Research*, 105(3), pp. 751–756. doi: 10.1007/s00436-009-1451-8.
- MOLYNEUX, D. H. (1974) 'Virus-like particles in *Leishmania* parasites', *Nature*, 249(5457), pp. 588–

589. doi: 10.1038/249588a0.
- Muller, M. (1993) 'Review Article: The hydrogenosome', *Journal of General Microbiology*, 139(12), pp. 2879–2889. doi: 10.1099/00221287-139-12-2879.
- Murakoshi, F., Nakaya, T. and Kato, K. (2020) 'Detection and Epidemiological Analysis of Symbiotic Viruses from Protozoa'.
- Provenzano, D., Khoshnan, A. and Alderete, J. F. (1997) 'Involvement of dsRNA virus in the protein composition and growth kinetics of host *Trichomonas vaginalis*', *Archives of Virology*, 142(5), pp. 939–952. doi: 10.1007/s007050050130.
- Rath, C. T. *et al.* (2019) 'Amazonian Phlebovirus (Bunyaviridae) potentiates the infection of *Leishmania (Leishmania) amazonensis*: Role of the PKR/IFN1/IL-10 axis', *PLOS Neglected Tropical Diseases*. Edited by W. O. Dutra, 13(6), p. e0007500. doi: 10.1371/journal.pntd.0007500.
- Rivera, W. L. *et al.* (2017) 'Detection and molecular characterization of double-stranded RNA viruses in Philippine *Trichomonas vaginalis* isolates', *Journal of Microbiology, Immunology and Infection*, 50(5), pp. 669–676. doi: 10.1016/j.jmii.2015.07.016.
- Robinson, R. A. *et al.* (2010) 'Emerging Infectious Disease Leads to Rapid Population Declines of Common British Birds', *PLoS ONE*. Edited by S. Rands, 5(8), p. e12215. doi: 10.1371/journal.pone.0012215.
- Ronet, C., Beverley, S. M. and Fasel, N. (2011) 'Muco-cutaneous leishmaniasis in the New World', *Virulence*, 2(6), pp. 547–552. doi: 10.4161/viru.2.6.17839.
- Roossinck, M. J. (2011) 'The good viruses: viral mutualistic symbioses', *Nature Reviews Microbiology*, 9(2), pp. 99–108. doi: 10.1038/nrmicro2491.
- S. B. Qiu (2012) 'High prevalence of *Trichomonas gallinae* in domestic pigeons (*Columba livia domestica*) in subtropical southern China', *African Journal of Microbiology Research*, 6(6). doi: 10.5897/AJMR12.001.
- Schantz, P. *et al.* (1995) 'Epidemiology and control of hydatid disease', in Thompson, R. C. A. and Lymbery, A. J. (eds) *Echinococcus and hydatid disease*. CAB International, p. 477 pp.
- Scheffter, S. M. *et al.* (1995) 'The Complete Sequence of *Leishmania* RNA Virus LRV2-1, a Virus of an Old World Parasite Strain', *Virology*, 212(1), pp. 84–90. doi: 10.1006/viro.1995.1456.
- Stabler, R. M. (1954) '*Trichomonas gallinae*: A review', *Experimental Parasitology*, 3(4), pp. 368–402. doi: 10.1016/0014-4894(54)90035-1.
- Tasca, T. and De Carli, G. A. (2003) 'Scanning electron microscopy study of *Trichomonas gallinae*', *Veterinary Parasitology*, 118(1–2), pp. 37–42. doi: 10.1016/j.vetpar.2003.09.009.
- VILLANÚA, D. *et al.* (2006) '*Trichomonas gallinae* in wintering Common Wood Pigeons *Columba palumbus* in Spain', *Ibis*, 148(4), pp. 641–648. doi: 10.1111/j.1474-919X.2006.00561.x.
- Wang, A. L. and Wang, C. C. (1986) 'The double-stranded RNA in *Trichomonas vaginalis* may originate from virus-like particles.', *Proceedings of the National Academy of Sciences*, 83(20), pp. 7956–7960. doi: 10.1073/pnas.83.20.7956.

- Weber, B. (2003) 'Double stranded RNA virus in South African *Trichomonas vaginalis* isolates', *Journal of Clinical Pathology*, 56(7), pp. 542–543. doi: 10.1136/jcp.56.7.542.
- Weber, F. *et al.* (2006) 'Double-Stranded RNA Is Produced by Positive-Strand RNA Viruses and DNA Viruses but Not in Detectable Amounts by Negative-Strand RNA Viruses', *Journal of Virology*, 80(10), pp. 5059–5064. doi: 10.1128/JVI.80.10.5059-5064.2006.
- Wendel, K. A. *et al.* (2002) 'Double-Stranded RNA Viral Infection of *Trichomonas vaginalis* Infecting Patients Attending a Sexually Transmitted Diseases Clinic', *The Journal of Infectious Diseases*, 186(4), pp. 558–561. doi: 10.1086/341832.
- Xu, M.-J. *et al.* (2014) 'Global characterization of microRNAs in *Trichomonas gallinae*', *Parasites & Vectors*, 7(1), p. 99. doi: 10.1186/1756-3305-7-99.
- Yang, P.-C. and Mahmood, T. (2012a) 'Western blot: Technique, theory, and trouble shooting', *North American Journal of Medical Sciences*, 4(9), p. 429. doi: 10.4103/1947-2714.100998.
- Yang, P.-C. and Mahmood, T. (2012b) 'Western blot: Technique, theory, and trouble shooting', *North American Journal of Medical Sciences*, 4(9), p. 429. doi: 10.4103/1947-2714.100998.
- Zang, S. and Lin, R.-J. (2016) 'Northwestern Blot Analysis: Detecting RNA–Protein Interaction After Gel Separation of Protein Mixture', in *Methods Mol Biol*, pp. 111–125. doi: 10.1007/978-1-4939-3591-8_10.
- Zangger, H. *et al.* (2013) 'Detection of Leishmania RNA Virus in Leishmania Parasites', *PLoS Neglected Tropical Diseases*. Edited by J. G. Valenzuela, 7(1), p. e2006. doi: 10.1371/journal.pntd.0002006.

Chapter 3

Validating the presence of dsRNA virus in *Trichomonas gallinae* using Transmission Electron Microscopy

Abstract

In this chapter, we employed several techniques to study the four sub-types of *T. gallinae* (C10, C3, C4 and A1) using Transmission Electron Microscopy (Kraemer *et al.*, 2019) and Scanning Electron Microscopy (Kassem and Gdoura, 2006). The use of different protocols enabled us to observe the change in the *T. gallinae* morphology. The growth of *T. gallinae* was successful and optimized as in Chapter 2.

The TEM grid was used to support thin sections of *T. gallinae* cells of C3, C4, A1 and C10 sub types, where C10 revealed some exosome-like structures. Negative-staining of supernatants under TEM in protocol 2 showed the Exosomes bodies, some of which contained electron dense material of a size consistent with virus particle and may represent the potential RNA virus in C10. The findings showed slower growth of *T. gallinae* sub-type C10. When using SEM the potentially virus-infected *T.gallinae* parasites collected from Socorro dove (identified as sub-type C 10) appeared smaller than those of other strains. The morphology of the subtypes (C4, C3, A10) was studied and flagella, Golgi apparatus, and axostyles were very clear. The findings showed that Subtype C10 size is significantly smaller than subtype C4 ($p=0.0001$). Manual counts of *T. gallinae* cells using Poly L Lysine coverslips were 17 cells/cm², while glass coverslips showed counts of 3 cells/cm², this may indicate the potential presence of virus-like-particles (VLP).

3.1 Introduction

Modern field-emission scanning electron microscopy FE-SEM is a highly powerful and versatile tool for the studies of cell and tissue ultrastructure alone or in combination with the biochemical data provided by fluorescence microscopy. Ultrastructural studies of cells and

tissues are usually performed using transmission electron microscopy (Jia *et al.*), which enables imaging at the highest possible resolution (Lewczuk and Szyrnska, 2021).

Several FE-SEM-based techniques for two-dimensional (2D) and three-dimensional (3D) ultrastructural studies of cells, tissues, organs, and organisms have been developed during the 21st century (Lucas *et al.*, 2012; Koga, Kusumi and Watanabe, 2018). These techniques have created a new era in structural biology and have changed the role of the scanning electron microscope (Kassem and Gdoura, 2006) in biological and medical laboratories. Since the first SEM equipment became commercially available in 1965 (Bogner *et al.*, 2007), these instruments have been used in biological laboratories almost exclusively to obtain topographical information over a large range of magnifications. For example, SEM was used to investigate the interaction of parasitic protozoa that involves the adhesion of the parasite to the host cell, which induces a response from the host cell (de Souza and Attias, 2018).

The early studies of *Trichomonas vaginalis* using both SEM and TEM revealed that the trichomonad body surface appears ruffled and creased with numerous crater-like depressions. Also, it was found that *T. vaginalis* has lattice-like and lamellar structures with unknown functions (Ovcinnikov *et al.*, 1975). Another study that used SEM showed erythrophagocytosis by two different strains of *T. vaginalis* as well as a contact-dependent mechanism relating to the hemolytic activity (Rosset *et al.*, 2002).

The study of the *T. gallinae* structures was similarly valuable, with SEM revealing the morphological features of the trophozoites; the emergence of the anterior flagellum, the structure of the undulating membrane, the position and shape of the pelta, axostyle and posterior flagellum and the pseudocyst forms (Tasca and De Carli, 2003).

Both *T. vaginalis* and *Tritrichomona foetus* are considered as good models for studying early eukaryotic cells which contain other organelles, such as hydrogenosomes and a

complex and elaborate cytoskeleton, which constitutes the mastigont system (Benchimol, 2004).

This chapter aims to fulfil specific aims 2,3 referred in chapter 1 by using the improved resolution of electron microscopy to validate the presence of virus in the isolates identified from the screen (Chapter 1) by visualising any virus particles in infected cells or supernatants. In addition, I investigate phenotypic differences between infected and closely related uninfected *T. gallinae* using newly established protocols for topological visualisation and measurement of the surface area of cells from culture.

Objectives

(1) To use SEM technology, to study the fine structure and morphology of *T. gallinae* subtypes and to look for any difference in size in *T. gallinae* protozoa with/without the presence of RNA-virus.

(2) To use TEM technology, to detect any virus-like particles in *T. gallinae* sub-types.

3.2 Materials and buffers:

The following materials were used during the preparation of *T. gallinae* samples for SEM and TEM study.

- A total of 2% aqueous phosphotungstic acid (adjusting pH to 7.3 using 1N NaOH) was filtered with 0.2µm syringe filter.
- Glutaraldehyde (Thermo Fisher Scientific, Loughborough, UK)
- Sodium phosphate, 0.2M buffer soln., pH 7.4 ((Thermo Fisher Scientific, Loughborough, UK).
- Glass coverslips. 10 m.m ((Thermo Fisher Scientific, Loughborough, UK)).
- poly(L-lysine)- coated glass coverslips (Electron Microscopy Sciences, Hatfield, UK).
- Osmium tetroxide solution (Sigma-Aldrich, St. Louis, USA).

-Sodium cacodylate, 0.1M buffer soln., pH 6.5, ((Thermo Fisher Scientific, Loughborough, UK)

3.3 Electron Microscopy Negative Staining Protocol using TEM

Here when negative staining was applied two protocols were conducted: A] Supernatants and B] Centrifugal filter.

3.3.1 Protocol (1).

A density of 10^5 cells/mL axenic culture of *T. gallinae* was transferred to a 1.5 ml Eppendorf tube and centrifuged for 5min at 1000 rpm, then supernatants were collected into 0.5 ml Eppendorf tubes. The grid was held with forceps and washed briefly by applying a drop (10 μ l) of 0.01% BSA for a few seconds and then drawn off from the edge of the grid with filter paper. A total of 2 μ l of the sample was placed immediately onto the grid and left for 4 minutes. Then drawing off *T. gallinae* from the edge of the grid with filter paper was done. 5-2% phosphotungstic acid was added for 1 minute and drawn off from the edge of the grid with filter paper. The grid was placed directly into the grid box and air-dried overnight before observation. The size and shape of the metal particles were observed by TEM. The JEM-2100 used is a multipurpose, 200 kV analytical electron microscope. Scale bars were added by using ImageJ Ver. 1.53s.

3.3.2 Protocol (2).

A density of 10^5 cells/mL axenic culture of *T. gallinae* was transferred to a 4ml Amicon® Ultra-4 Centrifugal Filter Unit and centrifuged for 15 mins at 6000 rpm (Sigma-Aldrich, St. Louis, USA). The filtrate from the filter produced from one spin column was taken using a pipette. From a second spin column, the ultrafiltrate was removed. The grid was held using forceps and the grid was washed briefly by applying a drop (10 μ l) of 0.01% BSA for 4-5 seconds and then drawing-off from the edge of the grid with filter paper was applied. A total of 2 μ l of the sample was applied immediately onto the grid and left for 3-5 minutes. Then drawing off from the edge of the grid with filter paper was repeated. A total of 4-2% phosphotungstic acid was added for 1 minute and drawn off from the edge of the grid with filter paper. The grid was placed directly into the grid box and air-dried overnight before observation. The size and shape of the metal particles were observed by TEM. Scale bars were added by using ImageJ Ver. 1.53s.

3.4 Using TEM to investigate *T. gallinae* internal morphology

Cells *T. gallinae* were fixed for 24 h with 2.5% glutaraldehyde in 0.1 M cacodylate buffer, pH 7.2. After fixation, the cells were washed in PBS and postfixed for 1 h in 1% OsO₄ containing 0.8% potassium ferrocyanide in 0.1 M cacodylate buffer (pH 7.2), then washed in PBS, dehydrated in acetone, and embedded in Epon-Araldite mixtures which is resin material. Ultrathin sections were stained with uranyl acetate and lead citrate and observed using a Hitachi HT 7800 transmission electron microscope (de Souza *et al.* 2022). This part of the work was carried out in collaboration with Dr. Marlene Benchimol from The Universidade Do Grande Rio, Duque, Brazil.

3.5 Field emission Scanning Electron Microscopy

In this chapter Field emission Scanning Electron Microscopy (FM-SEM) was conducted using a newly purchased a Zeiss Gemini 300 scanning electron microscope. Since I was the first biologist to use the machine protocols for its use on biological samples needed first to be established. To optimise the protocol to be used in the morphological evaluation of *Trichomonas gallinae* subtypes four different protocols each producing successively higher quality images were used:

3.5.1 Protocol (1).

A density of 10⁵ cells/mL axenic culture of *T. gallinae* was transferred to a 1.5 ml Eppendorf tube, then centrifuged for 10 min at 10000 rpm and the media were removed. The pellet was washed with sodium phosphate buffer (SPB) pH 7.4, then fixed with 4 % PFA, centrifuged 10 min at 10000 rpm and the liquid was removed. SPB was then added to the pellet, mixed and 10 µl of the cell suspension was added to the grid, left for 2 minutes then a further 10µl of cell suspension was added. This was left to dry overnight. Cells were observed using a Zeiss Gemini 300 scanning electron microscope. Scale bars were added by using ImageJ Ver. 1.53s.

3.5.2 Protocol (2).

A density of 10⁵ cells/mL axenic culture of *T. gallinae* was transferred to a 1.5 ml Eppendorf tube, then centrifuged for 10 min at 10000 rpm and the media were removed. The pellet was washed with SPB at pH 7.4. then fixed with 4 % PFA, left for 2 hours at room temperature, centrifuged for 10 min at 10000 rpm and the liquid was removed. SPB was added to the pellet,

mixed and 40 µl of the resulting liquid was added to glass coverslips. After fixation, dehydration with a series of ethanol concentrations 50%, 75%, 90% and 100% for 15 minutes was carried out. Cells of *T. gallinae* were coated with a 15-nm thick layer of sputtered gold and observed using a Zeiss Gemini 300 scanning electron microscope (Zeiss). Scale bars were added by using ImageJ Ver. 1.53s.

3.5.3 Protocol (3).

In this protocol, some modifications were made to the fixation. After using coverslips another technical issue emerged involving membrane preservation of the parasites where not much *T. gallinae* appearing under fixation, so glutaraldehyde was used instead of paraformaldehyde.

3.5.4 Protocol (4).

T. gallinae was adhered to poly-L-lysine-coated glass coverslips at a concentration of 10^5 cells/mL and were fixed in 2.5% glutaraldehyde in 0.1 M cacodylate buffer, pH 7.2 for 1 h. Next, the cells were washed in phosphate-buffered saline (PBS) and postfixed for 1 h in 1% Osmium tetroxide solution (OsO₄). Cells were exposed to 25%, 50%, 75%, 100% ethanol for 15 mins at each concentration. Coverslips were left to dry and then coated with a 15-nm thick layer of gold. and observed using a Zeiss Gemini 300 scanning electron microscope (de Souza *et al.*, 2022). Scale bars were added by using ImageJ Ver. 1.53s.

3.6 Cells area comparison of the two sub-types C10 and C4:

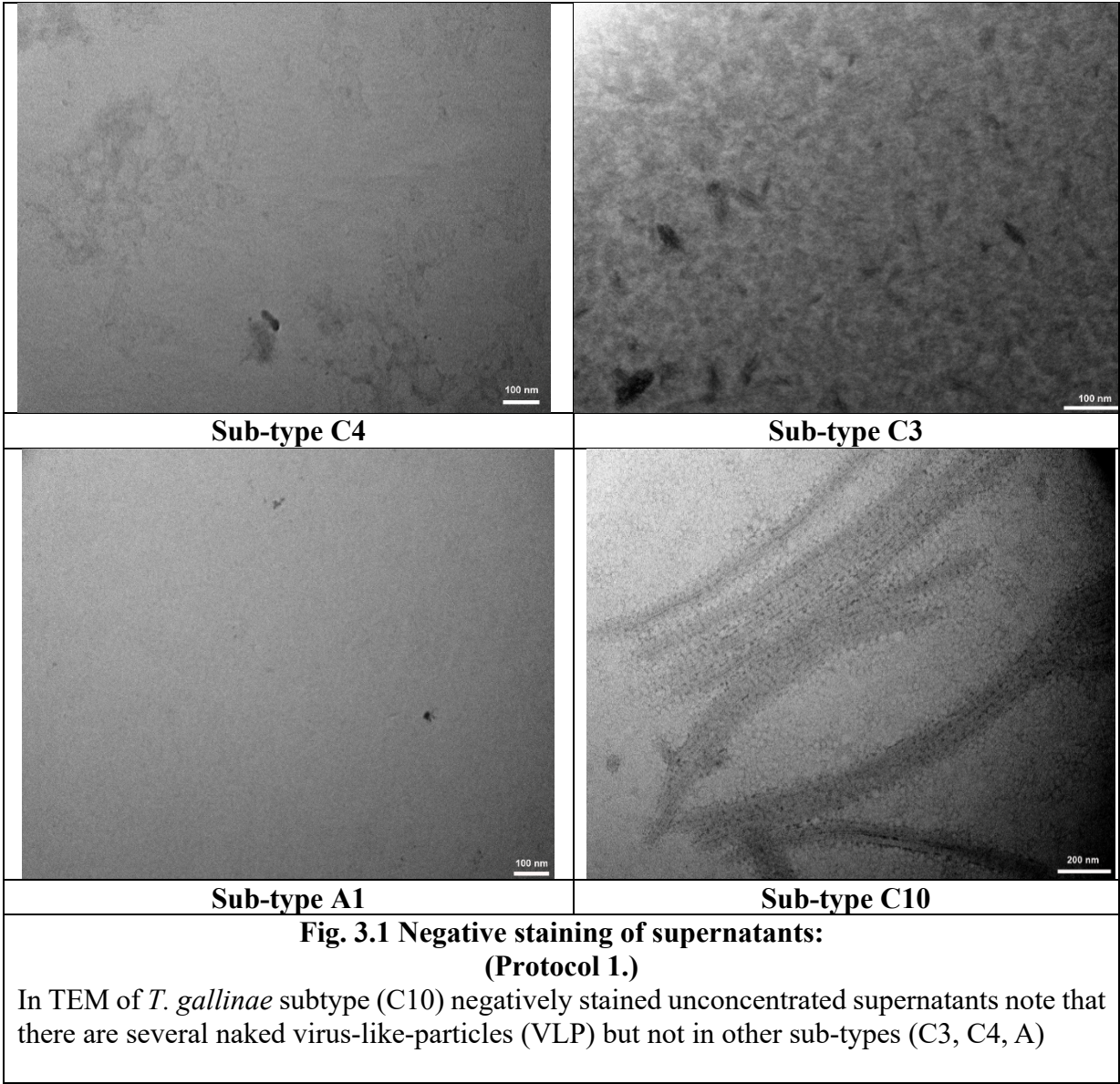
Cells area were measured using ImageJ ver. 1.53s and statistical analysis was conducted using GraphPad Prism 9.4.1. T-tests were used to compare cell area of the two subs-typ.

3.7 Results

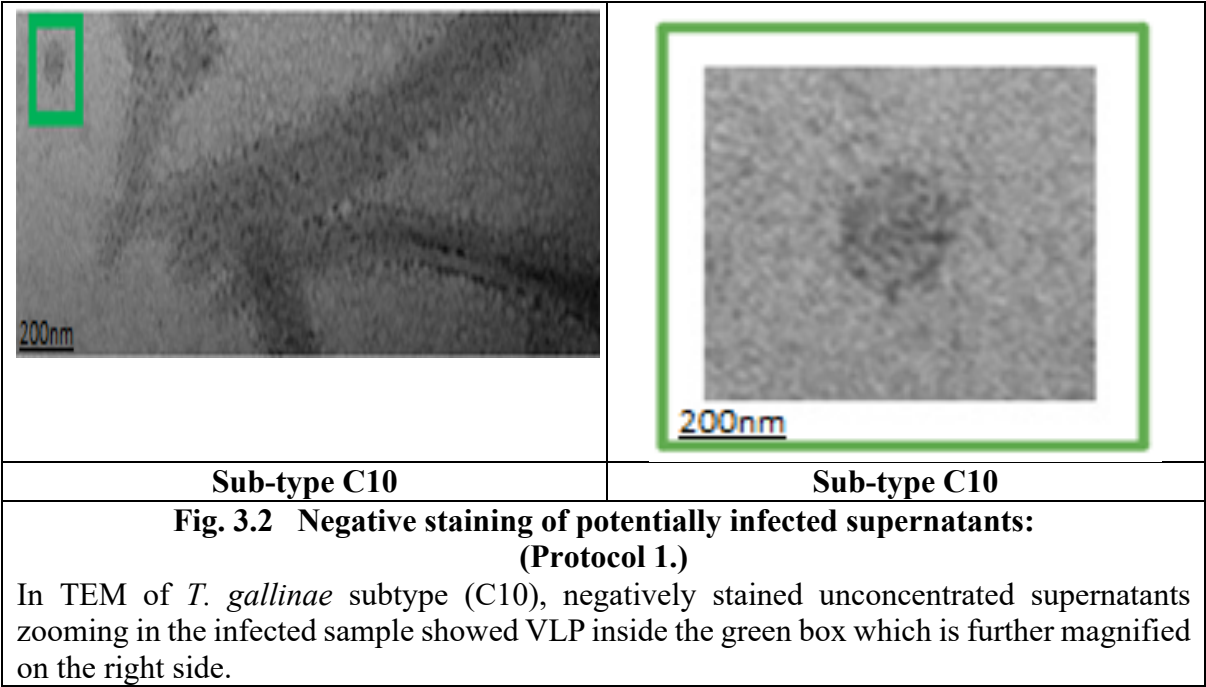
3.7.1 Negative staining supernatants confirms icosahedral virus-like particles (VLPs) in potentially infected C10 isolate:

Naked virus-like-particles (VLP) were observed from unconcentrated supernatants of *T. gallinae*, subtype (C10) negatively stained and visualized by TEM. Enlargement of sub-type C10 and change in its structure indicated the virions in protocol 1 but not in other sub-types (C3, C4, A) (Fig.3.1). Zooming in on the sub-type C10 potentially infected sample showed VLP inside the green box which is further magnified on the right side (Fig.3.2).

Negative staining air dried supernatants:

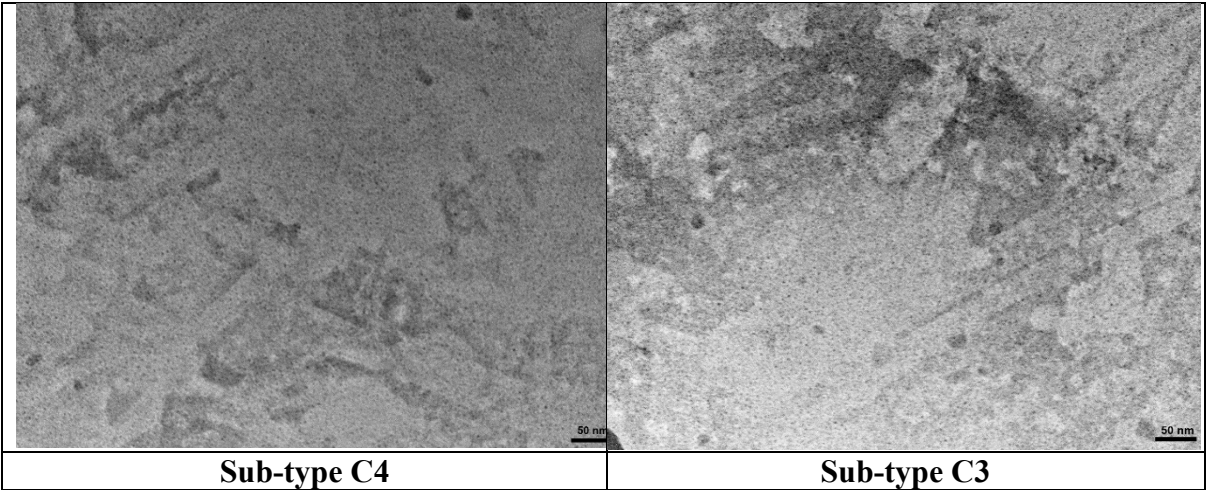


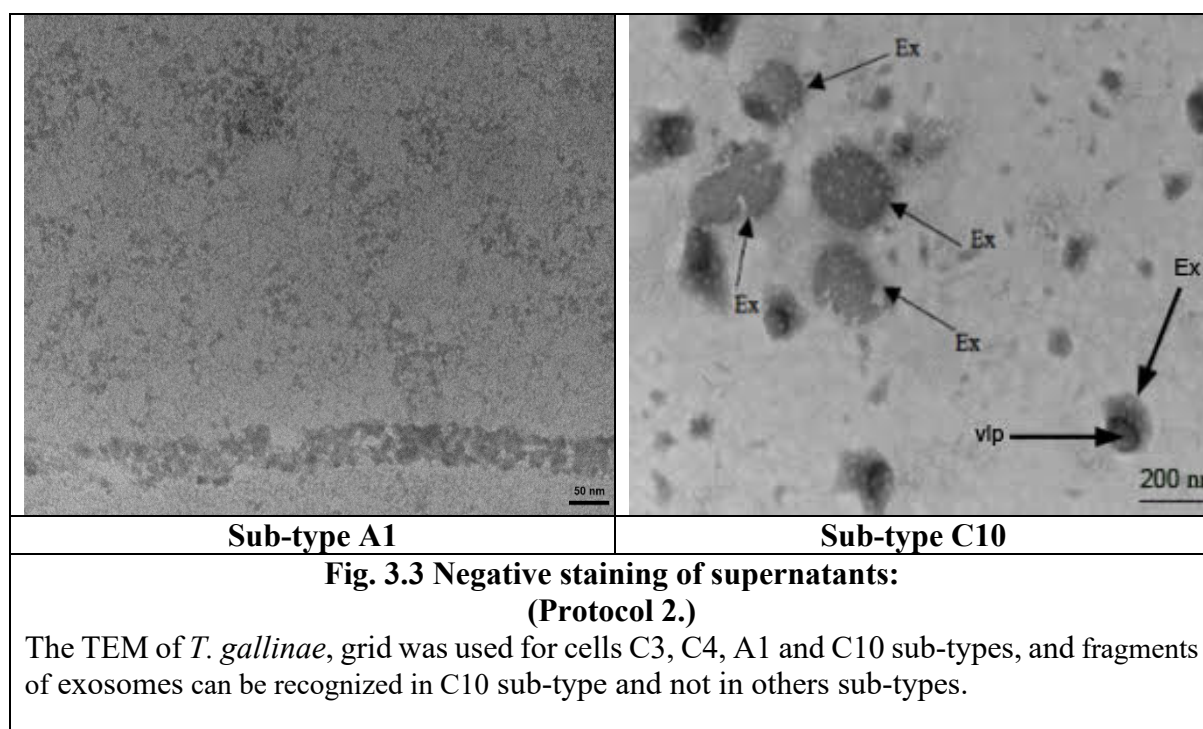
The negative staining of potentially infected supernatants is indicating the virus-like particles in sub-type C10.



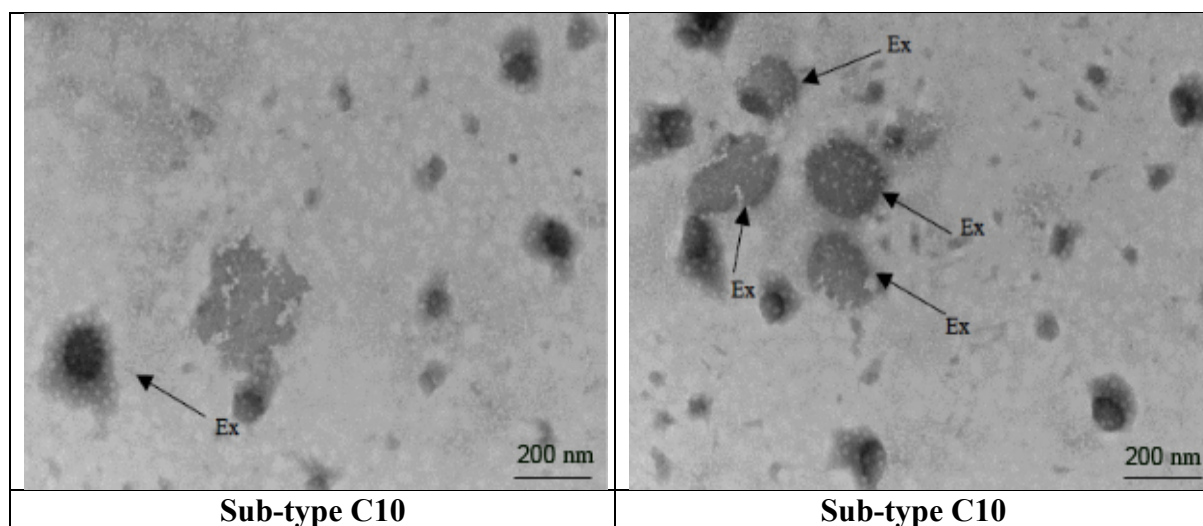
3.7.2 Negative staining of concentrated supernatants reveals abundant exosomes with putative VLPs in infected C10 isolate:

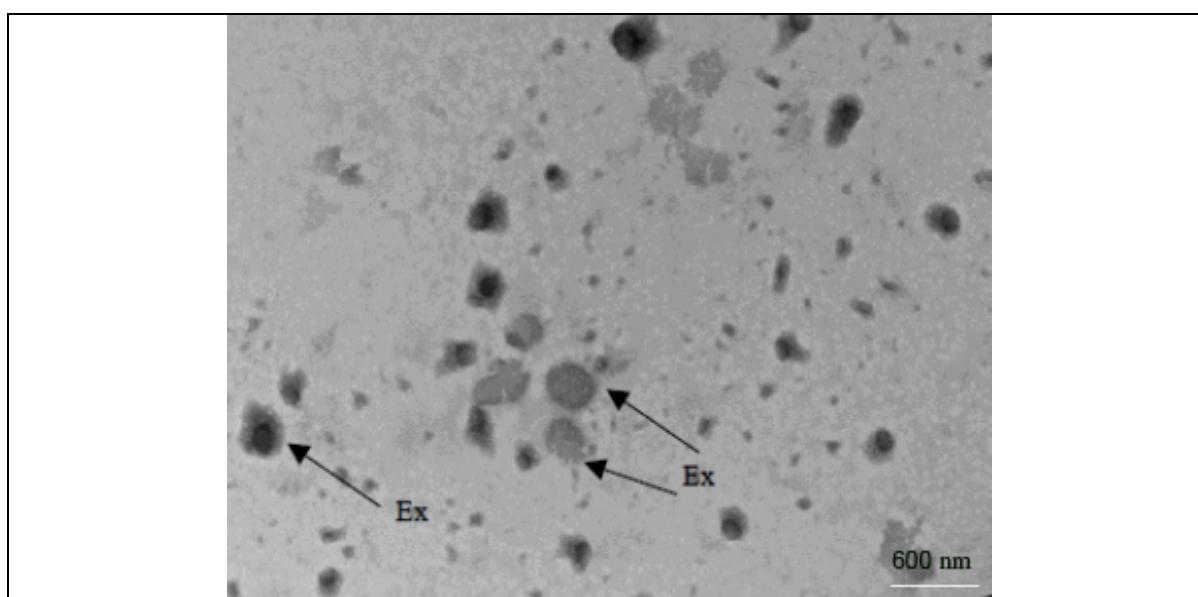
The TEM grid was used to support thin sections of *T. gallinae* cells of C3, C4, A1 and C10 sub-types, where sub-type C10 revealed some structures resembling exosomes as in fig. 3.3.





Negative-staining of supernatants under TEM in protocol 2 showed exosome bodies some of which contained electron dense material of a size consistent with virus particle and may represent the potential RNA virus in sub-type C10 as shown in (Fig 3.4).





Sub-type C10

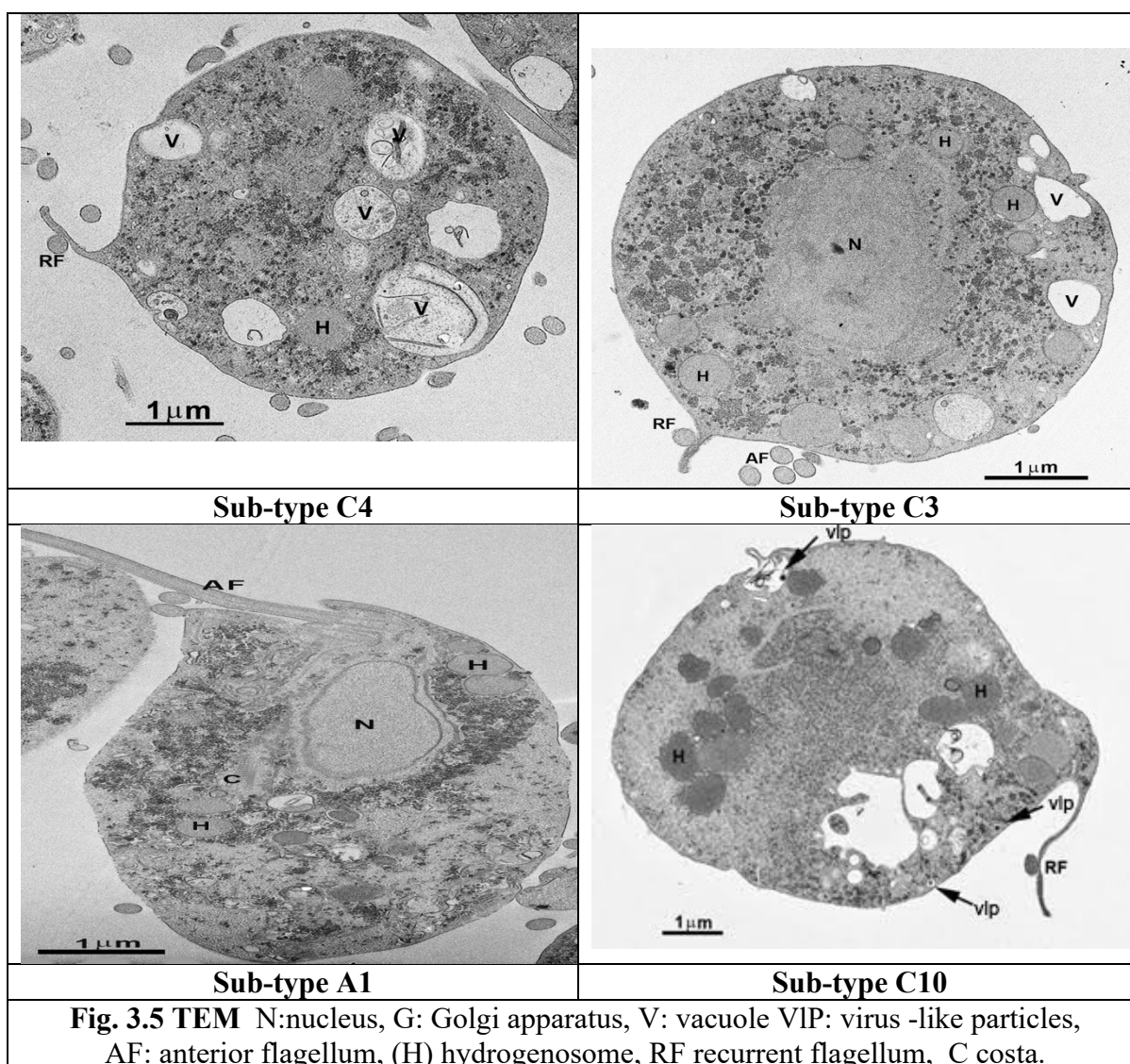
**Fig. 3.4 Negative staining of infected supernatants:
(Protocol 2.) Ex: Exosomes**

In TEM by using negative-staining of supernatants the grids showed exosome bodies some of which contained electron-dense material of a size consistent with virus particles in sub-type C10.

3.7.3 Confirmation of virus like particles using TEM of sectioned *Trichomonas gallinae*

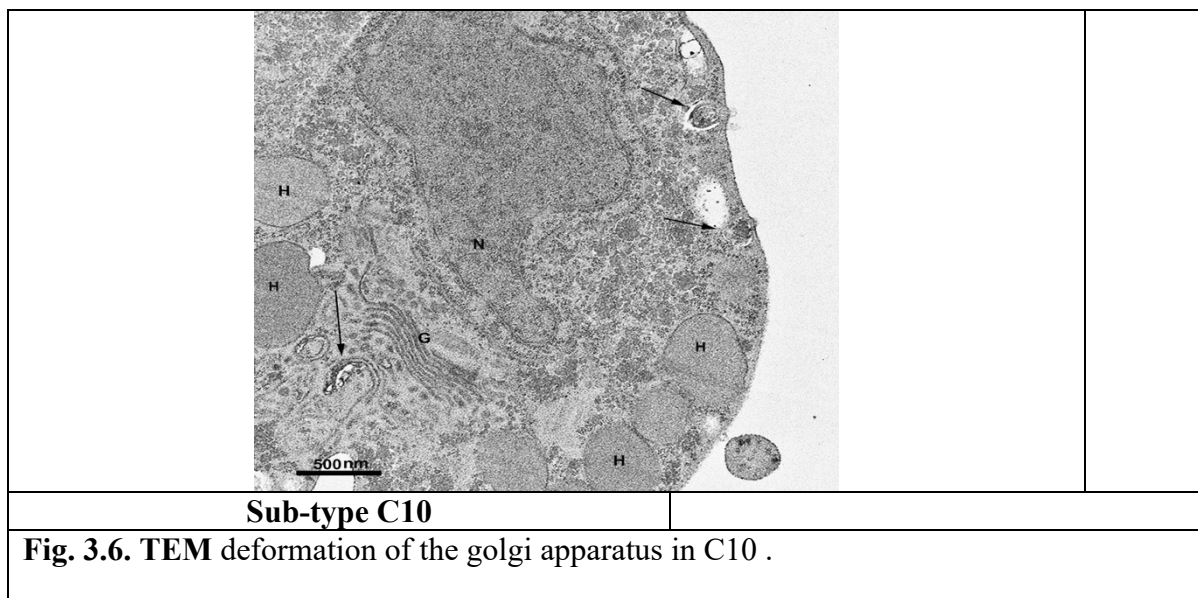
Samples of isolates from the putatively infected sub-type C10 and the C3, C4 and A1 lineages were embedded and sectioned prior to visualizing using TEM. VLP was evident in subtype C10 as shown in Fig. 3.5.

TEM revealed negative control samples of (C4, A1) contained large vacuoles full of membrane - signs of digestion of other cells and autophagy, but no viral particles were observed in Fig.3.5. Sub-type C3 cells have large vacuoles filled with debris created during digestion. TEM was used to reveal details of the morphology of *T. gallinae*; the nucleus, Golgi apparatus, and the vacuoles are shown in Fig.3.5. to Fig.3.6.



TEM showed the detailed structure of Golgi apparatus where the cristae are very clear in addition to the viral like-particles in sub-type 10 (Fig. 3.5).

TEM revealed evidence of plasma membrane disruption alongside granular structures which may be a VLP budding from the cell surface in sub-type C10. Arrows indicate the presence of putative viral particles in the potentially infected cell as well as deformation of golgi (Fig. 3.6).



3.7.4 Scanning Electron Microscope

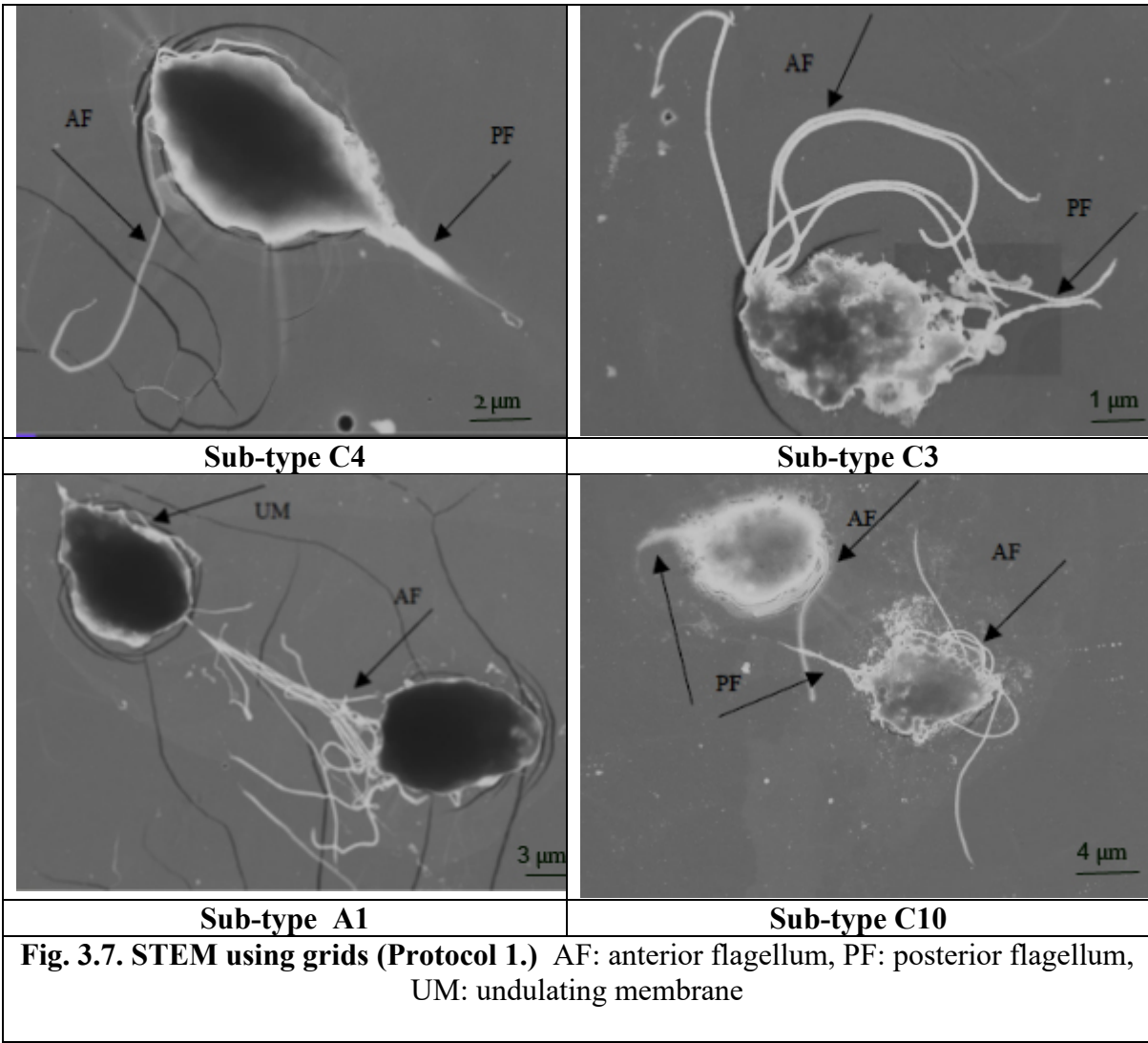
The use of Scanning Electron Microscope provides detailed images of the surfaces of cells and whole organisms. Using grids, the film was cracked around the parasites and this probably occurred during grid preparation for TEM, or the cells were very heavy for the grid. When coverslips were used improved images were obtained and the morphology of *T. gallinae* was very clear.

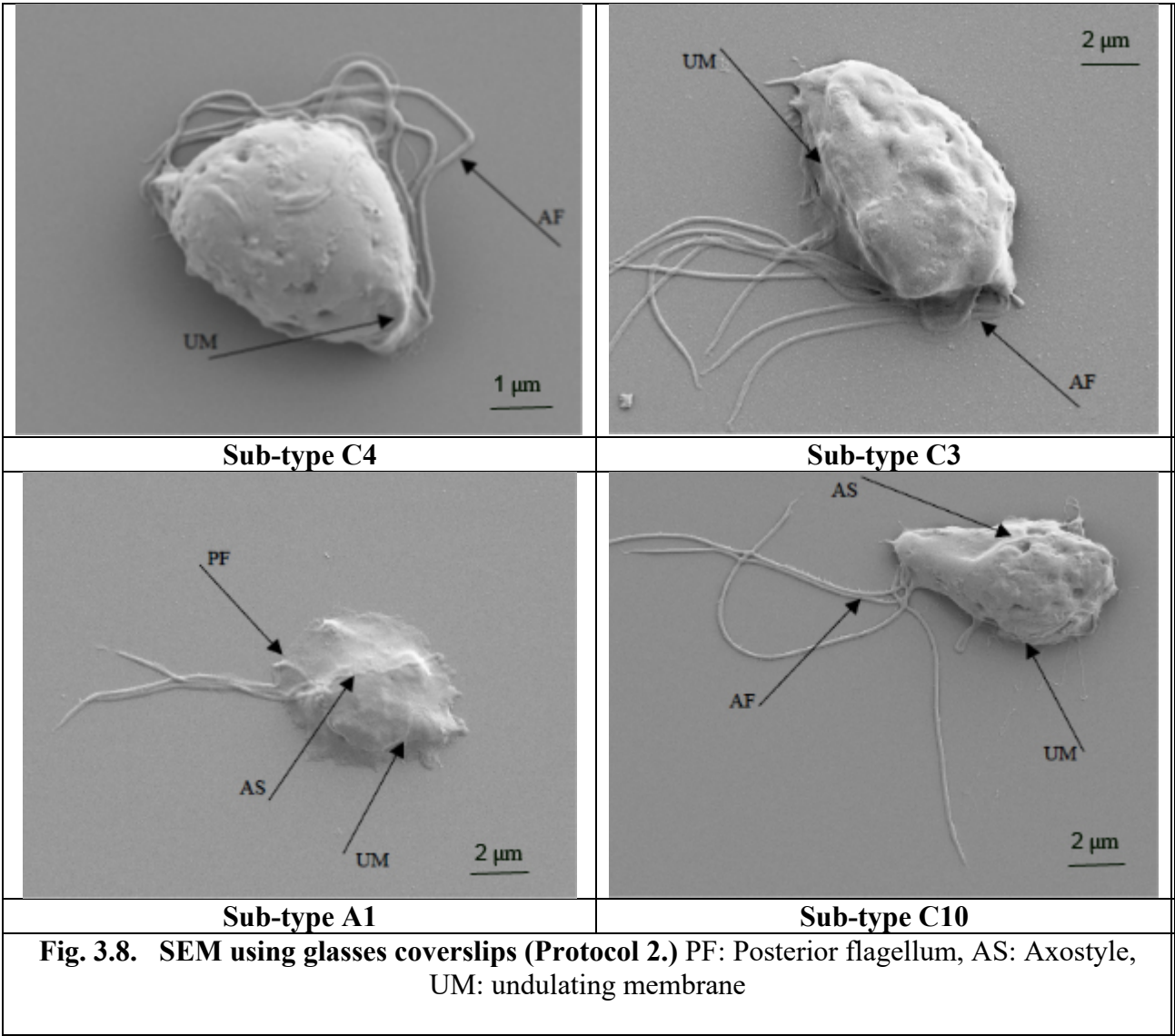
In addition, during the work, the fixative glutaraldehyde was used instead of paraformaldehyde to obtain a better view of the cell membrane. Finally, a poly-L-Lysine coverslip was used to promote cell adhesion to solid substrates by enhancing electrostatic interaction between negatively charged ions of the cell membrane and the slide.

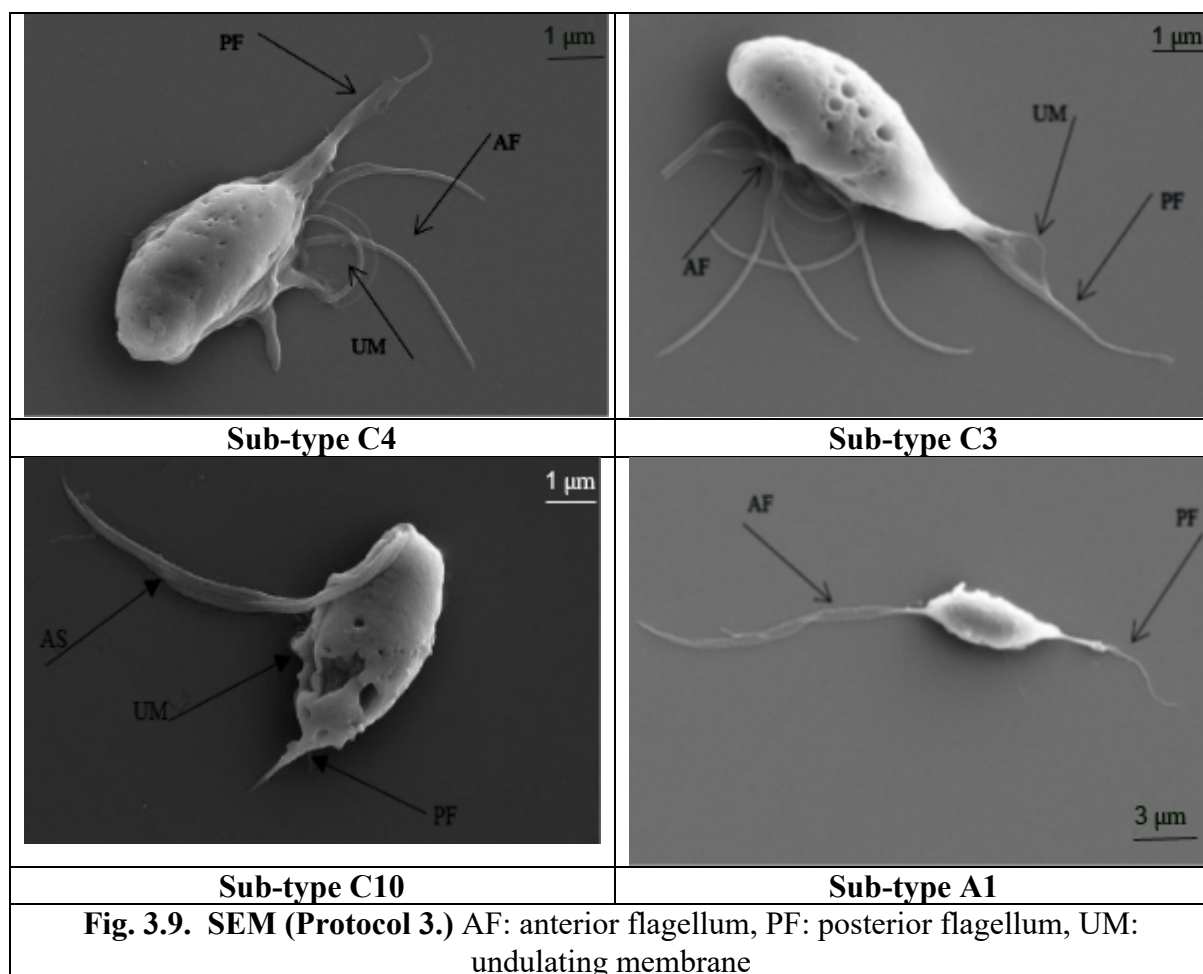
When using SEM the potentially virus-infected *T.gallinae* parasites collected from Socorro dove (identified as sub-type C 10) appeared smaller than sub-type C4. In addition tiny particles that may be viral shedding were noticed on the surface of cells. The features of the morphology of *T. gallinae* (Fig.3.7) such as the spherical/ovoidal appearance of the *T.gallinae* protozoa in samples of the four sub-types C4, C3, A1, C10 (Wood pigeon from Norfolk; Pink pigeon

from Bristol Zoological Gardens; common buzzard from UK Zoological collection; and Socorro dove UK Zoological Collection) were apparent using SEM. The flagella are very obvious both anterior and posterior. The recurrent flagellum is also obvious in the four lineages (Fig.4.1). The undulating membrane was visualized during SEM process in sub-type C3; in addition protozoan cells varied in size (Fig3.14)(Fig. 3.8 (d) in sub-type C10 (d) fig. 3.9) and in sub-type A1 (Fig.3.10).

All *T. gallinae* lineages demonstrated the appearance of the posterior flagellum (Fig.3.7).

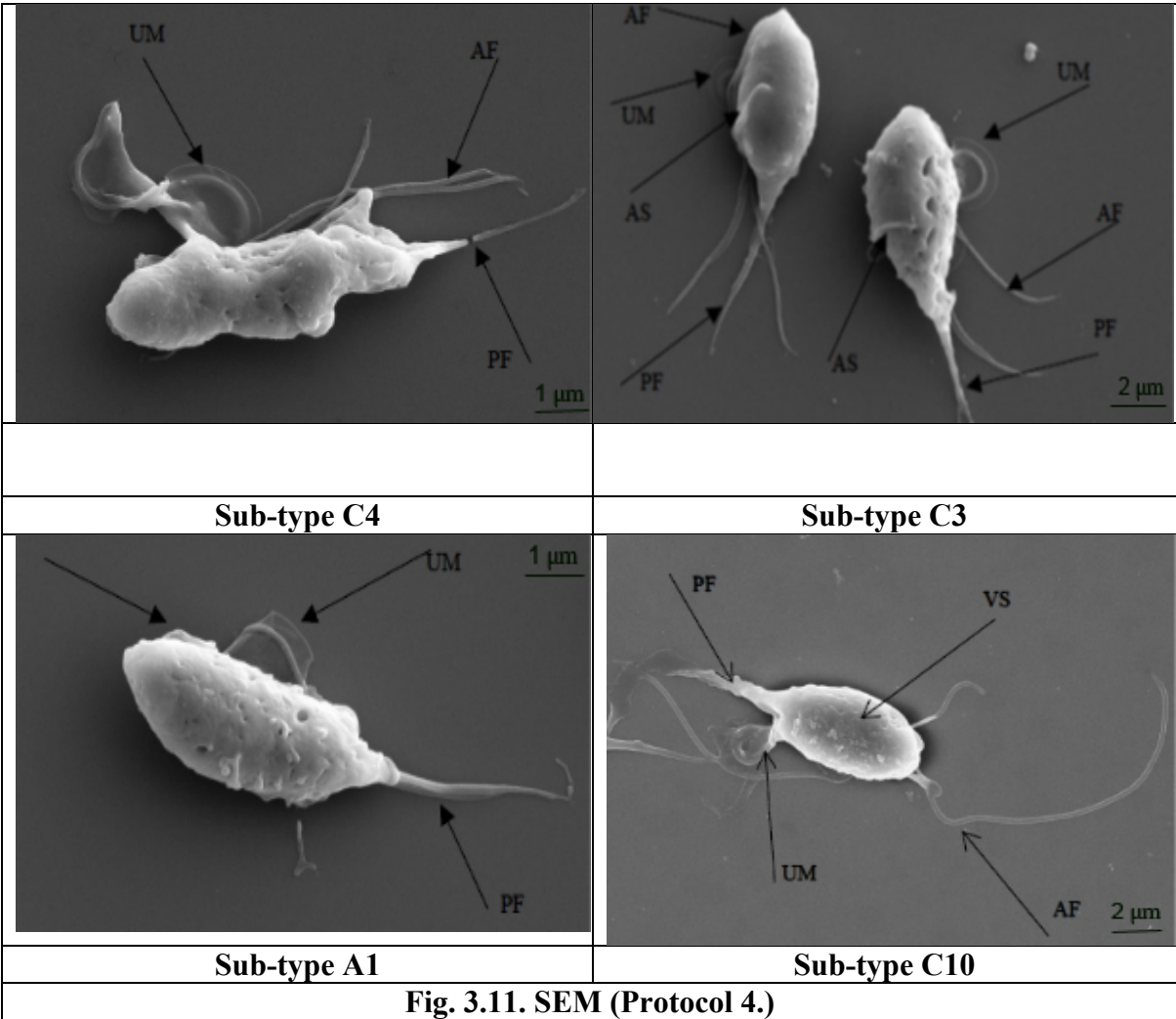
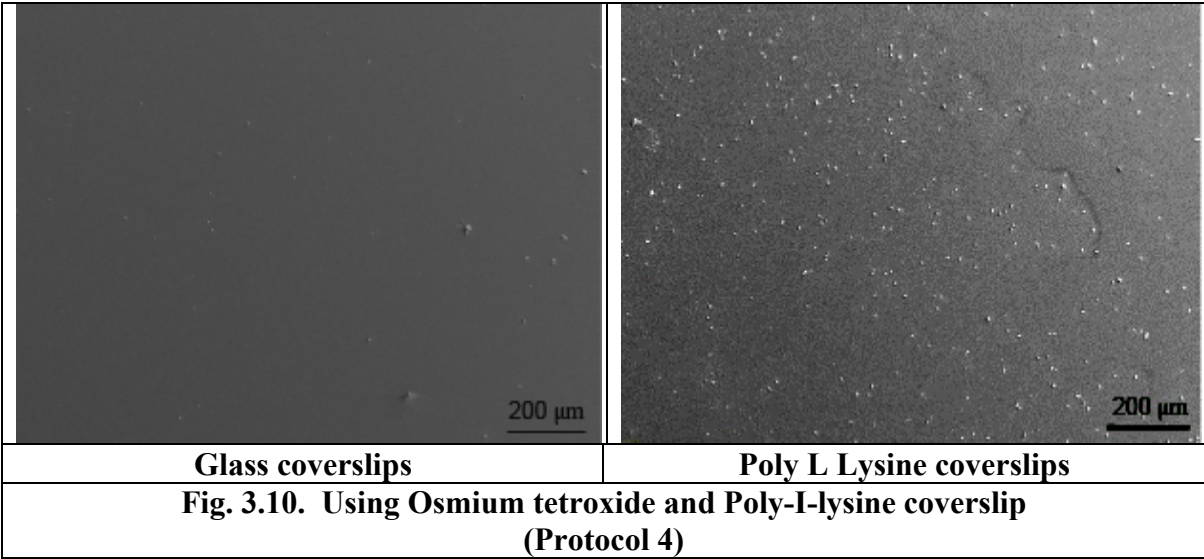






3.7.5 Results for Protocol 4 Using Osmium tetroxide and Poly L lysine coverslip

Poly-L-Lysine helped the *T. gallinae* cells to attach to the surface. The undulating membrane appears more clearly in addition to the flagella (Fig. 3.10 and 3.11). The manual count of *T. gallinae* cells when using Poly L Lysine coverslips was 17 cells/cm² and 3 cells/cm² when using glass coverslips.



Viral shading, tiny particles that might be viral shedding were noticed on the surface of cells as in Fig. 3.12.

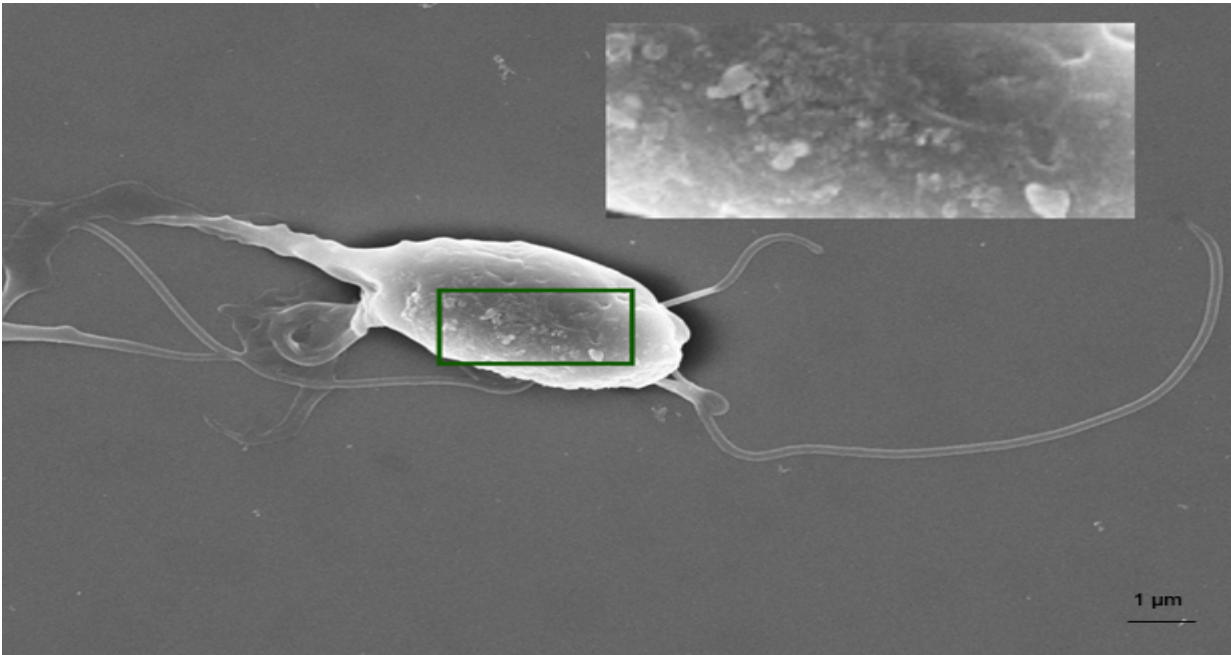
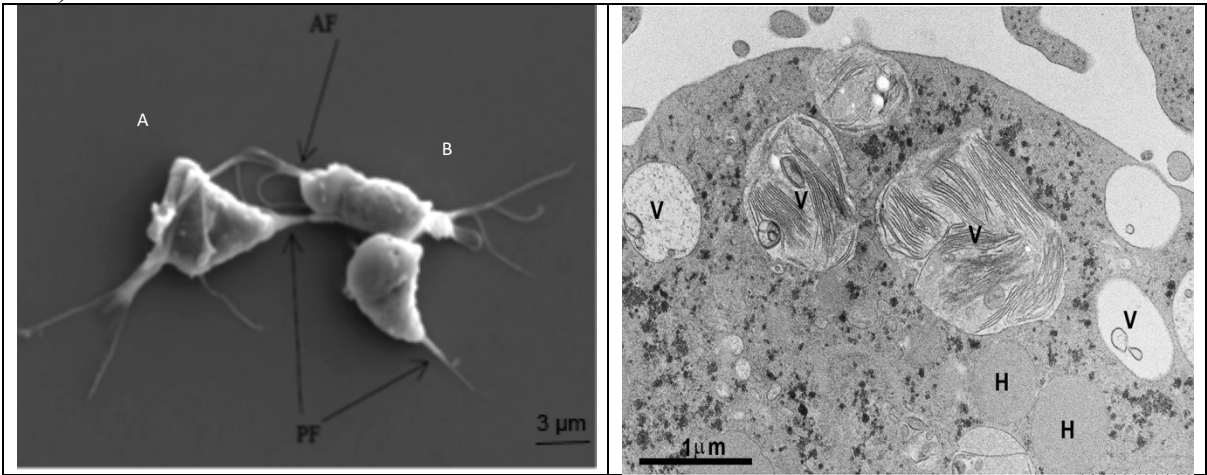


Fig. 3.12. Viral shedding in Sub-type C10

Cell division, phagocytosis of *T. gallinae* is well appeared as in a sample of sub-type C4 (Fig. 3.13).



A. SEM for Sub-type C4	B. TEM for Sub-type C4
<p>Fig. 3.13.</p> <p>A. SEM showing the cell in negative control C4 uninfected sample in process of division{a} and cell in process of phagocytosis{b}.</p> <p>B. TEM shows cell negative control C4 uninfected sample with large vacuoles with signs of digestion and autophagy.</p>	

The findings showed that Subtype C10 is size in terms of surface area is significantly smaller C4 *T.gallinae* (****= P =value< 0.0001)as in fig. 3.14.

Cell Area of *T. gallinae* sub-types using Scanning Electron Microscopy

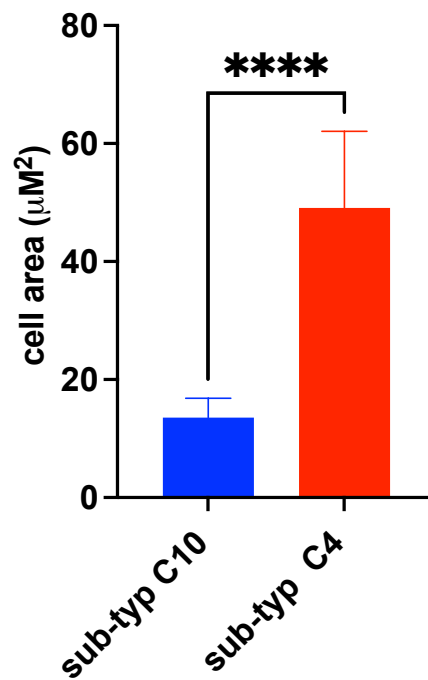


Fig. 3.14. Cell area comparison of the two subtypes C10 and C4.

Unpaired T- test found there was significant difference between the two groups (sub-types C10) and (sub-type C4) (****= P =value< 0.0001, $t=12.27$, $df=38$) ($n=40$).

3.8 Discussion

The current chapter focused on studying the morphology and structure of *T. gallinae* sub-types cultured from four bird species namely sub-type C4 from a common buzzard *Buteo buteo*, sub-type C3 (pink pigeon *Columba nesoenas*), sub-type A1 from a greenfinch *Chloris chloris*, and sub-type C10 from a Socorro dove *Zenaida graysoni*

The rapid advances in EM have given rise to a huge increase in the number of structures routinely being determined to high resolution. Using TEM microscopy revealed the exosomes and virus-like particles in *T. gallinae* cells. However, SEM technique revealed clear morphology and the structure of *T. gallinae* cells to explore the flagella, axostyle and undulating membrane.

Also, using TEM putative virus-like RNA -particles were found in the cells of sub-type C10 using the negative staining of infected supernatant. The presence of RNA-particles is evidenced by the presence of exosomes. Exosomes derived from virus-infected cells may contain various viral components with different functions together with altered protein and RNA cargo of host cell origin (Crenshaw *et al.*, 2018; Saad *et al.*, 2021).

In the current study the presence of exosomes in *T. gallinae* is a crucial indicator of the potential existence of RNA virus. The recent literature recorded that the exosomes shed by *T. vaginalis* virus TVV-infected parasites may represent a potential novel tool for TVV communication within the microenvironment as observed for other viruses (Ju *et al.*, 2021). *Leishmania* virus has a major impact on the protein content of parasite's exosomes via modulation of mRNA translation and exploits *Leishmania* for packing viral particles into the exosomes to be released into the extracellular environment (Atayde *et al.*, 2019). The presence of naked virion and exosomes in the current cultured *T. gallinae* may be a potential cause of the pathogenicity of such parasites in birds.

It was found that *T. vaginalis* cells frequently contain a dsRNA virus named *Trichomonasvirus* (TVV) of *Totiviridae* group that was suspected to modulate the outcome of *T. vaginalis* infection. It was confirmed that TVV particles are released from infected *T. vaginalis* cells to the extracellular environment via sEVs and induced proinflammatory responses in human HaCaT cells (Rada *et al.*, 2022). Considering the high prevalence of TVV harboring *T. vaginalis* clinical isolates, the release of TVV via small exosomal vesicles (sEVs) might be critical for the development of pathologies related directly to trichomoniasis, as well as other pathologies related to modulation of the immune response such as the increased risk of preterm birth, susceptibility to HIV-1, and human papillomaviruses in *T. vaginalis*-infected patients (Rada *et al.*, 2022).

T. gallinae is a potential model for examining and designing future therapeutic drugs in birds. The observed exosomes in the current study should be investigated for RNA-viruses or proteome in future research.

The presence of TVV may alter gene expression in *T. vaginalis* as documented by the increased level of surface immunogenic protein P270, and changes in cysteine proteinase expression profiles in the infected parasite (Alderete, 1999). This may indicate the reason why *T. gallinae* sample of C10 subtype cells contained the virion while other sub-type isolates did not .

The Golgi apparatus is a highly dynamic organelle whose function primarily includes saccule formation and utilization of such saccules in vesicle formation at the opposite face for delivery (James Morré and Mollenhauer, 2007). In general, certain viruses utilize the cellular trafficking and secretory pathway of the ER-Golgi transport system to replicate/release their progeny (Robinson *et al.*, 2018). Poliovirus (PV) utilizes the components of the ADP-ribosylation factor (Arf) family of small GTPases (Belov *et al.*, 2007) and cellular COP-II proteins (Rust *et al.*, 2001) to form membrane-bound replication complex for viral replication, indicating that PV hijacks the components of the cellular secretory pathway for replication.

Metonaviridae (Fontana *et al.*, 2010) and peribunyaviridae (Fontana *et al.*, 2008) hijack the Golgi complex to re-construct it as a viral factory for viral replication. For example, RUBV (Fontana *et al.*, 2010) and BUaNV (Fontana *et al.*, 2008) infections modify cell structural morphology and remodel the Golgi complex as a viral factory during the entire life cycle. Furthermore, host secretory signalling is also crucial for innate and acquired immune responses, such as the exportation of proinflammatory and antiviral cytokines.

To study the fine structure and morphology of *T. gallinae* subtypes and to detect any difference in size in *T. gallinae* protozoa with/without the presence of RNA-virus. We followed four protocols started by using the grid, then sputtered gold, fixation using glutaraldehyde and finally Poly-L-Lysine coated slides to obtain the best quality images of the structure of *T. gallinae*. The improvement in using the protocols obtained clear images of *T. gallinae* external structure including the undulating membrane, axostyle, flagellum and the viral shedding in the infected cells revealed by SEM, wherein we found a statistically significant difference ($p=0.0001$) between potentially infected subtype C10, and uninfected subtype C4.

Similar to our study it was reported that *T. gallinae* shares morphological similarity with other trichomonads and will contribute to a better understanding of spatial relationships of surface structures in this flagellate protozoan (Tasca and De Carli, 2003). Other studies focused on the understanding of the flagella biology in pathogenic trichomonads (Coceres *et al.*, 2021).

In the current study the cell division noticed for *T. galiane* mimics that occurring in *T. vaginalis* where Midlej and Benchimol (2010) observed that cell division only occurs after adhesion. The target cells were detached from the substrate while dozens of trichomonads were clustered around them, inducing cell death by apoptosis (condensed chromatin, membrane blebbing) and necrosis (plasma membrane rupture, organelle liberation). Organelles, nuclei and other cellular debris were promptly phagocytosed by the trichomonads (Midlej and Benchimol, 2010).

TEM was found to be a helpful tool in revealing the internal organelles of *T. gallinae* cells like, Golgi apparatus, vacuoles and the nucleus. Viral particles were also evident when using TEM and plasma membrane disruption and the granular structure. The only sample found hosting the viral particles was sub-type C10 from a Socorro dove *Zenaida graysoni*. The current findings are the first evidence for the presence of viral-RNA in *T. gallinae* cells as protozoan parasites. It's importance may help towards the drug design and designing vehicle's to kill *T. gallinae* cells in the host birds.

SEM was useful to explore more detailed visualization of the three-dimensional organization of the mastigont system *T. foetus* using high resolution (de Andrade Rosa, de Souza and Benchimol, 2013). Also SEM and TEM were used to study *T. vaginalis* organelles like the anterior flagella, the recurrent flagellum, the undulating membrane, and the axostyle and the posterior tip of the cell.

In addition it shows the structure of the cell interior like the nucleus, the Golgi complex, hydrogenosomes, the endoplasmic reticulum, and an endocytic vacuole (Gomes Vancini and Benchimol, 2005).

Based on the categorization of virus families by their genetic material, mode of replication and structural properties, the most extensively characterized viral endosymbionts of protozoan parasites of medical relevance are small, non-enveloped, double-stranded (ds) RNA viruses of the family *Totiviridae* (Hillman and Cohen, 2021).

In Brazil, researchers have shown that *T. gallinae* shares morphological similarities with other trichomonads (Tasca and De Carli, 2003). Another Brazilian study focused on *T. foetus* and using SEM found that human erythrocytes did not adhere to the trophozoites; in contrast, horse erythrocytes adhered to the surface of the parasites and were phagocytosed for up to 90 min (De Carli *et al.*, 2004). Also, SEM confirmed that the trichomonad associated with *Callithrix penicillata* (Black-pencilled marmoset) had four anterior flagella (AF) and one posterior or

recurrent flagellum that was associated with the main body of the cell to form the distinct UM (Dos Santos *et al.*, 2017). A fine-structure study using SEM and TEM found that *T. suis* and *T. foetus* are identical morphologically (Mattos *et al.*, 1997).

T. gallinae isolates studied here under SEM obtained images highlighting the plasticity of the trophozoites (from ovoid to pyriform). The four anterior flagella originated from a common region (the periflagellar canal) located at the apical pole of the cell. From this periflagellar canal, the recurrent flagellum emerges and forms an undulating membrane without a free end portion of the flagellum.

The axostyle projection varied within each isolate, but it was clearly apparent its proportional greater size in the trichomonads from the vulture isolates due to their smaller cell size (Martinez-Diaz *et al.*, 2015). In the present studies *T. gallinae* subtypes C10 and A1 showed the presence of axostyle in the body cell.

In the current study, the virus particles observed using TEM examination were consistent with the results of TEM examination from the *T. vaginalis* ultracentrifugation retentate and negative staining using 2% uranyl acetate and grids (Gerhold *et al.*, 2009).

Scanning electron microscopy was used to study the interphasic *T. foetus* in axenic cultures, where the protozoan presents a teardrop shape, three anterior flagella, and a recurrent one that runs toward the posterior region of the cell (Benchimol, 2004). Direct detection of virus-like particles in *T. foetus* by electron microscopy was possible after the trichomonads were treated with cytoskeleton-affecting chemicals including colchicine, vinblastine, taxol, nocodazole, and griseofulvin (Gomes Vancini and Benchimol, 2005; de Andrade Rosa, de Souza and Benchimol, 2013) used high-resolution scanning electron microscopy of the cytoskeleton of *T. foetus* to determine the three-dimensional organization of the mastigont system, and the presence of new structures, such as the costa accessory filament, and the presence of two groups

of microtubules that form the pelta-axostylar system (de Andrade Rosa, de Souza and Benchimol, 2013).

Identification of viruses in trichomonads by electron microscopy of thin sections is strong evidence that further supports our findings. Where they the same methodology we applied grid and negative staining for the studying of ultrastructure analysis of typical 33-nm dsRNA viruses in *T. vaginalis* (Benchimol *et al.*, 2002).

Following purification, virus-like particles were not observed by transmission electron microscopy, nor were dsRNA segments visualized in agarose gels after electrophoresis of extracted RNA from any of the 21 *T. gallinae* isolates. However, virus particles and dsRNA segments were detected from a previously determined virus-infected *T. vaginalis* isolate as a control using identical purification procedures by (Gerhold *et al.*, 2009). Subsequent reverse transcription-polymerase chain reaction analysis of the dsRNA of the virus in this isolate revealed a novel sequence of the RNA-dependent RNA polymerase gene of *T. vaginalis* viruses (Gerhold *et al.*, 2009).

The virus in the present study represented as virus-like particles (VLPs) in *T. gallinae* and this has been shown as the first evidence of such a relationship between avian parasites and virus. An alternative to using infectious viruses to attack parasites, is their use as VLPs to deliver toxic antiparasitic agents to the parasite host cells. VLPs consist of the assembled viral coat protein subunits that provide empty viral shells which can be loaded with the desired material. The outer surface can also be decorated with targeting moieties, either genetically or chemically (Lomonossoff and Evans, 2011; Steele *et al.*, 2017).

Also there is potential use of the viral symbiont for molecular manipulation of the parasite host. Although some of these viruses appear to have no effect on their parasite hosts, others either have a clear direct negative impact on the parasite or may, in fact, contribute to the virulence of parasites for humans (Barrow *et al.*, 2020).

3.9 References

- Alderete, J. F. (1999) 'Iron Modulates Phenotypic Variation and Phosphorylation of P270 in Double-Stranded RNA Virus-Infected *Trichomonas vaginalis*', *Infection and Immunity*. Edited by V. A. Fischetti, 67(8), pp. 4298–4302. doi: 10.1128/IAI.67.8.4298-4302.1999.
- de Andrade Rosa, I., de Souza, W. and Benchimol, M. (2013) 'High-resolution scanning electron microscopy of the cytoskeleton of *Trichomonas foetus*', *Journal of Structural Biology*, 183(3), pp. 412–418. doi: 10.1016/j.jsb.2013.07.002.
- Atayde, V. D. *et al.* (2019) 'Exploitation of the Leishmania exosomal pathway by Leishmania RNA virus 1', *Nature Microbiology*, 4(4), pp. 714–723. doi: 10.1038/s41564-018-0352-y.
- Barrow, P. *et al.* (2020) 'Viruses of protozoan parasites and viral therapy: Is the time now right?', *Virology Journal*, 17(1), p. 142. doi: 10.1186/s12985-020-01410-1.
- Belov, G. A. *et al.* (2007) 'Hijacking Components of the Cellular Secretory Pathway for Replication of Poliovirus RNA', *Journal of Virology*, 81(2), pp. 558–567. doi: 10.1128/JVI.01820-06.
- Benchimol, M. (2004) 'Trichomonads under Microscopy', *Microscopy and Microanalysis*, 10(5), pp. 528–550. doi: 10.1017/S1431927604040905.
- Benchimol, M., Chang, T.-H. and Alderete, J. F. (2002) 'Visualization of new virus-like-particles in *Trichomonas vaginalis*', *Tissue and Cell*, 34(6), pp. 406–415. doi: 10.1016/S0040816602000757.
- Bogner, A. *et al.* (2007) 'A history of scanning electron microscopy developments: Towards "wet-STEM" imaging', *Micron*. Oxford, England, 38(4), pp. 390–401. doi: 10.1016/j.micron.2006.06.008.
- De Carli, G. A., Tasca, T. and Borges, F. P. (2004) '*Trichomonas foetus* : a scanning electron microscopy study of erythrocyte adhesion associated with hemolytic activity', *Veterinary Research*, 35(1), pp. 123–130. doi: 10.1051/vetres:2003042.
- Coceres, V. M. *et al.* (2021) 'Ultrastructural and Functional Analysis of a Novel Extra-Axonemal Structure in Parasitic Trichomonads', *Frontiers in Cellular and Infection Microbiology*, 11, p. 757185. doi: 10.3389/fcimb.2021.757185.
- Crenshaw, B. J. *et al.* (2018) 'Exosome Biogenesis and Biological Function in Response to Viral Infections', *The Open Virology Journal*, 12(1), pp. 134–148. doi: 10.2174/1874357901812010134.
- Fontana, J. *et al.* (2008) 'The unique architecture of Bunyamwera virus factories around the Golgi complex', *Cellular Microbiology*, 10(10), pp. 2012–2028. doi: 10.1111/j.1462-5822.2008.01184.x.
- Fontana, J. *et al.* (2010) 'Three-dimensional structure of Rubella virus factories', *Virology*, 405(2), pp. 579–591. doi: 10.1016/j.virol.2010.06.043.
- Gerhold, R. W. *et al.* (2009) 'Examination for double-stranded RNA viruses in *Trichomonas gallinae* and identification of a novel sequence of a *Trichomonas vaginalis* virus', *Parasitology Research*, 105(3), pp. 775–779. doi: 10.1007/s00436-009-1454-5.

- Gomes Vancini, R. and Benchimol, M. (2005) 'Appearance of virus-like particles in *Trichomonas foetus* after drug treatment', *Tissue and Cell*, 37(4), pp. 317–323. doi: 10.1016/j.tice.2005.03.009.
- Hillman, B. I. and Cohen, A. B. (2021) 'Totiviruses (totiviridae', in *Encyclopedia of Virology*, pp. 648–657.
- James Morré, D. and Mollenhauer, H. H. (2007) 'Microscopic Morphology and the Origins of the Membrane Maturation Model of Golgi Apparatus Function', in *Int Rev Cytol*, pp. 191–218. doi: 10.1016/S0074-7696(07)62004-X.
- Ju, Y. *et al.* (2021) 'The Role of Exosome and the ESCRT Pathway on Enveloped Virus Infection', *International Journal of Molecular Sciences*, 22(16), p. 9060. doi: 10.3390/ijms22169060.
- Kassem, H. H. and Gdoura, N. K. M. (2006) 'Hydatidosis in camels (*Camelus dromedarius*) slaughtered at Sirt Abattoir, Libya.', *Journal of the Egyptian Society of Parasitology*, 36(2 Suppl), pp. 1–10.
- Koga, D., Kusumi, S. and Watanabe, T. (2018) 'Backscattered electron imaging of resin-embedded sections', *Microscopy*, 67(4), pp. 196–206. doi: 10.1093/jmicro/dfy028.
- Kraemer, M. U. G. *et al.* (2019) 'Utilizing general human movement models to predict the spread of emerging infectious diseases in resource poor settings', *Scientific Reports*, 9(1), p. 5151. doi: 10.1038/s41598-019-41192-3.
- Lewczuk, B. and Szyryńska, N. (2021) 'Field-Emission Scanning Electron Microscope as a Tool for Large-Area and Large-Volume Ultrastructural Studies', *Animals*, 11(12), p. 3390. doi: 10.3390/ani11123390.
- Lomonossoff, G. P. and Evans, D. J. (2011) 'Applications of Plant Viruses in Bionanotechnology', in *Curr Top Microbiol Immunol*, pp. 61–87. doi: 10.1007/82_2011_184.
- Lucas, M. S. *et al.* (2012) 'Bridging Microscopes', in *Methods Cell Biol*, pp. 325–356. doi: 10.1016/B978-0-12-416026-2.00017-0.
- Martínez-Díaz, R. A. *et al.* (2015) 'Trichomonas gypaetini n. sp., a new trichomonad from the upper gastrointestinal tract of scavenging birds of prey', *Parasitology Research*, 114(1), pp. 101–112. doi: 10.1007/s00436-014-4165-5.
- Mattos, A. *et al.* (1997) 'Fine structure and isozymic characterization of trichomonadid protozoa', *Parasitology Research*, 83(3), pp. 290–295. doi: 10.1007/s004360050249.
- MIDDLEJ, V. and BENCHIMOL, M. (2010) 'Trichomonas vaginalis kills and eats – evidence for phagocytic activity as a cytopathic effect', *Parasitology*, 137(1), pp. 65–76. doi: 10.1017/S0031182009991041.
- Ovcinnikov, N. M. *et al.* (1975) 'Further studies of Trichomonas Vaginalis with transmission and scanning electron microscopy.', *Sexually Transmitted Infections*, 51(6), pp. 357–375. doi: 10.1136/sti.51.6.357.
- Rada, P. *et al.* (2022) 'Double-Stranded RNA Viruses Are Released From Trichomonas vaginalis Inside Small Extracellular Vesicles and Modulate the Exosomal Cargo', *Frontiers in Microbiology*, 13, p. 893692. doi: 10.3389/fmicb.2022.893692.

- Robinson, M. *et al.* (2018) 'Viral journeys on the intracellular highways', *Cellular and Molecular Life Sciences*, 75(20), pp. 3693–3714. doi: 10.1007/s00018-018-2882-0.
- Rosset, I. *et al.* (2002) 'Scanning electron microscopy in the investigation of the in vitro hemolytic activity of *Trichomonas vaginalis*', *Parasitology Research*, 88(4), pp. 356–359. doi: 10.1007/s00436-001-0555-6.
- Rust, R. C. *et al.* (2001) 'Cellular COPII Proteins Are Involved in Production of the Vesicles That Form the Poliovirus Replication Complex', *Journal of Virology*, 75(20), pp. 9808–9818. doi: 10.1128/JVI.75.20.9808-9818.2001.
- Saad, M. H. *et al.* (2021) 'A Comprehensive Insight into the Role of Exosomes in Viral Infection: Dual Faces Bearing Different Functions', *Pharmaceutics*, 13(9), p. 1405. doi: 10.3390/pharmaceutics13091405.
- dos Santos, C. S. *et al.* (2017) 'Morphological, ultrastructural, and molecular characterization of intestinal tetratrichomonads isolated from non-human primates in southeastern Brazil', *Parasitology Research*, 116(9), pp. 2479–2488. doi: 10.1007/s00436-017-5552-5.
- de Souza, T. G. *et al.* (2022) 'Effects of amiodarone, amioder, and dronedarone on *Trichomonas vaginalis*', *Parasitology Research*, 121(6), pp. 1761–1773. doi: 10.1007/s00436-022-07521-8.
- de Souza, W. and Attias, M. (2018) 'New advances in scanning microscopy and its application to study parasitic protozoa', *Experimental Parasitology*, 190, pp. 10–33. doi: 10.1016/j.exppara.2018.04.018.
- Steele, J. F. C. *et al.* (2017) 'Synthetic plant virology for nanobiotechnology and nanomedicine', *WIREs Nanomedicine and Nanobiotechnology*, 9(4). doi: 10.1002/wnan.1447.
- Tasca, T. and De Carli, G. A. (2003) 'Scanning electron microscopy study of *Trichomonas gallinae*', *Veterinary Parasitology*, 118(1–2), pp. 37–42. doi: 10.1016/j.vetpar.2003.09.009.

Chapter 4

***Trichomonas gallinae* virus TGV-1 is most closely related to TVV-1.**

Abstract

The current study has used transcriptomics to confirm the presence of a novel virus in *T. gallinae*. The sample of C10 subtype investigated expresses viral transcripts at a high level which were absent in the three other isolates (of subtypes C3, C4 and A1) for which transcriptomes were also obtained. RNA-seq technology was used to sequence cDNA generated from total RNA samples. The *Trichomonas gallinae* virus (TGV) dependent RNA polymerase and capsid proteins sequences were compared and showed the high similarity with *T. vaginalis* virus of the *Totiviridae* family of dsRNA viruses. In a phylogenetic (Maximum Likelihood - ML) tree generated by translating the polymerase and capsid sequences and concatenating them, the new *T. gallinae* virus (TGV1) clustered with but was clearly segregated from the TVV1 family and did not branch basally to the TVV virus clade raising the possibility that *T. vaginalis* may itself not be a monophyletic group as these viruses may have been introduced to *T. vaginalis* from founding events. As with other Trichomonad viruses, the TGV1 genome consists only of capsid and polymerase. As with other TVV viruses there is no gap between the two genes which actually with overlap each other. A Neighbour-Net analysis indicates that the TGV 1 isolate and TVV isolates appear to have evolved independently with little evidence for genetic exchange between the major lineages (TVV1, TGV1, TVV2, TVV3, TVV4) although some genetic exchange may have occurred between viruses within TVV lineages. Strong similarities in the capsid proteins between TGG and TVV lineages enabled the design of primers and epitopes to the conserved regions which may enable PCR and mAb based diagnosis of the virus in infections with avian trichomoniasis.

4.1 Introduction

The presence of disease course modifying viruses in trichomonads raises substantial questions for the study of *Trichomonas gallinae*. It has been proposed for *Trichomonas vaginalis*, that the presence of the virus far from disables infection, but actually contributes to disease pathogenesis by acting as an adjuvant, promoting inflammation and making infected strains more, rather than less, virulent.

4.1.1 A brief history of transcriptomics

‘Transcriptomes’ is a term whose first use, to signify an entire set of transcripts, has been attributed to Charles Auffray (Pietu *et al.*, 1999). The term transcriptome is now widely understood to mean the complete set of all the ribonucleic acid (Hepatitis, Immunology and Viral Diseases Panels, USJCMSP AIDS, ARI *et al.*, 2019) molecules expressed in some given entity, such as a cell, tissue, or organism (Morozova, Hirst and Marra, 2009; Wolf, 2013).

The transcriptome can be conceptualized as the total set of RNA species, including coding and noncoding RNAs (ncRNAs), that are transcribed in a given cell type, tissue, or organ at any given time under normal physiological or pathological conditions. This concept was then applied to the study of large-scale gene expression in the yeast *S. cerevisiae* (Velculescu *et al.*, 1997; Dujon, 1998; Piétu *et al.*, 1999).

However, due to the importance of messenger RNAs (mRNAs), which represent protein-coding RNAs, the term transcriptome is often associated with this set of RNAs. Researchers later coined the analogous term miRNome to refer to the total set of mi(cro)RNAs. The proteome is conceptually similar to the transcriptome and refers the total set of proteins translated in a given cell type, tissue, or organ at any given time during normal physiological or pathological conditions (Passos, 2022).

Although the first method used to analyze transcriptional gene expression emerged in 1980 with the development of Northern blot hybridization (Wreschner and Hersberg 1984), this method was not, and still is not, capable of being performed on a large scale, and thus cannot be considered a transcriptome approach. In 1990s, the human genome project, through partially automated DNA sequencing, had the ambition to identify, characterize, and analyse all of the genes in the human genome (Watson 1990; Cantor 1990). This revolutionary approach led to thousands of entries that were constructed via the tag-sequencing of randomly selected cDNA clones (Adams *et al.*, 1991, 1992, 1993; Okubo *et al.*, 1992; Takeda *et al.*, 1993).

As mentioned above, the first transcriptome analysis was performed on large nylon arrays using high-density filters containing colony cDNA (or PCR products) followed by quantitative measurements of the amount of hybridized probe at each spot. A common platform used spotted cDNA arrays, where cDNA clones representing genes were robotically spotted on the support surface either as bacterial colonies or as PCR products. These “macroarrays,” or high-density filters, were made on nylon membranes measuring approximately 10 cm². Although this is now considered a dated approach, it was nonetheless effective enough to test sets of hundreds, or even a few thousand, genes (Passos, 2022).

The development of high-throughput techniques for concurrently measuring the expression levels of thousands of genes, mostly based on DNA microarrays (Bumgarner, 2013) or on RNA sequencing (RNA-seq) techniques (Cockrum *et al.*, 2020), allowed monitoring cell’s transcriptional activity across multiple conditions, opening broad perspectives for functional genomics (Williams *et al.*, 2021).

The past two decades have seen the development of methods that allow for a nearly complete analysis of the transcriptome, in the form of microarrays and, more recently, RNA-Seq, which are the most popular technologies used in genome-scale transcriptional studies. These high-throughput gene expression analysis systems generate large and complex datasets, and the development of computational methods to obtain biological information from the generated data has been the primary challenge in bioinformatics analysis (Fig 4.1) (Passos, 2022).

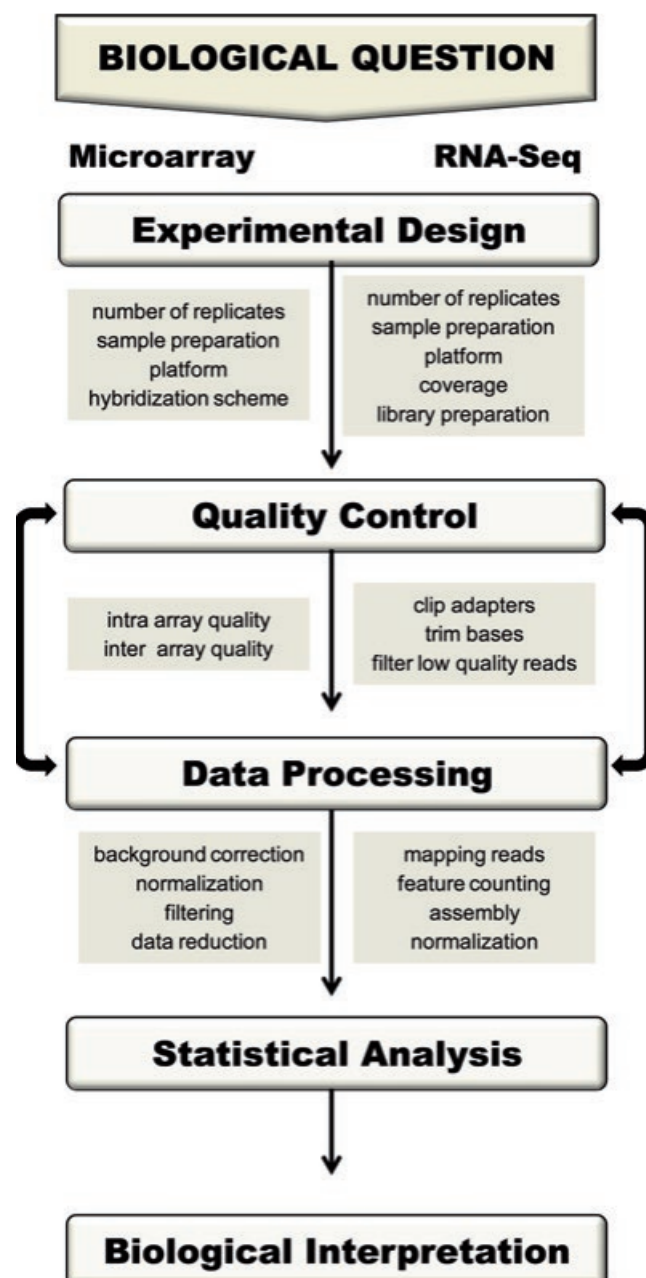


Fig. 4.1 An overview of the steps in a typical gene expression microarray or RNA-Seq experiment (Passos, 2022).

At its most basic, a transcriptome can encompass all cellular RNAs in the sample studied. It may include data on their transcription and expression levels, function, location, trafficking, and degradation. It may include the structures of transcripts and their parent genes with regard to start sites, 5' and 3' end sequences, splicing patterns, and post-transcriptional modifications (Wang *et al.*, 2009). Transcriptomics covers all types of transcripts, including messenger RNAs(mRNAs), microRNAs (miRNAs), and different types of long noncoding RNAs (lncRNAs).

4.1.2 RNAseq

Recent years have seen the emergence of RNA sequencing (RNA-seq), which encompasses a variety of next-generation sequencing techniques for determining the sequence and potentially also the levels of RNA transcripts (Nagalakshmi *et al.*, 2008; Chu and Corey, 2012). Only the more abundant transcripts are usually detected by traditional approaches like EST sequencing whereas RNA-seq, when employed with adequate sequencing depth (100–1000 reads per base pair of a transcript), is capable of delivering an almost complete capture of a transcriptome (Martin and Wang, 2011). Furthermore, RNA-seq allows for a full genome-wide assessment of transcripts, with a wide dynamic range of expression levels (Nookaew *et al.*, 2012).

As summarized in the left panel of Figure 4.2, most RNA-seq approaches to date have used indirect methodologies in which extracted mRNAs or total RNAs are first converted into a library of cDNAs containing sequencing adapters. A high-throughput DNA sequencing technology is then used to sequence the cDNA fragments from one end or both ends, rendering an output which is comprised of short sequences (Metzker, 2010).

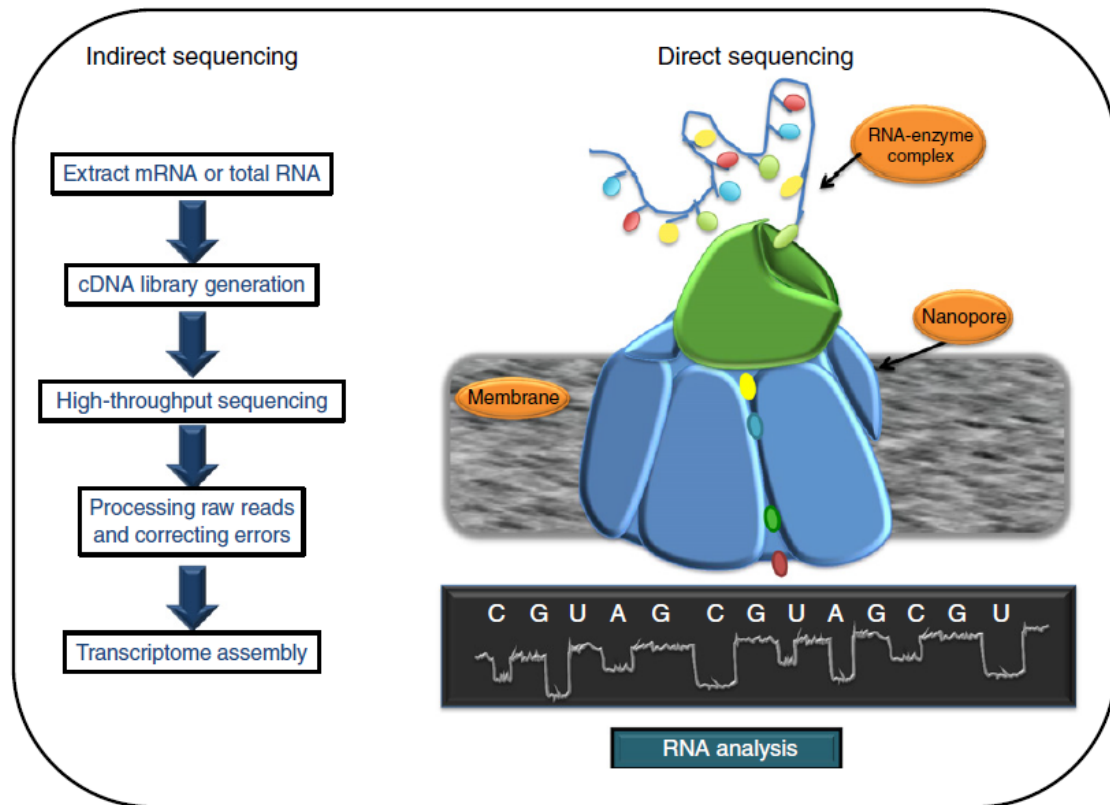


Figure 4.2 Indirect and direct approaches to RNA-seq. Early high-throughput approaches to RNA-seq have utilized cDNA (left) but new alternatives such as nanopore sequencing (right) can sequence RNA directly. In one implementation of this strategy, the RNA strand binds to an enzyme or other immobilizing molecule (green) which ratchets the RNA one base at a time through a molecular nanopore channel (Kuhlmann *et al.*, 2017) embedded in a membrane. The nanopore conducts an electrical current across the membrane. As each RNA base passes through the nanopore it disrupts the current in a characteristic way, allowing the base to be identified (Adopted from (Bettencourt *et al.*, 2016)).

With the rapid evolution of assembly algorithms and improvements in data quality, newer RNA sequence technologies, for example single-molecule real-time sequencing technology (SMRT) or nanopore sequencers (Maitra, Kim and Dunbar, 2012; Mikheyev and Tin, 2014) providing longer reads up to several kilobases, which make them capable of fully sequencing a transcript in a single run.

The RNA-Seq methodology uses next-generation sequencing (Kraemer *et al.*, 2019) to sequence cDNAs generated from RNA samples producing millions of short reads. The number of reads mapped within a genomic feature of interest (such as a gene or an exon) can be used as a measurement of the feature's abundance in the analysed sample. Typical RNA-Seq

procedure is depicted in Fig. 4.3. Briefly, RNAs are converted to a library of cDNA fragments with adaptors attached to one or both ends. The molecules, with or without amplification, are then sequenced with high-throughput technology, and short sequences from one end or both ends are obtained. The reads are typically 30–400 bp, depending on the DNA sequencing technology used (Chang, 2016).

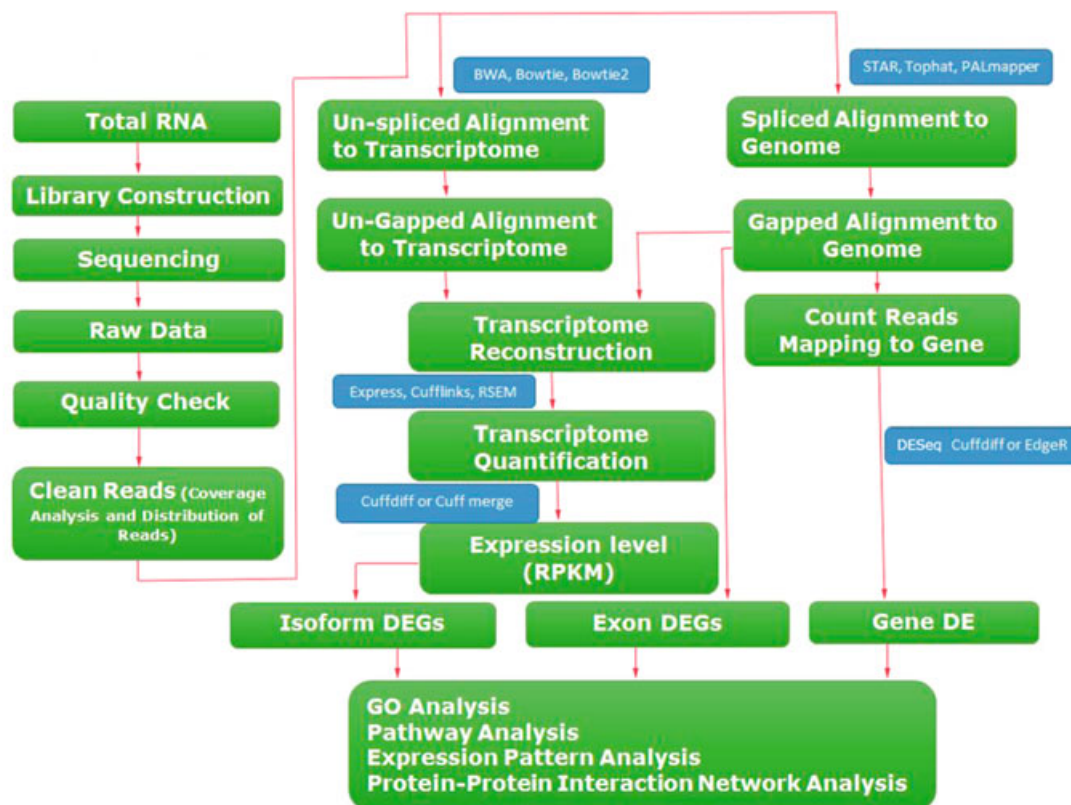


Fig. 4.3 RNA-Seq workflow. RNA-Seq begins with isolation of high-quality total RNA followed by conversion into cDNA, fragmentation, and adaptor ligation. Fragmented cDNA is used to construct a library for sequencing. Raw data, consisting of reads of a defined length, are preprocessed according to a set of quality control metrics, such as base quality, minimum read length, untrimmed adaptors, and sequence contamination. After filtering and trimming, reads are aligned to a reference genome or transcriptome depending on the objective of the experiment and the nature of the samples. Subsequently aligned reads are assembled. RNA-Seq assembly involves merging reads into larger contiguous sequences based on similarity. After assembly, reads are quantified in order to measure transcriptional activity. Read counts are generally computed in RPKM or FPKM in order to perform further downstream analysis, such as differential expression, pathway and gene set overrepresentation analysis, and interaction networks. From (Chang, 2016).

4.1.3 RNAseq in Trichomonads

In a study carried out in Germany they found among transcriptome data thousands of instances, in which reads mapped onto genomic loci not annotated as genes, some reaching up to several kilobases in length (Woehle *et al.*, 2014). At first sight these appear to represent long non-coding RNAs (lncRNAs), however, about half of these lncRNAs have significant sequence similarities to genomic loci annotated as protein-coding genes. This provides evidence for the transcription of hundreds of pseudogenes in the parasite. Conventional lncRNAs and pseudogenes are expressed in *T. vaginalis* through their own transcription start sites and independently from flanking genes in *T. vaginalis*. Expression of several representative lncRNAs was verified through reverse-transcriptase PCR in different *T. vaginalis* strains and case studies exclude the use of alternative start codons or stop codon suppression for the genes analysed (Woehle *et al.*, 2014). Taking advantage of the genome draft assembly for *T. foetus* K1 strain17, (Alonso *et al.*, 2022) generated a guided transcriptome assembly for three publicly available transcriptomics pieces of data: PIG30/1 (Kraemer *et al.*), G10/1 (feline) and BP-4 (bovine) isolates. The abundance of expressed transcripts was determined confirming considerable similarities between BP-4 and PIG30/1 and marked differences in those isolates connected to G10/1. Using a comparative procedure, (Alonso *et al.*, 2022) found a set of pathogenic factors mainly expressed in G10/1 that were predicted to codify for BspA-like proteins, tetraspanin proteins, metalloproteases, papain-like proteases, calpain-like proteases, subtilisin-like proteases and Myb-like DNA binding proteins (MYB), these last known in other pathogens as key transcription factors. Another finding was revealing expression patterns for MYB proteins in G10/1 isolate, and by an *in-silico* promoter analysis, and observing the presence of DNA motifs in the sequences, suggesting that these transcription factors could be involved in gene transcriptional regulation in *T. foetus* (Alonso *et al.*, 2022).

The increased expression of both the BspA and Pmp protein family in the human pathogen *T. vaginalis* raises the question about their distinct roles during infection, or more precisely whether those proteins are implicated in directly mediating adhesion to human host tissue as has been previously speculated (Hirt *et al.*, 2007; Noël *et al.*, 2010).

(Handrich *et al.*, 2019) sequenced the transcriptomes of five trichomonad species and screened for the presence of BspA and Pmp domain-containing proteins and characterized individual candidate proteins from both families in *T. vaginalis*. Their findings demonstrated that (i) BspA and Pmp domain-containing proteins are universal to trichomonads, but specifically expanded in *T. vaginalis*; (Mitrea *et al.*, 2014) in line with a concurrent expansion of the endocytic machinery, there is a high number of BspA and Pmp proteins which carry C-terminal endocytic motifs; and (Mitrea *et al.*, 2014) both families traffic through the ER and have the ability to increase adhesion performance in a non-virulent *T. vaginalis* strain and *Tetratrichomonas gallinarum* by a so far unknown mechanism (Handrich *et al.*, 2019)

From different studies it was suggested that *T. gallinae* invasion of the pigeon mouth may modulate Long non-coding RNAs (lncRNAs) expression and their target genes. Moreover, co-expression analysis identified crucial lncRNA-mRNA interaction networks (Yuan *et al.*, 2021). It was reported that mapping the RNA-Seq transcripts to the genome revealed that the majority of genes predicted within repetitive elements are not expressed. Also they identified a novel species of small RNA that maps bidirectionally along the chromosomes and is correlated with reduced protein-coding gene expression and reduced RNA-Seq coverage in repetitive elements. This novel small RNA family may play a regulatory role in gene and repetitive element expression. Recent results identify a possible small RNA pathway mechanism by which the parasite regulates expression of genes and TEs and raise intriguing questions as to the role

repeats may play in shaping *T. vaginalis* genome evolution and the diversity of small RNA pathways in general (Warring *et al.*, 2021).

4.1.4 **Trichomonas virus in trichomonad transcriptomes**

The complete cDNA sequences of three trichomonas virus strains was reported, one from each of the three known species, infecting a single, agar-cloned clinical isolate of *T. vaginalis*, confirming the natural capacity for concurrent (in this case, triple) infections in this system. We furthermore report the complete cDNA sequences of 11 additional trichomonas virus strains, from four other clinical isolates of *T. vaginalis* (Goodman *et al.*, 2011).

A viral sequence mining was conducted in publicly available transcriptomes across 60 RNA-Seq accessions representing at least 13 distinct *T. vaginalis* isolates. The results led to sequence assemblies for 27 novel trichomonas virus strains across all four recognized species. Using a strategy of de novo sequence assembly followed by taxonomic classification, we additionally discovered six strains of a newly identified fifth species, for which we propose the name *T. vaginalis* virus 5, also in genus *Trichomonas* virus (Manny *et al.*, 2022). Although developed independently from the work reported below, the strategy is essentially analogous to the one which I have employed.

4.1.3 **The aim of the present study was:**

1. To use RNAseq of putatively infected and uninfected lines to evaluate the presence of RNA virus in the trichomonas lines investigated.
2. To assemble from the transcriptomic data the genome(s) of any RNA viruses present.
3. To compare the virus genomes obtained for insight into their evolution and potential diagnostics for the presence of virus.

4.2 Materials and Methods

4.2.1 Earlham institute collaboration

RNA samples once prepared and validated for quality were provided to the Earlham Institute's pipeline group who prepared the libraries and undertook the NGS and provided the data in the form of short reads. Thanks to Dr. Sally Waring and Prof. Neil Hall for overseeing the bioinformatic analysis of the *T. gallinae* transcriptome and in particular the identification and assembly of the *T. gallinae* virus.

Table 4.1 Measurement of QC of samples for our Low throughput RNA pipeline

Sample ID		RNA Qubit	DNA Qubit	
Sample	Sample ID	ng/μl	ng/μl	%DNA
1	A55236	43.00	2.36	5.49
2	A55237	112.00	12.40	11.07
3	A55238	9.40	0.49	5.23
4	A55239	6.54	0.20	3.06

4.2.2 Extraction of RNA from *Trichomonas gallinae* isolates for detection of dsRNA

A total of 21 *T. gallinae* isolates listed in Table 1. were grown and RNA was extracted using the TRIZOL Thermo Fisher protocol (Graves *et al.*, 2019). Here a total of 1 mL of Trizol™ Reagent was added to every 50–100 mg of tissue for all samples. A centrifuge was used to pellet the cells, after which the supernatant was discarded. 0.75 mL of Trizol™ Reagent per 0.25 mL of sample at a concentration of 1×10^7 cell was then added to the pellet. The cells were not washed prior to the addition of Trizol™ Reagent to avoid mRNA degradation. The lysate was then pipetted up and down several times in order to homogenize it. A volume of 0.2 mL of chloroform per 1 mL of Trizol™ Reagent used for lysis, was added to the cultures. The tubes were then securely capped and incubated was for 2–3 minutes. The samples were then centrifuged for 15 minutes at $12,000 \times g$ at 4°C. The mixture separated into a lower red phenol-

chloroform, an interphase, and a colourless upper aqueous phase. The aqueous phase containing any dsRNA was then transferred to a new tube. This was carried out by angling the tube at 45° and pipetting out the solution. 0.5 mL of isopropanol was added to the aqueous phase, for every 1 mL of the Trizol™ Reagent used for lysis. Incubation took place for a period of 10 minutes. Centrifuging was then conducted for 10 minutes at $12,000 \times g$ at 4°C. The total RNA precipitate formed a white gel-like pellet at the bottom of the tube. The supernatant was discarded using a micropipette. The next step was to wash the RNA pellet once with 75% ice-cold ethanol. A mix of 1 mL of 75% cold ethanol per 1 mL of TRIzol reagent was used., after which the pellet was resuspended in 1 mL of 75% ethanol per 1 mL of TRIzol™ Reagent used for lysis. Some of the samples were required to be kept in storage. For this, 75% ethanol was used at a temperature of -20°C. This allows samples to be retained for one year. For short term storage of one week, a temperature of 4°C is adequate. The sample was then vortexed briefly, then centrifuged for 5 minutes at $7500 \times g$ at 4°C. The supernatant was then discarded using a micropipette. Any RNA pellet was left on the bench to air dry for 5–10 minutes. 30 µl of RNase-free water was added to the pellet of the RNA. The RNA samples were examined using agarose gel electrophoresis (1.5. gm agarose/100m; TAE and 5 µl ethidium bromide) Firstly, 3.5 µl nuclease-free water was added to 4 µL of the extracted RNA plus 1.5 µL DNA and loading dye. Previously, I had added 1 µL of the extracted RNA and 1.5 µL of loading dye, along with 4 µL nuclease-free water (Graves *et al.*, 2019).

4.2.3 Methods for identification of trichomonas (+virus) RNA-seq

The libraries for this project were constructed at the Earlham Institute, Norwich, UK using the NEBNext Ultra II RNA Library prep for Illumina kit (E7760L) and NEBNext Mul_plex Oligos

for Illumina® (96 Unique Dual Index Primer Pairs) (E6440S) at a concentration of 10uM. 100ng of depleted RNA was fragmented for 12 minutes at 94°C, and first strand cDNA was synthesised. This process reverse transcribes the RNA fragments primed with random hexamers into first strand cDNA using reverse transcriptase and random primers. The second strand synthesis process removes the RNA template and synthesizes a replacement strand to generate ds cDNA. Decoloniality is retained by adding dUTP during the second strand synthesis step and subsequent cleavage of the uridine containing strand using USER Enzyme (a combination of UDG and Endo VIII). NEBNext Adaptors were ligated to end-repaired, dA-tailed DNA. The NEBNext Adaptors with novel hairpin loop structure are designed to ligate with high efficiency and minimize adaptor-dimer formation. The loop contains a U, which is removed by treatment with USER Enzyme to open the loop and make it available as a substrate for PCR. The ligated products were subjected to a bead-based purification using Beckman Coulter AMPure XP beads (A63882) to remove most of un-ligated adaptors. Adaptor Ligated DNA was then enriched by receiving 8 cycles of PCR (30 secs at 98°C, 8 cycles of: 10 secs at 98°C _75 secs at 65°C _5 mins at 65°C, final hold at 4°C). Barcodes are incorporated during PCR using NEBNext Mul_plex Oligos for Illumina® (96 Unique Dual Index Primer Pairs) thereby allowing multiplexing. The quality of the resulting libraries was determined using Agilent High Sensitivity DNA Kit from Agilent Technologies (5067-4626) and the concentration measured with a High Sensitivity Qubit assay from ThermoFisher (Q32854). The final libraries were equimolar pooled, and q-PCR was performed to accurately quantify only the molecules with both adapters. The library pool was diluted down to 0.5 nM using EB (10mM Tris pH8.0) in a volume of 18µl before spiking in 1% Illumina phiX Control v3. This was denatured by adding 4µl 0.2N NaOH and incubating at room temperature for 8 mins, which it was neutralised by adding 5ul 400mM tris pH 8.0. A master mix of EPX1, EPX2, and EPX3 from Illumina's Xp 2-lane kit was made and 63µl added to the denatured pool leaving

90µl at a concentration of 100pM. This was loaded onto a NovaSeq SP flow cell using the NovaSeq Xp Flow Cell Dock. The flow cell was then loaded onto the NovaSeq 6000 along with an NovaSeq 6000 SP cluster cartridge, buffer cartridge, and 300 cycle SBS cartridge. The NovaSeq was running NVCS v1.7.0 and RTA v3.4.4 software and was set up to sequence with 150bp paired-end reads. The data was de-multiplexed and converted to fastq using bcl2fastq2 .

4.2.4 Virus genome assembly and identification.

Raw 2 x150 bp reads (106,644,150 total read pairs) were trimmed to remove adapter contamination using Trim Galore version 0.5.0. Trimmed reads were assembled using Trinity version 2.9.1 (Grabherr *et al.*, 2011). The assembled contigs were used to make a BLAST database and searched with a BLASTx search using 27 full length *Trichomonas vaginalis* virus genomes as a query – see table (BLAST+ version 2.10.0 used for database construction and BLASTx search (Camacho *et al.*, 2009). The BLASTx search returned a single contig, 4647 nt long, with 458 hits. This contig was run through the NCBI ORFfinder (<https://www.ncbi.nlm.nih.gov/orffinder/>) which identified two open reading frames. Each protein was run through the BLASTp webserver search against the nr database, which identified one as the RNA dependent RNA polymerase and the other as the capsid protein.

Table 4.2. TVV genomes used to identify TGV genome in Trinity assembly

Accession	sequence_name
NC_003824.1	Trichomonas vaginalis virus, complete genome
NC_003873.1	Trichomonas vaginalis virus II, complete genome
NC_004034.1	Trichomonas vaginalis virus 3, complete genome
JF436871.1	Trichomonas vaginalis virus 2 isolate C351, complete genome
JF436870.1	Trichomonas vaginalis virus 2 isolate C76, complete genome
JF436869.1	Trichomonas vaginalis virus 1 isolate C344, complete genome
MW978698.1	Trichomonas vaginalis virus 3 strain TVV3-G3(HMS), complete genome
MW978697.1	Trichomonas vaginalis virus 2 strain TVV2-G3(HMS), complete genome
NC_038700.1	Trichomonas vaginalis virus 4 strain TVV4-OC3, complete genome
NC_027701.1	Trichomonas vaginalis virus 1 strain TVV1-UR1-1, complete genome
KM268110.1	Trichomonas vaginalis virus 3 strain TVV3-UR1-1, complete genome
KM268109.1	Trichomonas vaginalis virus 2 strain TVV2-UR1-1, complete genome
KM268108.1	Trichomonas vaginalis virus 1 strain TVV1-UR1-1, complete genome
HQ607523.1	Trichomonas vaginalis virus 1 strain TVV1-OC5, complete genome
HQ607521.1	Trichomonas vaginalis virus 1 strain TVV1-OC4, complete genome

HQ607517.1	Trichomonas vaginalis virus 1 strain TVV1-OC3, complete genome
HQ607516.1	Trichomonas vaginalis virus 1 strain TVV1-UH9, complete genome
HQ607513.1	Trichomonas vaginalis virus 1 strain TVV1-UR1, complete genome
HQ607524.1	Trichomonas vaginalis virus 2 strain TVV2-OC5, complete genome
HQ607518.1	Trichomonas vaginalis virus 2 strain TVV2-OC3, complete genome
HQ607514.1	Trichomonas vaginalis virus 2 strain TVV2-UR1, complete genome
HQ607525.1	Trichomonas vaginalis virus 3 strain TVV3-OC5, complete genome
HQ607519.1	Trichomonas vaginalis virus 3 strain TVV3-OC3, complete genome
HQ607515.1	Trichomonas vaginalis virus 3 strain TVV3-UR1, complete genome
HQ607526.1	Trichomonas vaginalis virus 4 strain TVV4-OC5, complete genome
HQ607522.1	Trichomonas vaginalis virus 4 strain TVV4-1, complete genome
HQ607520.1	Trichomonas vaginalis virus 4 strain TVV4-OC3, complete genome

4.2.5 Protein alignment and phylogenetic tree.

The TGV RNA dependent RNA polymerase and capsid protein sequences were added to those from *T. vaginalis* virus and a selection of other *Totiviridae* viruses based on the table presented in Fraga et al., 2012. Each protein family was aligned using the Clustal Omega webserver (<https://www.ebi.ac.uk/Tools/msa/clustalo/>) and alignments were viewed and concatenated in Geneious Prime® 2022.2.1. A maximum likelihood tree was built for the concatenated alignment using the IQ-TREE web server (<http://iqtree.cibiv.univie.ac.at>) with ultrafast bootstrap analysis (Trifinopoulos *et al.*, 2016).

Table 4.3 Totiviridae genomes used for the

Virus name	Code	GenBank accession No.	Genome length (nt)	RNA-dependent RNA polymerase accession	capsid protein accession
Trichomonas gallinae virus	TGV		4647		
Trichomonas vaginalis virus	TVV1-1	NC_003824	4647	NP_620730.2	NP_620729.1
	TVV1-T5	U57898	4648	AAC55469.2	AAC55468.1
	TVV1-IH2	DQ270032	4647	ABC86751.1	ABC86750.1
	TVV1- Changhun	DQ528812	4291	ABF57713.1	ABF57712.1
	TVV1-UR1	HQ607513	4684	AED99812.1	AED99811.1
	TVV1-UH9	HQ607516	4678	AED99814.1	AED99813.1
	TVV-OC3	HQ607517	4648	AED99816.1	AED99815.1
	TVV1-OC4	HQ607521	4680	AED99818.1	AED99817.1
	TVV1-OC5	HQ607523	4680	AED99820.1	AED99819.1
	TVV2-1	AF127178	4674	NP_624323.2	NP_624322.1
	TVV2-UR1	HQ607514	4674	AED99806.1	AED99805.1
	TVV2-OC3	HQ607518	4674	AED99808.1	AED99807.1
	TVV2-OC5	HQ607524	4671	AED99810.1	AED99809.1
	TVV3-1	AF325840	4844	NP_659390.1	NP_659389.1
	TVV3-UR1	HQ607515	4845	AED99800.1	AED99799.1
	TVV3-OC3	HQ607519	4846	AED99802.1	AED99801.1
	TVV3-OC5	HQ607525	4842	AED99804.1	AED99803.1
	TVV4-1	HQ607522	4943	AED99796.1	AED99795.1
	TVV4-OC3	HQ607520	4944	AED99794.1	AED99793.1
	TVV4-OC5	HQ607526	4942	AED99798.1	AED99797.1
	TVV1- C344	JF436869	4657	AET81012.1	AET81011.1
	TVV2-C76	JF436870	4689	AET81014.1	AET81013.1
	TVV2- C351	JF436871	4686	AET81016.1	AET81015.1
	TVV3- G3(HMS)	MW978698	4820	QYV44575.1	QYV44574.1

	TVV2- G3(HMS)	MW978697	4656	QYV44573.1	QYV44572.1
	TVV1- UR1-1	KM268108	4666	AKE98367.1	AKE98368.1
	TVV2- UR1-1	KM268109	4657	AKE98370.1	AKE98369.1
	TVV3- UR1-1	KM268110	4825	AKE98371.1	AKE98372.1
Giardia lamblia virus	GLV1	L13218	6277	AAB01579.1	AAB01578.1
	GLV2	AF525216	6237	AAM77694.1	AAM77693.1
Giardia canis virus	GCV	DQ238861	6276	ABB36743.1	ABB36742.1
Leishmania virus	LRV1-1	M92355	5284	NP_041191.1	NP_041190.1
	LRV2-1	U32108	5241	AAB50031.1	AAB50030.1
	LRV1-4	U01899	5283	NP_619653.1	NP_619652.1
Saccharomyces cerevisiae virus	ScVL-A	J04692	4579	AAA50507.1	AAA50506.1
	ScVL-BC	U01060	4615	AAB02146.1	AAB02145.1
Eimeria brunette virus	EbV1	AF356189	5358	AAK26438.1	AAK26437.1
Botryotinia fuckeliana totivirus	BfTV1	NC_009224	5261	YP_001109580.1	YP_001109579.1
Chalara elegans RNA virus 1	CeRV1	AY561500	5310	AAS68036.1	AAS68035.1
Coniothyrium minitans mycovirus	CmRV	AF527633	4975	AAO14999.1	AAO14998.1
Epichloe festucae virus 1	Efv1	AM261427	5109	CAK02788.1	CAK02787.1
Gremmeniella abietina virus	GaRV-L1	AF337175	5133	AAK11656.1	AAK11655.1
	GaRV-L2	AY615210	5129	AAT48885.1	AAT48884.1
Helicobasidium momp totivirus 1-17	HmTV1-17	AB085814	5207	BAC81754.1	BAC81753.1
Helminthosporium victoriae virus 190S	HvV190S	HVU41345	5179	AAB94791.2	AAB94790.2
Magnaporthe oryzae virus	MoV1	AB176964	5359	BAD60833.1	BAD60832.1
	MoV2	AB300379	5193	BAF98178.1	BAF98177.1
Sphaeropsis sapinea virus	SsRV1	AF038665	5163	AAD11601.1	AAD11600.1
	SsRV2	AF039080	5202	AAD11603.1	AAD11602.1

4.3 Results

4.3.1 The *T.gallinae* sample identified as C10 subtype but not those of the C3, C4, or A1 subtypes show high levels of viral transcript.

In the present study RNA quality was checked for degradation, purity, and quantity before it was passed to the pipeline team at the Earlham Institute. The Nanodrop device was used to measure the fluorescent absorbance of nucleic acid samples typically at 260 and 280 nm (Table 4.1). The results of paired end sequencing for the cDNA libraries of the four isolates tested are described in Table 4.2

Table 4.4 Outcomes from paired end sequencing of cDNA libraries

SampleName	El Sample Name	Submitter Sample Name	Sample ID	#Reads	Mean Q30 To Base R1	Mean Q30 To Base R2	Barcode	Run Alias	Lane
R0603-S0001_C3_A5	R0603-S0001	C3	A55236	160,215,265	150	150	CACGCAAT	210413_A00	1
R0603-S0002_C10_A	R0603-S0002	C10	A55237	106,644,150	150	150	GGAATGTC	210413_A00	1
R0603-S0003_A_A55	R0603-S0003	A	A55238	126,637,411	150	150	TGGTGAAG	210413_A00	1
R0603-S0004_C4_A5	R0603-S0004	C4	A55239	113,606,489	150	150	GGACATCA	210413_A00	1
Total				507,103,315					
				AVG	126,775,829				
				STDV	23,783,265				
				CV	0.19				

	Total read pairs	Total read pairs after rRNA removal	Total read pairs not mapped to genome
C3	160,215,265	14,881,040	628,157
C10	106,644,150	9,406,131	1,078,520
A1	126,637,411	10,821,266	251,982
C4	113,606,489	8,509,211	346,774
	total annotated genes	total genes with >0 mapped read pairs	% genes with mapped read pairs
C3	23,270	16,518	71
C10	23,270	18,098	78
A1	23,270	13,920	60
C4	23,270	14,566	63

All samples yielded greater than 100,000 reads of data of 150 bp. The *T. gallinae* reference genome (A1) is approximately 55 Mb and contains approximately 22,000 protein coding genes. The cDNAs sequenced contained predominantly ribosomal cDNAs because of the high level

of expression of the ribosomal genes. Initially the rRNA and then genomic *T. gallinae* sequences were removed bioinformatically to leave a pool of novel sequences from which assembly was attempted (lower part of Table 4.2). From these initial transcriptome statistics it was clear that the C10 isolate had more read pairs that did not align to the *T. gallinae* genome and correspondingly that the C10 isolate has a higher proportion of unmatched expressed genes, especially bearing in mind that it has a lower number of read pairs overall. Overall the coverage of each of the protein coding host genes was low due to large loss associated with rRNA removal (~10 million per isolate).

Initially the unmapped read pairs from each isolate were assembled into scaffolds using Spades (<https://emea.illumina.com/products/by-type/informatics-products/basespace-sequence-hub/apps/algorithmic-biology-lab-spades-genome-assembler.html>) the longer, more highly expressed (based on reads per kb) scaffolds were selected, open reading frames identified (using NCBI ORF finder <https://www.ncbi.nlm.nih.gov/orffinder/>) and the translated protein sequences then used to manually interrogate the NCBI nr Database using blastp (<https://blast.ncbi.nlm.nih.gov/Blast.cgi?PAGE=Proteins>). Several of the larger contigs with the highest reads per scaffold (and thus presumed the highest expression levels) from C10 but none from any of the other isolates showed their top blast hit to TVV1 capsid protein (not shown).

On the basis of this initial analysis a complete assembly from the read pair library was undertaken for the C10 transcriptome, using the Trinity assembler described in section 4.2.4 of the methods above. A complete and novel viral genome was thereby obtained (Fig. 4.4).

A)

>TGGV1
 CCCAGATGGGTATTCTTGACATACTAATCGCCTTGAGAGGACCTTCTTAACATGGAGGGATCGACGGGTGCCCTTCAAGAACTCTCAGACCTACGAGCAATCTATTGTGCAACACGAACCGGATACCTACGAAGC
 CCGGCAAGTGATCGGATAGGGCCTAAGTTTATCGTCTGCCGAGGCGAGCATGCTGGGTAGAGACATTCCACATCCGGATTGAGTAGCATCAGTCTAGGATAAATGCTCGGCTAGTTTACTGAGTGGTGGTGAATGTTTC
 GCGTATTGACCATGGCTGAGCTTAGTTTCAAGGAAGTGGTCCACTTAATGGCGATTAAATGATGATAAGAAATCGTCAGGTATGGCTTCCCGCCACAGGAGGCAAAATAAAGTGGCAAAATATGATTTTATTTATGATT
 TTTGAAGCAGCAGGATACCAATCTCAATCATGCGAATTGTCAAATTAATCGTAAAGCAGGTGGTGAATATAGATCCGACAACTGGGGAGATGCCGTATGAGGTTGACACACACAGTTTCAAGTGTATAGCCGATC
 TTGCAGTTCACTCGCGCAACAACTCGAACTCGACTTCGGTTTGGGCAAGATGTCAACAAGCAGTCAGGACCGATTCTATCCCACTAAATTCACCAGAAGCTTACAAAGAGCTGGCCAAAGAGCATCAGCTCTCTGTATCAG
 AAGAAGGCCCTTATGACGACATGAACCTCGAAGTAATACTAGATCTTATGCAAACTCAGACTTAAGTATCGCAACTGTGCCGCTGGTTTCTACACAGCGTTGAGTGACAGCCAGAAATGATCAAGCAATAAGCACTGCT
 GACCACCGTTCCGATTTTGGCTCAGCATCAGTGCAACATCACACGCGACACCAACGCCGCAAGATGCTCACACATGATATCTTCTCCTCAGAGCAGAGGAATGCTCAAAACAGAGAAAGGGATATCCAGAACGATGTCAA
 CTATGGGGTATGTCACATCAAGAACTGCCTGCAAGGCGACACATCATAGCTCCAGACACAATCACAATCTCGCTCCCAACGAATCCTTAGGTCAAAGTTGGTGGTGGCGGATTGGCTGCTTCGATCTTATCCAA
 TCGATGAATACACACGAAATATACATTTACGTGCTCCAGGTGCTGAACCACTTAACAGCGTTACAGACACCAACATTACTGAAGCAATTACGATTTTACTCGGAATGGCCAAAGACGCCAGGCGAGCTCAGTGATGCT
 CTCGAAACTTTCTCTACGTCCAAGTTTACAGATGGTCTCAGGCCACACTCGCTATACACAGAGGGAGGAGTTGTCCGGAAGATGATCTTCCGCGTTCCAACTTGAAACCAACACGGCATGTTCTACTACAAACTTGCCTAC
 TCAAGATTGACCTCAATTAAGCGCCAGATGATCTAGTCTCCGCAAGAATCTCATCTGCGCTGGAGGAGTCTGCAACAACGCAACTAGCGCTCTGCTACAGGCGCTCTCAGCTGCAAAAGTCCGATAGCATCAATGGGA
 GAGTAATGATGCTATCTCAACCGCTCAAAAGCGCTCGCAACACAGATACTTAAGAGCGCGATTCTTCAAGATTCCAATCGCCCAAGCTACCGTCACTAACGTCGCAATCTACACACGTCGCGTCCGTGACGATCCCAATACAA
 GAGGCAGCTCGCGAGATCTTGCCCAACTATTGGAGCAGGTGCTGAAGTCAATCATCGATATAGAAGAATATCATTAATCAGCAACGCTCTGATCAACGCTCAACAGCGCAATCGCCGCGAGAGAAATTCGCTACAG
 CGTTTCATCAACAGATTCAACGATCCGAGTACGCCCTACATGTTTCGGCATCAAGGGCAACGGTGTTCAGCGCTCGAAGGTGCTGTCACGTCAAAAAATTGATGAAGAAGTCCAATCTTGATGAAAGTGGCGACATCCGCA
 CTGCCCAATCTCCGCGACAAGCTATGCCGCAACACGATTAGACATCAAGCTCGTGCAGAGACGCAAGATGCTTATCAGCACACTCGACGGCAGGCTCATCGAGATCGGCTCTACCAAGCTAAAGGCTTCTCAGATA
 TCGGCTGGAAATTGAGAGGTAAGGTCATGAAGCTTACGAGATAAAGAGTCCACTCTTCCACAAGCTCAAATACAGCGTACTGCTCAACGCTGCACTCATCAAACTCAGCAAAATGTTCTTGGACCATTTGCGCGATACC
 ATCGCGCCCATTTTTCGTAAGGCGCTAGCTTTTGGACCGCTATGCCGACTGTCTACTATTACTGAACCAAGCAATGCCAGAAAGTCAACAATAAAGTACAGATACATCTACAGTCCGGTATATGATGATATCCCTG
 TCTGATCATCTACAAAAACACTAGCAATCGAGGTGACACGCCCTCCATTGGATCAGCCAGATGAGTTGATTGTCTGAAGAAGAATGATAATTGATAAATTGTACAAAAATTAACCTTATAAAAGCCGAATACATATGA
 TAACCCAGATAAGTTAGTAAGCAAGGAACAAGAAGATCCCTTTCCCGCTAAAGCAACACACAGCAGCTAGGAACAAGGTTAATCTATACGACAGCTATCTTGGAAATGAGAGTAAGCTATCGAAGCGAGCTTTCATACCAAG
 GAACTTATAAGATATTGTGTCGGTCTATTGGTATGGGGTGAAGTAGCAGTATTGGAGCATCCCAAGAGATTATAGATTCACTGATTTCTGCGCTTCAAGGAGACAAAGGCCCACTACTAGTGTATAGGAA
 GGGCGAGCACTGGTTGAAGCAAGCTGGTATGGCTTTGACCCGATCTACGCTTATTATCGAGCTAAACACATTACTGGGTAGAGGAGCTGGCGAAGGCGATGGCGCAAGGATATTGCAATCTGATGACGGTATAAAC
 TCTCAAGAGGTACCGGTGACGAAATTGCACTACGACCTTCTAAGGCACTCTATTCAAGAAATATAAGTAAGCGTGAATCCCAAGTTTCTCAGACCAATTAGACATGCGCTTATTGGTGTAAGACAGGTTCCCACTACT
 ACCGAGACCAAGAACTAGACCAACCAAGCTACCAACCAAGCACTAGAAAAGAATTGTTGATATTGGGATAAAGGCTACCTGGAAATCAAGAAACCGGAGTCTATATACTCAGGCGAGAAATCAGAGCATGGAAGG
 TTAGATTATCTACAACCTGCACTCGGTGATATATCTATTGACTAGTCTTAAATACATTGAGAGCAGTGAGAGATGAACAGGCCATCTGTGTCACAGGCGAGATAGGCAAGTCCGAGATATATCTGAAGGTCAACCG
 ATACAAGTACAAGGCGATGTAGACTACAGCACTTCAACAGCGACACACCAATGAAGTCTATGCAAAATGTTGTCAGAGAGCTGAGGAGTACTTACCAGAGTGCGATGTCGCGATGAAGTGGTGCATAAAGTCTTTCG
 AGAATATGCAACACCAAGGCTCATAGGTGGATAGCACCTGCCAAGCGGCCACCGCGGCACCACTTTCATCAACAGCATCTCAACTGGTGCTACCTACGCTAGCAGAGGGGCTCAGTTTCGATGACCAAGTGTGCGCGG
 AGACGATGTCTATGCTGACCAACAGCCTATCAGGCTCACTTCTATATCTCTTAAGTTCCGCTTTAATCAAGCAAGCAGAGCAGCGGCACACGTTGGAGAATTCTTAGGAAACACGCTACTGACGCGGGGCTCTATGCT
 CTATCCGGCAAGAGCGTGCTAGCTTGTGTTAGCGGCACTGGGTATCAGATGCAAGAGGCAATCTGCTCACTAGCCCCACTACAGAACGCTTTCGACAGAAATCCGAGCGGCTGGCATCTTAGGAGCATGGAAGG
 GTCAATTGGGACATACCGAGATCCAGGAGAGATACGCACTTACACAGCAGACAGCAATTGTGGGCTTGAATTCTAAAGCTGCAAGGCGCAGGATTCATCCAGCACTAGAAAACACAGTGTGGTTCATCAGTGAGCAGAGGCA
 CGCGAACTCGGCTCGCTTCACTGCGCACAGGAATGGCTAGCTGACCTGTGCGCTAAAGTACGCTGGAAGGAGCTAAACGAGCGGACAGCATGCTTACGCTCGCGGCTTAAGAAAGTTAAACCAACACGCGCATCCA
 AGAAAACATAAGTGTGTACAGGGAAGCTCGGTTGGAAGCGGACAGTGGCGGAACCATAGTCCCGACAAAGGTGCCAGACCTACGACACAAGGGCTGTGTGAGCGCGATGATGAAGCAGAAAGGAAACAA
 AAGCTGAGAACTCAGACGAGTATGCAGTGGGCTCAAGCTATGAAGCAACAGCATGCTTCTGGCGATTTCGCTGCTGACGTGCCAGGCTGAGAGTGCCTGCTTACAAGCTGATCCCGCTACCTCATAGACG
 TACGCTACGTCGAAAGCTTGAGTTAGTTTCTACCCAAAGACAGGTTACCAAGCACCATC

B)

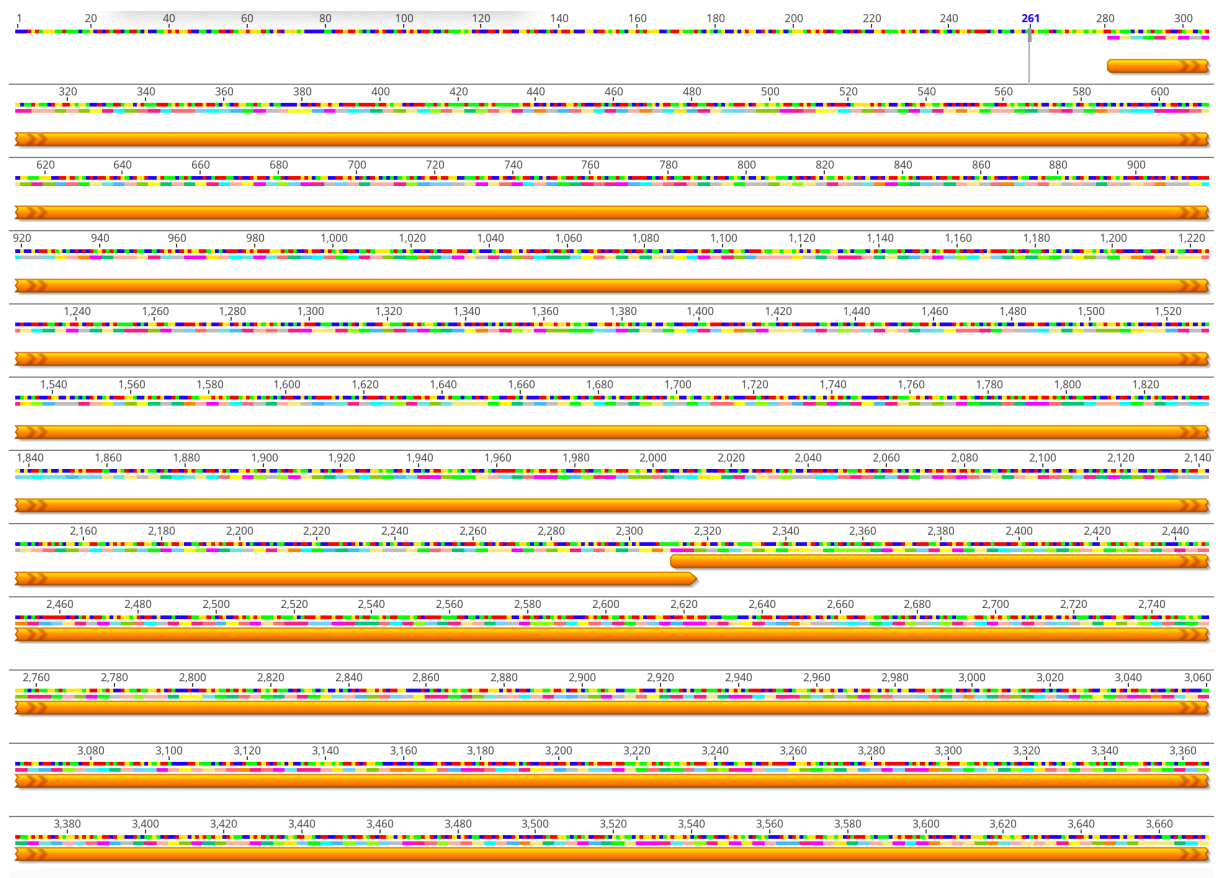


Figure 4.4.

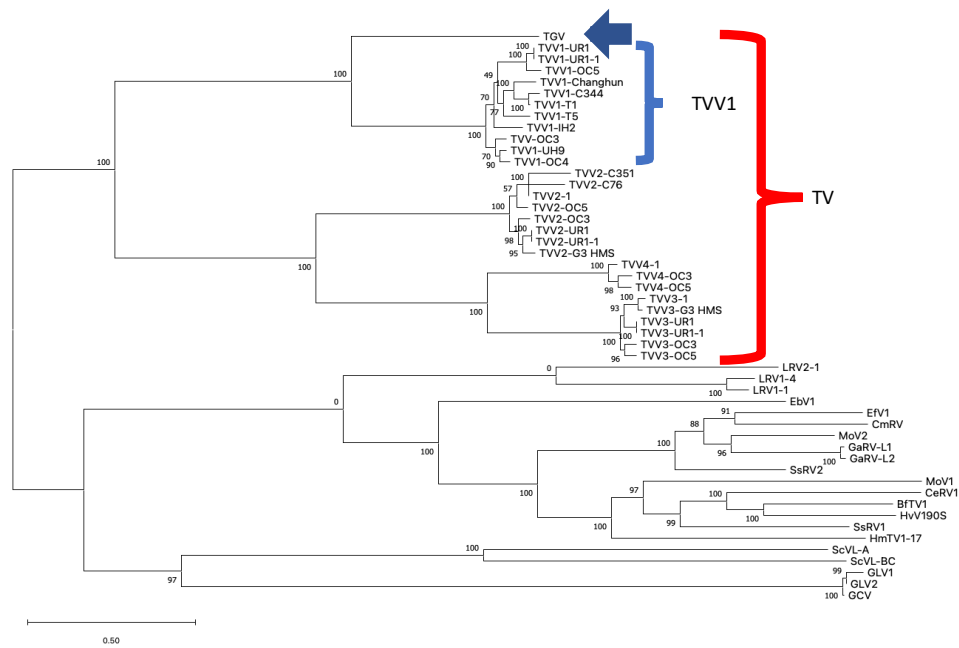
A) The complete cDNA sequence of the genome of TVV1. The genome is 4647bp in length and is exclusively composed from two overlapping reading frames which are in the same direction, with the viral capsid protein lying 5' to the viral polymerase.

B) Capsid and Polymerase open reading frames are overprinted for 6 nucleotides, they are unidirectional and out of phase as is typical for the other *Trichomonas* viruses - so far characterized. Prepared by Dr. S. Warring using ingenious software (<https://www.geneious.com>)

4.3.2 Phylogenetic analysis

Like all of the *Totiviridae*, the *T. gallinae* virus (TGV1) genome consists only of capsid and polymerase. As with all of the other *Trichomonas* viruses there is no gap between the two genes which overlap each other. Blastn interrogation with the nucleic acid sequence showed only relatively weak sequence identity with the top hits which were TVV viruses (not shown). Much better “hits” were obtained using the translated protein sequences from the capsid and polymerase proteins. For this reason, phylogenetic analysis was undertaken based on the predicted amino-acid sequences. Analysis was undertaken for the maximum number of character transitions by concatenating the complete amino acid sequences encoded by each of the genes.

A)



B)

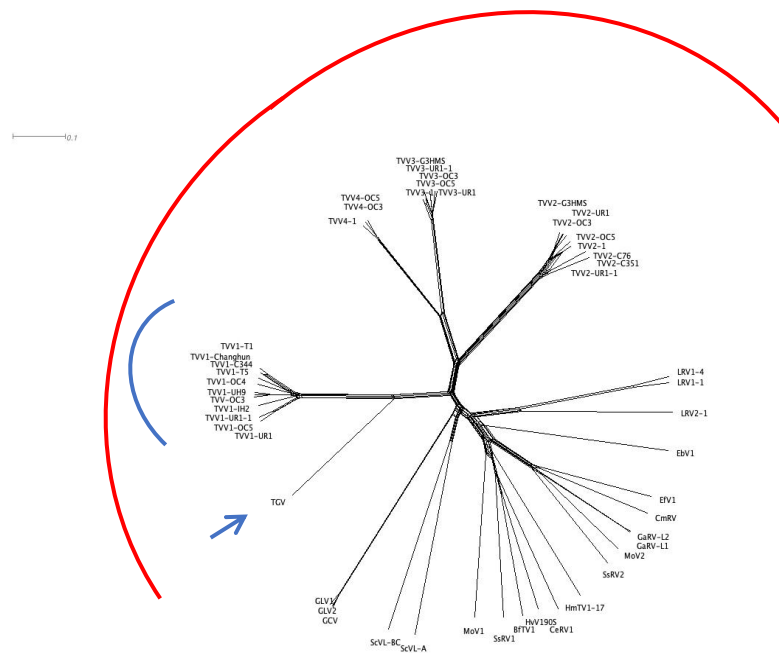


Figure 4.5 Phylograms of the protein sequences encoded by TGV1 compared with other related viruses of the *Totiviridae* A) Maximum Likelihood tree with bootstraps which clearly delineate a clade of Trichomonas viruses within the *Totiviridae* (red bracket) and a subclade of TVV1 viruses with which the *Trichomonas gallinae* (arrow) virus is associated (blue bracket). B) Neighbour net analysis supports a discrete evolution of a clade of

Trichomonas viruses (red arc) and discrete evolution of the TVV1 clade (blue arc) with which the TGV1 (arrow) is associated.

In Figure 4.5A Trichomonas viruses (TVs) were observed to form a well-supported clade discrete from other viruses of the *Totiviridae*. TGV1 was nested within this clade and so is a new TV. Within the TVs, TVV1 viruses cluster closely together in a well-supported clade, TGV1 is just outside of this group but clearly associated with it – thus TVV1 viruses are more like each other than TGV but are more like TGV1 than any of the other TVV clades even though the host species are quite different. The result is unexpected if *T.s vaginalis* has a monophyletic origin and is evolved from *T. gallinae* since the most parsimonious co-evolution of viruses with *T. vaginalis* would place any *T. gallinae* viruses outside of the root of the *T. vaginalis* viruses.

In Figure 4.5B, Neighbour-net analysis was also conducted to evaluate whether homoplasy or recombination between lineages might have contributed to a misleading positioning of the taxon on the maximum-likelihood tree. This analysis closely corresponded to the phylogenetic tree confirming TVs as a discrete clade from other members of the *Totiviridae*. There is no evidence of genetic exchange affecting relationships between taxa and the branch length of TGV1 is similar to the other groups of TVs suggesting independent evolution since divergence with no obvious signs of homoplasy.

4.3.3 Design of diagnostics for TVV1 like virus in other *T. gallinae* strains.

TVV1 viruses are the most prevalent group of TVs in *Trichomonas vaginalis*. It seems unlikely that the virus found in this study will be the only *Trichomonas gallinae* lineage affected by such viruses and the tracts of nucleotide and amino-acid sequence identity common between TGV and TVV1 provide an opportunity to design probes which may be used diagnostically to evaluate the prevalence of TGVs of this kind in *T. gallinae* isolates. Since the capsid protein is constrained structurally by its function in containing the genome and is antigenic I chose to consider it as the target for these new diagnostic tests. The translated 678 amino-acid capsid sequence is shown in Figure 4.6

```
MFRVLTMAELSSGSGPLNGDLNDDKNRQVMASPPQEANKISGTNYDFIYDFLKHAQDTNLQSHANCQLTRK
AGGELDPTNWGDVAVMRLTHTVSSVIADLAVHSRNNLELDFGLGQDVTRQSGPISIPNSPERYKELAKSISSLY
QKKAFMTDMNSQVILDLMQNSDLSIATVAAGFYTALSARHEVIKAISTADHRSDFAAISATSHAAPNAAARCSH
MISSFLRAECSNRERDIQNDVNLWGIVHIKETALQGDNIIRPDTITIFAPNESLGQSWWCAIWLLSIFIQSMKY
NTKIYIYVAPGAVTHLTAFTDTNITEAITILLGMAKDARQLSDALETFLYVQGLQMVIQPHSLYTEGGVVRKMIF
AVPNLKPFGMFTTKLAYSRLTSIKRPDDLVSANKFICAGGVCTTQLALCYQAALSCKGPPIAHWESNDAISTAQK
RLANRYLRGRFFTVPQAQATVTNVAIYTRAVRDDPKYKSQLGEILPQLFGAGAEVIIDIEEDIINSSNV SINANKRN
RRQRKFRTAFINRFNDPEYAYMFGIKGNGVQRLEGVVTSKIDEEVQYLMKGGDIRNCPILRTSYAANNLDIKL
VAEDED AFISTLDGRLEIGLYQAKAFSDIGWNSRGKVMKPYEIRAPLFHNVQIQRTAATVDSIKVTTMVSGPLR
DTIAPHFC
```

Figure 4.6 The 678 amino-acid sequence for the capsid protein of TGV1

The capsid sequence was aligned to a TVV1 genome in MEGAX with a CLUSTAL sequence alignment employing MUSCLE (Figure 4.7). The alignment identifies several conserved stretches of amino acids common between the alleles. To determine whether these stretches might be antigenic open source epitope prediction software (<http://tools.iedb.org/main/bcell/>) was utilised to identify the likely B-cell epitopes in the capsid protein and those present in the conserved areas listed (Figure 4.8 A) since several were present in a relatively short peptide chain it (Figure 4.8 B) it is possible that this could be synthesised and used as an inoculum for a diagnostic peptide antibody and basis for future monoclonal antibodies.

CLUSTAL multiple sequence alignment by MUSCLE (3.8)

```

capsid|TGV
AED99811.1|TVV1-UR1
AED99813.1|TVV1-UH9
MFRVLTMaelSSGSGLNGDLNDDKNRQVMASPPQEANKISGNTY-----DFIYDF
-----MEASANGLSHDDNANKSQNVGPSTLPGSDKQGGENHENSFNSFSNDFFFNF
-----MEASANGLSHDENATRSQNVGPSTLPGSDKQGGEKHENSFNSFSNDFFFNF
      :.:.:. . * . * . . . : * . . . : : * . * : :
      ****:

capsid|TGV
AED99811.1|TVV1-UR1
AED99813.1|TVV1-UH9
LKHAQDTNLQSHANCQLTRKAGGELDPTNWGDVAMRLTHTVSSVIADLAVHSRNNLELDF
LRTSTSTHISDSPGVSVFVKDGTPTYSATIQSAGVRLTHNVVASAVQLNITANNTLEVDY
LRISAQTHISDSPGVSVFIKDGTPYSSTTIPSAVGRLLTHNVVASAVQLNVTADNVLEVDY
* . : . * : . . . . : * * . . . . * * * * * : . * : : * * * :
      ****:

capsid|TGV
AED99811.1|TVV1-UR1
AED99813.1|TVV1-UH9
GLGQDVTRQSGPISIPNSPERYKELAKSISLQYKKAFTMDMNSQVILDLMQNSDLISIA
GFGQDVSRATGTITIPIDFGEKYKEVARALSLVFSKKGMDLVTSTQTVQDTLMNSDLTIA
GFGQDVSRSTGTITIPIDFGEKYKETARALATIFSCKGMAVDVTSQTVQETLKNSDLTIA
* : * * * : * . * * * : . * * * * . : : * * * : * : * * * :
      ****:

capsid|TGV
AED99811.1|TVV1-UR1
AED99813.1|TVV1-UH9
TVAAGFYTAL SARHEVIKAI STADHRSDFAISATSHAAPNAARCSHMISFLRAEECS
TVAAGYYTALAARHELTKEASVAHRIPFVTALSDTFTAADNAQRSSHVISSCLRCPASN
TVAAGYYTALAARHELTQVSVASHTIPFVTALSDTLSAAQGAQRSSHVISSCLRCPHSN
* * * * * : * * * * * : * * * * * : * * * * * : * * * * * : * * * * * :
      ****:

capsid|TGV
AED99811.1|TVV1-UR1
AED99813.1|TVV1-UH9
NRERDIQNDVNLWGI VHIKETALQGDNIIRPDTITIFAPNESLGQSWWCAIWLLSIFIQS
NAQRQVTVGTMWNTNVSVENLAVQGAAIPNPNDVSFFIPNKALPSSWWCAIWLLNAFLHS
NVQHDVIGIGTDMWNNVSVESLSPQNMVAVPNPNDVSFFIPNKALPPPWWCAIWLLNAFLHS
* : : : . . : : * : : : : * : : : : * : : : : * : : : : * : : : :
      ****:

capsid|TGV
AED99811.1|TVV1-UR1
AED99813.1|TVV1-UH9
MKYNTKIYIYVAPGAVTHLTAFTDTNITEAITILLGMAKDARQLSDALETFLYVQGLQMV
FVAQTRFHIFITPGETYNLAPFTDADIYEAIPVLLAMSKSSRPVPESVESMLYAYGTQMV
FVAPTRFHIFIAIPGETYHLAPFTDADVYEAIPIMLAMSKAARPVPESVESMLYAYGTQMI
: * : : : : * : : * : * : : * : : : * : : : : * : : : : * : : : :
      ****:

capsid|TGV
AED99811.1|TVV1-UR1
AED99813.1|TVV1-UH9
IQPHSLYTEGGVVRKMI FAVPNLKPHGMFTTKLAYSRLTSIKRPDDLVSANKFICAGGVC
IQPHSLYTEGGIIRKMI FTVPHLPAHG YFVTNAEYSRYMNI AVPNDRPTAKDYIIGVGTG
IQPHSLYTEGGLIRMI FTVPHLPAHG YFVTNSEYSRYMNI AVPNDRPSAKDFIIGAGTG
* * * * * : * * * * * : * * * * * : * * * * * : * * * * * : * * * * * :
      ****:

capsid|TGV
AED99811.1|TVV1-UR1
AED99813.1|TVV1-UH9
TTQLALCYQAALSCCKGPIAIHWESNDAISTAQKRLANRYLRGRFFTVPIAQATVTNVAIY
LLQVILAYQAALFSCGGPIALHWHANDAI SHGMDTVAAYLEGRYFTIPMAINVATNIAQY
LLQITLAYQAALFSCAGPIALHWHNDIAISQGMDTIASTYLEGRYFTIPIAVAVATNVAQY
* : * * * * * : * * * * * : * * * * * : * * * * * : * * * * * : * * * * * :
      ****:

capsid|TGV
AED99811.1|TVV1-UR1
AED99813.1|TVV1-UH9
TRAVRDPKYSQGLGEILPQLFGAGAEVIDIEEDIINSSNVSNANKRNRQRKFRFAF
TTGVRADPPQYKHS LDRILPRIFGPSTDTVFNFIESAITSWVSINATKRNGRARKFRFAF
TTMVRADPPQYRHTLDRILPRIFGPSTDTVFNFIESAISWVSIDARRNRGRARKFRFAF
* * * * * : * * * * * : * * * * * : * * * * * : * * * * * : * * * * * :
      ****:

capsid|TGV
AED99811.1|TVV1-UR1
AED99813.1|TVV1-UH9
INRFNDPEYAYMFYIKNGVQRLEGVVTSKIDEEVQYLMKGGDIRNCPIRLTSYAANN DL
INRFHDPEFAYMFYITGNGIERMEGKVTSNIAQVEYLTNGGDLRNCPIRLTLKAAEAE
INRFHDPEFAYMFYITGNGIERMEGKVTSTISQEVGYLLHGGDLRNCPIRLTLKAAERDE
* * * * * : * * * * * : * * * * * : * * * * * : * * * * * : * * * * * :
      ****:

capsid|TGV
AED99811.1|TVV1-UR1
AED99813.1|TVV1-UH9
DIKLVAEDED AFISTLDGRLIEIGLYQAKAFSDIGWNSRGKVMKPYEIRAPLFHNQVQIR
TVTFMCTGKIGSIF AIDGMTRTFKRYQTIDLAELGWTSHGKVMKPYAFRAPVIOGITVCK
TITFMCKEKAGTLFAMDGTMRFKRFETIDLTQLGWTSHGKVMKPYAFRAPVIOGITICN
: : : : . : : : * : : : : : : * : * * * * * : * * * * * :
      ****:

capsid|TGV
AED99811.1|TVV1-UR1
AED99813.1|TVV1-UH9
TAATVDSIKVTTMVSGPLRDTIAPHFC
TAYTSTAIDIVTTVFGLRLRVGLTFE
TAYTTTAIDIVTTVFGLRQRVGLTFE
* * * : * : . * * * * : . . *

```

Figure 4.7 alignment of the protein sequences encoded by TGV1 capsid compared with TVV1

A)

20	516	530	NANKRNRQRKFRFA	15
21	532	537	INRFND	6
22	551	556	VQRLEG	6
23	564	564	E	1
24	567	578	QYLMKGGDIRNC	12

B)

NANKRNRQRKFRFAINRFNDPEYAYMFYIKNGVQRLEGVVTSKIDEEVQYLMKGGDIRNC

Figure 4.8A A) epitope predictions and B) conserved peptide with multiple epitopes

The nucleotide sequence of the TGV1 capsid protein gene (Figure 5.8) was also aligned to highlight target regions of conservation from which diagnostic primers sets might be

selected. Just two stretches showed enough conservation to be potentially useful nucleotides 937-1116 and 1537-1748 both showed over 70% identity with regions of >10 nucleotides with 100% identity between TGV1 and TVV1 viruses suggesting several possible primer sets were possible from each target region.

TGV capsid complete CDs

```
ATGTTTCGCGTATTGACCATGGCTGAGCTTAGTTTCAGGAAGTGGTCCACTTAATGGCGATTAAATGATGATAAGAAT
CGTCAGGTTATGGCTTCCCCGCCACAGGAGGCAAATAAAATAAGTGGCACAAATTATGATTTTATTTATGATTTTTGA
AGCACGCACAGGATACCAATCTACAATCACATGCGAATTGTCAATTAAGTCGTAAAGCAGGTGGTGAATTAGATCCGA
CAAAGTGGGGAGATGCCGTCATGAGGTTGACACACACAGTTTCAAGTGTATAGCCGATCTTGACAGTTCACTCGCGCA
ACAACCTCGAAGTCTGACTTCGGTTTGGGCCAAGATGTCACAAGACAGTCAGGACCGATTTCTATCCCACTAAATTCAC
CAGAACGTTACAAAGAGCTGGCCAAGAGCATCAGCTCTCTGTATCAGAAGAAGGCCTTTATGACCGACATGAAGTCG
CAAGTAATACTAGATCTTATGCAAACTCAGACTTAAGTATCGCAACTGTCGCCGCTGGTTTCTACACAGCGTTGAGT
GCACGCCACGAAGTGATCAAAGCAATAAGCACTGCTGACCAACCGTTCCGATTTTGCCTCAGCCATCAGTGCAACATCA
CACGCAGCACCAAACGCCGCAAGATGCTCACACATGATATCCTCATTCTCAGAGCAGAGGAATGCTCAAACAGAGA
AAGGGATATCCAGAACGATGTCAACTTATGGGGTATCGTCCACATCAAAGAACTGCCCTGCAAGGCGACAACATCA
TACGTCCAGACACAATCACAATCTTCGCTCCCAACGAATCCTTAGGTCAAAGTTGGTGGTGCGCGATTTGGCTGCTTTC
GATCTTTATCCAATCGATGAAATACAACACGAAAATATACATTTACGTGCTCCAGGTGCTGTAACCCACTTAACAGCG
TTCACAGACACCAACATTACTGAAGCAATTACGATTTTACTCGGAATGGCCAAAGACGCCAGGCAGCTCAGTGATGCT
CTCGAAACTTTCCTCTACGTCCAAGGTTTACAGATGGTCATCCAGCCACACTCGCTATACACAGAGGGAGGAGTTGTC
CGGAAGATGATCTTCGCCGTTCCAACTTGAAACACACGGCATGTTCACTACAAAACCTGCCTACTCAAGATTGACCT
CAATTAAGCGCCCAGATGATCTAGTCTCCGCCAAGAACTTCATCTGCGCTGGAGGAGTCTGCACAACGCAACTAGCGC
TCTGCTACCAGGCCGCTCTCAGCTGCAAAGGTCCGATAGCCATCCATTGGGAGAGTAATGATGCTATCTCAACCGCTC
AAAAGCGCCTCGCAAACAGATACTTAAGAGGCCGATTCTTCACAGTTCCAATCGCCCAAGTACCGTCACTAACGTCG
CAATCTACACACGTGCCGTCCGTGACGATCCCAAATACAAGAGCCAGCTCGGCGAGATCTTGCCCAACTATTTGGAG
CAGGTGCTGAAGTCATCATCGATATAGAAGAAGATATCATTAACTCCAGCAACGTCTCGATCAACGCTAACAAGCGCA
ATCGCCGCCAGAGAAAATTCCGTACAGCGTTTCATCAACAGATTCAACGATCCGGAGTACGCCTACATGTTCCGGCATCA
AGGGCAACGGTGTTTCAGCGCCTCGAAGGTGTCGTACGTCAAAAATTGATGAAGAAGTCCAATACTTGATGAAAGGT
GGCGACATCCGCAACTGCCCAATCCTCCGCACAAGCTATGCCGCAAACAACGATTTAGACATCAAGCTCGTCGCAGAA
GACGAAGATGCCTTCATCAGCACACTCGACGGCAGGCTCATCGAGATCGGCCTTACCAAGCTAAGGCCTTCTCAGAT
ATCGGCTGGAATTCGAGAGGTAAAGGTCATGAAGCCTTACGAGATAAGAGCTCCACTCTCCACAACGTCCAAATACA
GCGTACTGCTGCAACGGTCGACTCCATCAAAGTCACGACAATGGTCTCTGGACCATTGCGCGATACCATCGCGCCCCA
TTTTTGCTAG
```

Figure 4.8 complete CDs of the TGV capsid protein gene.

A) 937-TTCACAGACACCAACATTACTGAAGCAATTACGATTTTACTCGGAATGGCCAAA-GAC-
GCCAGGCAGCTCAGTGATGCTCTCGAACTTTCTCTACGTCCAAGGTTTACAGATGGTC
ATCCAGCCACACTCGCTATACACAGAGGGAGGAGTTGTCCGGAA-
GATGATCTTCGCCGTTCCAACTTGAAACCACACGGCATGTTCACTACAAAATTGCCTA
CTCAA-1116

Score	Expect	Identities	Gaps	Strand
70.7 bits(77)	2e-07	129/183(70%)	6/183(3%)	Plus/Plus
Query 1	TTCACAGACACCAACAT-TACTGAAGCAATTACGATTTTACTCGGAATGGCCAAAGACGC			
Sbjct 1259	TTCACAGATGCCGATATCTAC-GAGGCTATTCTATCTTACTTGAATGTGCGAAA-ACAT			
Query 60	CAGGC-AGCTCAGTGATGCTCTCGAACTTTCTCTACGTCCAAGGTTTACAGATGGTC			
Sbjct 1317	CACGCCAGTTCAGAAAGCG-TCGAAAGCATGCTCTACGCATACGGCGCGCAGATGGTT			
Query 118	ATCCAGCCACACTCGCTATACACAGAGGGAGGAGTTGTCCGGAAGATGATCTTCGCCGTT			
Sbjct 1376	ATCCAGCCACACTCGCTTTACACAGAAGGCGGTATAGTCAGAAGAATGATCTTTACCGTC			
Query 178	CCA 180			
Sbjct 1436	CCA 1438			

B) 1537-TCGATCAACGCTAACAAGCGCAATCGCCGCCAGAGAAAATTCCG-
TACAGCGTTCATCAACAGATTCAACGATCCGGAGTACGCCTACATGTTTCGGCATCAAGG
GCAACGGTGTTCAGCGCCTCGAAGGTGTCGTACGTCAAAAATTGATGAA-
GAAGTCCAA-
TACTTGATGAAAGGTGGCGACATCCGCAACTGCCCAATCCTCCGCAC-1748

Score	Expect	Identities	Gaps	Strand
122 bits(134)	3e-22	154/212(73%)	0/212(0%)	Plus/Plus
Query 1537	GTCTCGATCAACGCTAACAAGCGCAATCGCCGCCAGAGAAAATTCCGTACAGCGTTCATC			
Sbjct 1852	GTCTCAATCAATGCTACGAAACGCAACGGCCGTGCCAGAAAGTTCAGGACGGCTTTCATC			
Query 1597	AACAGATTCAACGATCCGGAGTACGCCTACATGTTTCGGCATCAAGGGCAACGGTGTTCAG			
Sbjct 1912	AACCGCTTTCATGATCCAGAATTGCTTACATGTTTCGGCATTACTGGCAATGGCATCGAG			
Query 1657	CGCCTCGAAGGTGTCGTACGTCAAAAATTGATGAAGAAGTCCAATACTTGATGAAAGGT			
Sbjct 1972	CGGATGGAAGGTAAAGTCACGTGCAACATCGCACAGGAAGTTGAATACCTCACCAACGGT			
Query 1717	GGCGACATCCGCAACTGCCCAATCCTCCGCAC 1748			
Sbjct 2032	GGTGACCTTCGCAACTGCCCAATCCTCCGCAC 2063			

Figure 4.9 (A and B) Two conserved target regions (>70% identity) of the capsid gene in the TGV genome against which primers will be made for RT-PCR based detection.

4.4 Discussion

Trichomonas gallinae is a serious infection of birds which causes avian trichomonosis (canker/frounce) and is a commercial threat to avian livestock particularly columbids and raptors but is occasionally a cause of infection in poultry. The pathology is highly variable, predominantly asymptomatic or mild but some strains cause lethal infections. In the closely related human pathogen *Trichomonas vaginalis*, viruses are known to modulate virulence (Fichorova *et al.*, 2013).

The full-length protein-coding sequences for six TVV strains that have been deposited into GenBank, allowed for phylogenetic comparisons among these viruses as well as with other members of the family *Totiviridae*. From such analyses, it was clear that TVVs constitute a monophyletic cluster distinguishable from all other viruses in the family, including from members of the genus *Giardiavirus*, to which TVVs had been previously assigned on a tentative basis before the recently approved proposal to segregate them into their own new genus, *Trichomonasvirus* (TV). Moreover, the TVs appear to be more closely related to protozoan viruses in the genus *Leishmanivirus* and to fungal viruses in the genus *Victorivirus* than to other protozoan and fungal viruses in the respective genera *Giardiavirus* and *Totivirus* (Goodman *et al.*, 2011).

A total of 35 dsRNA viruses were identified from 18 *T. vaginalis* isolates in Philippine. Multiple TVV species were observed in six of the 18 *T. vaginalis* cultures. Phylogenetic analyses show monophyly in TVV1 and TVV2 whereas TVV3 and TVV4 appear paraphyletic. (Rivera *et al.*, 2017). A new virus of *T. gallinae* closely related to one group of *T. vaginalis* viruses has been discovered. In this chapter I have been able to report that this virus consists of two genes encoding respectively the viral capsid and the viral polymerase. Using this sequence we identify conserved nucleotides able to act as targets of primers for diagnostic PCR in anticipation of a relationship between strain virulence and presence of the virus. I focussed

on the capsid protein as the source for these since it is well conserved and likely more abundant more antigenic the polymerase.

4.4.1 Surprising phylogeny

The evolutionary relationship between *T. gallinae* (*sensu lato*) and *T. vaginalis* is much discussed but remains unresolved. Some alleles show striking similarity between *T. vaginalis* and some but not other *T. gallinae* isolates. Thus there is some indication that *T. vaginalis* shares relatively recent common ancestry with some *T. gallinae* clades which in turn suggests a zoonotic origin. *T. vaginalis*, has a large, complex genome that although haploid overall is polyploid with respect to some alleles it is possible that it has a hybrid origin from multiple and diverse trichomonads including but not restricted to *T. gallinae*. It has not yet been established whether the origins of *T. vaginalis* are monophyletic and it may be that modern strains include a mosaic of genes acquired more recently from *T. gallinae* amongst genes from older previously evolved *T. vaginalis* lineages.

If *T. vaginalis* had evolved directly from *T. gallinae* diverging after a single species jump then the most straightforward expectation would be that any virus would have begun to diverge at the same point and that any *T. gallinae* viruses would branch prior to the radiation of the *T. vaginalis* viruses which have been characterised. The observation that TGV1 nests amongst the TVV viruses and is more akin to TVV1 than any of the other TVV clades suggest that this cannot be the case. Neighbour-net analysis provides no indication that the evolutionary rate is massively different in the different hosts or that there is any recombination between the TVV and TGV viruses which have likely evolved independently of each other since the hosts trichomonads have diverged. It is however consistent with the hypothesis that modern *T. vaginalis* may be a hybrid of an earlier *T. vaginalis* parasite which hosted the TVV2, 3 and 4 viruses with a more recent *T. gallinae* zoonosis which contained a TVV1/TGV1 like progenitor.

4.4.2 Future Work

The transcriptome of the C10 line firmly establishes the presence of trichomonas viruses in *Trichomonas gallinae* isolates but further study of the effect of these viruses on avian trichomonosis will be greatly enhanced by the establishment of a diagnostic tool kit containing specific antibody and PCR probes. Based on the presence of a single founding TGV we cannot fully anticipate the genetic diversity of these viruses and it is clearly likely that even if most are part of a single family ideally design of diagnostics would encompass a range of viral isolates. I reasoned though that in all likelihood TGV viruses would be more like TGV1 than TVV1 and so that by designing probes able to recognize both at conserved region it was likely that these probes would be likely to recognize a good proportion of other TGV viruses. Further an antibody able to recognize the viral capsid would greatly facilitate both follow-on studies of TGV life-cycle and pathogenesis and potentially enable screening of *T. gallinae* isolates for virus to establish the prevalence of the virus. Similarly, A PCR based screen for the virus would be highly desirable and so I have laid the groundwork in this chapter for diagnostic and epidemiologic studies to follow.

References 4.5:

- Adams, M. D. *et al.* (1991) 'Complementary DNA Sequencing: Expressed Sequence Tags and Human Genome Project', *Science*, 252(5013), pp. 1651–1656. doi: 10.1126/science.2047873.
- Adams, M. D. *et al.* (1992) 'Sequence identification of 2,375 human brain genes', *Nature*, 355(6361), pp. 632–634. doi: 10.1038/355632a0.
- Adams, M. D. *et al.* (1993) 'Rapid cDNA sequencing (expressed sequence tags) from a directionally cloned human infant brain cDNA library', *Nature Genetics*, 4(4), pp. 373–380. doi: 10.1038/ng0893-373.
- Alonso, A. M. *et al.* (2022) 'In-depth comparative analysis of *Trichomonas foetus* transcriptomics reveals novel genes linked with adaptation to feline host', *Scientific Reports*, 12(1), p. 10057. doi: 10.1038/s41598-022-14310-x.
- Bettencourt, C. *et al.* (2016) 'Gene co-expression networks shed light into diseases of brain iron accumulation', *Neurobiology of Disease*, 87, pp. 59–68. doi: 10.1016/j.nbd.2015.12.004.
- Bumgarner, R. (2013) 'Overview of DNA Microarrays: Types, Applications, and Their Future', *Current Protocols in Molecular Biology*, 101(1). doi: 10.1002/0471142727.mb2201s101.
- Camacho, C. *et al.* (2009) 'BLAST+: architecture and applications', *BMC Bioinformatics*, 10(1), p. 421. doi: 10.1186/1471-2105-10-421.
- Cantor, C. R. (1990) 'Orchestrating the Human Genome Project', *Science*, 248(4951), pp. 49–51. doi: 10.1126/science.2181666.
- Chang, J. T. (2016) *Transcriptomics and Gene Regulation, Transcriptomics and Gene Regulation*. Edited by J. Wu. Springer Netherlands (Translational Bioinformatics). Available at: http://link.springer.com/10.1007/978-94-017-7450-5_4.
- Chu, Y. and Corey, D. R. (2012) 'RNA Sequencing: Platform Selection, Experimental Design, and Data Interpretation', *Nucleic Acid Therapeutics*, 22(4), pp. 271–274. doi: 10.1089/nat.2012.0367.
- Cockrum, C. *et al.* (2020) 'A primer for generating and using transcriptome data and gene sets', *Development*, 147(24). doi: 10.1242/dev.193854.
- Dujon, B. (1998) 'European functional analysis network (EUROFAN) and the functional analysis of the *Saccharomyces cerevisiae* genome', *Electrophoresis*, 19(4), pp. 617–624.
- Fichorova, R. N. *et al.* (2013) 'The Villain Team-Up or how *Trichomonas vaginalis* and bacterial vaginosis alter innate immunity in concert', *Sexually Transmitted Infections*, 89(6), pp. 460–466. doi: 10.1136/sextrans-2013-051052.
- Goodman, R. P. *et al.* (2011) 'Trichomonasvirus: a new genus of protozoan viruses in the family Totiviridae', *Archives of Virology*, 156(1), pp. 171–179. doi: 10.1007/s00705-010-0832-8.
- Grabherr, M. G. *et al.* (2011) 'Full-length transcriptome assembly from RNA-Seq data without a reference genome', *Nature Biotechnology*, 29(7), pp. 644–652. doi: 10.1038/nbt.1883.
- Graves, K. J. *et al.* (2019) 'Trichomonas vaginalis Virus Among Women With Trichomoniasis and Associations With Demographics, Clinical Outcomes, and Metronidazole Resistance', *Clinical*

- Infectious Diseases*, 69(12), pp. 2170–2176. doi: 10.1093/cid/ciz146.
- Handrich, M. R. *et al.* (2019) 'Characterization of the BspA and Pmp protein family of trichomonads', *Parasites & Vectors*, 12(1), p. 406. doi: 10.1186/s13071-019-3660-z.
- Hepatitis, Immunology and Viral Diseases Panels, USJCMSP AIDS, ARI, C. *et al.* (2019) '20th International Conference on Emerging Infectious Diseases in the Pacific Rim Organized by the United States-Japan Cooperative Medical Sciences Program (USJCMSP)', *Vaccines*, 7(2), p. 35. doi: 10.3390/vaccines7020035.
- Hirt, R. P. *et al.* (2007) 'Trichomonas vaginalis surface proteins: a view from the genome', *Trends in Parasitology*, 23(11), pp. 540–547. doi: 10.1016/j.pt.2007.08.020.
- Kraemer, M. U. G. *et al.* (2019) 'Utilizing general human movement models to predict the spread of emerging infectious diseases in resource poor settings', *Scientific Reports*, 9(1), p. 5151. doi: 10.1038/s41598-019-41192-3.
- Kuhlmann, F. M. *et al.* (2017) 'Antiviral screening identifies adenosine analogs targeting the endogenous dsRNA Leishmania RNA virus 1 (LRV1) pathogenicity factor', *Proceedings of the National Academy of Sciences*, 114(5). doi: 10.1073/pnas.1619114114.
- Maitra, R. D., Kim, J. and Dunbar, W. B. (2012) 'Recent advances in nanopore sequencing', *ELECTROPHORESIS*, 33(23), pp. 3418–3428. doi: 10.1002/elps.201200272.
- Manny, A. R. *et al.* (2022) 'Discovery of a Novel Species of Trichomonasvirus in the Human Parasite Trichomonas vaginalis Using Transcriptome Mining', *Viruses*, 14(3), p. 548. doi: 10.3390/v14030548.
- Martin, J. A. and Wang, Z. (2011) 'Next-generation transcriptome assembly', *Nature Reviews Genetics*, 12(10), pp. 671–682. doi: 10.1038/nrg3068.
- Metzker, M. L. (2010) 'Sequencing technologies — the next generation', *Nature Reviews Genetics*, 11(1), pp. 31–46. doi: 10.1038/nrg2626.
- Mikheyev, A. S. and Tin, M. M. Y. (2014) 'A first look at the Oxford Nanopore MinION sequencer', *Molecular Ecology Resources*, 14(6), pp. 1097–1102. doi: 10.1111/1755-0998.12324.
- Mitreä, D. M. *et al.* (2014) 'Structural polymorphism in the N-terminal oligomerization domain of NPM1', *Proceedings of the National Academy of Sciences*, 111(12), pp. 4466–4471. doi: 10.1073/pnas.1321007111.
- Morozova, O., Hirst, M. and Marra, M. A. (2009) 'Applications of New Sequencing Technologies for Transcriptome Analysis', *Annual Review of Genomics and Human Genetics*, 10(1), pp. 135–151. doi: 10.1146/annurev-genom-082908-145957.
- Nagalakshmi, U. *et al.* (2008) 'The Transcriptional Landscape of the Yeast Genome Defined by RNA Sequencing', *Science*, 320(5881), pp. 1344–1349. doi: 10.1126/science.1158441.
- Noël, C. J. *et al.* (2010) 'Trichomonas vaginalis vast BspA-like gene family: evidence for functional diversity from structural organisation and transcriptomics', *BMC Genomics*, 11(1), p. 99. doi: 10.1186/1471-2164-11-99.
- Nookaew, I. *et al.* (2012) 'A comprehensive comparison of RNA-Seq-based transcriptome analysis

- from reads to differential gene expression and cross-comparison with microarrays: a case study in *Saccharomyces cerevisiae*', *Nucleic Acids Research*, 40(20), pp. 10084–10097. doi: 10.1093/nar/gks804.
- Okubo, K. *et al.* (1992) 'Large scale cDNA sequencing for analysis of quantitative and qualitative aspects of gene expression', *Nature Genetics*, 2(3), pp. 173–179. doi: 10.1038/ng1192-173.
- Passos, G A (2014) *Transcriptomics in Health and Disease*. 2nd Edn. Edited by Geraldo A. Passos. Cham: Springer International Publishing. doi: 10.1007/978-3-319-11985-4.
- Piétu, G. *et al.* (1999) 'The Genexpress IMAGE Knowledge Base of the Human Brain Transcriptome: A Prototype Integrated Resource for Functional and Computational Genomics', *Genome Research*, 9(2), pp. 195–209. doi: 10.1101/gr.9.2.195.
- Rivera, W. L. *et al.* (2017) 'Detection and molecular characterization of double-stranded RNA viruses in Philippine *Trichomonas vaginalis* isolates', *Journal of Microbiology, Immunology and Infection*, 50(5), pp. 669–676. doi: 10.1016/j.jmii.2015.07.016.
- Takeda, J. *et al.* (1993) 'A molecular inventory of human pancreatic islets: sequence analysis of 1000 cDNA clones', *Human Molecular Genetics*, 2(11), pp. 1793–1798. doi: 10.1093/hmg/2.11.1793.
- Trifinopoulos, J. *et al.* (2016) 'W-IQ-TREE: a fast online phylogenetic tool for maximum likelihood analysis', *Nucleic Acids Research*, 44(W1), pp. W232–W235. doi: 10.1093/nar/gkw256.
- Velculescu, V. E. *et al.* (1997) 'Characterization of the Yeast Transcriptome', *Cell*, 88(2), pp. 243–251. doi: 10.1016/S0092-8674(00)81845-0.
- Wang, R.-S. *et al.* (2009) 'Modeling post-transcriptional regulation activity of small non-coding RNAs in *Escherichia coli*', *BMC Bioinformatics*, 10(S4), p. S6. doi: 10.1186/1471-2105-10-S4-S6.
- Warring, S. D. *et al.* (2021) 'Small RNAs Are Implicated in Regulation of Gene and Transposable Element Expression in the Protist *Trichomonas vaginalis*', *mSphere*. Edited by K. S. Ralston, 6(1). doi: 10.1128/mSphere.01061-20.
- Watson, J. D. (1990) 'The Human Genome Project: Past, Present, and Future', *Science*, 248(4951), pp. 44–49. doi: 10.1126/science.2181665.
- Williams, P. S. *et al.* (2021) 'Microfluidic chip for graduated magnetic separation of circulating tumor cells by their epithelial cell adhesion molecule expression and magnetic nanoparticle binding', *Journal of Chromatography A*, 1637, p. 461823. doi: 10.1016/j.chroma.2020.461823.
- Woehle, C. *et al.* (2014) 'The parasite *Trichomonas vaginalis* expresses thousands of pseudogenes and long non-coding RNAs independently from functional neighbouring genes', *BMC Genomics*, 15(1), p. 906. doi: 10.1186/1471-2164-15-906.
- Wolf, J. B. W. (2013) 'Principles of transcriptome analysis and gene expression quantification: an <scp>RNA</scp>-seq tutorial', *Molecular Ecology Resources*, 13(4), pp. 559–572. doi: 10.1111/1755-0998.12109.
- Wreschner, D. H. and Herzberg, M. (1984) 'A new blotting medium for the simple isolation and Identification of highly resolved messenger RNA', *Nucleic Acids Research*, 12(3), pp. 1349–

1360. doi: 10.1093/nar/12.3.1349.

Yuan, J. *et al.* (2021) 'Transcriptome Analysis Revealed Potential Mechanisms of Resistance to Trichomoniasis gallinae Infection in Pigeon (*Columba livia*)', *Frontiers in Veterinary Science*, 8, p. 672270. doi: 10.3389/fvets.2021.672270.

Chapter 5

5. General Discussion

Canker and frounce are serious and often deadly pathologies arising in columbids, passerines and birds of prey due to infection with *Trichomonas gallinae* which are associated with huge die-offs and thus *T. gallinae* is a pathogen which provides an existential threat to some avian species. Avian trichomoniasis is well documented in most countries and literature as a parasitic disease caused by the flagellated protozoan parasite *T. gallinae* (Stabler, 1954). This parasite infects the upper digestive tract of domestic and wild birds, including the mouth, crop, esophagus and pharynx, causing erosions and necrotic lesions, as well as necrotic foci within internal organs, such as the liver and lungs. Severe cases can be deadly in the early days following infection (AMIN *et al.*, 2014; Grunenwald *et al.*, 2018). However infection with *T. gallinae* is not only not always fatal, indeed a majority of the infections detected in columbids are considered asymptomatic and it is very possible that infection with avirulent *T. gallinae* provides at least some protection against more virulent strains. Thus, an understanding of strain virulence and pathogenicity is essential to the understanding and management of this pathogen. During the course of my PhD studies, I researched the possibility that the pathology of avian trichomonosis was modulated by the presence of viruses – not co-infections of the host but rather of a variety specific to the pathogen.

5.1 Screening an archive of genetically diverse *Trichomonas gallinae* isolates from the UK.

A total of 21 isolates of *T. gallinae* were cultured and screened for dsRNA to investigate the possible presence of dsRNA viruses. Two isolates (C10 and C3) appeared positive on agarose these were unusual zoo isolates being derived from a Socorro dove (now extinct in the wild) and a pink pigeon (classified by IUCN as Endangered). In both cases the birds they were taken

from had been routinely screened and were asymptomatic. To characterize these lines further, in order to ascertain whether the screen results could be attributable to the presence of an infecting dsRNA virus a reduced panel of the C10, C3, a related common but often virulent strain of *T.gallinae* C4 and the highly virulent A1 strain were selected for further characterization. Northwestern dot blotting indicated some evidence for increased dsRNA in the C10 and C3 strains, however fluorescence staining for dsRNA showed a clear punctate peripheral staining pattern consistent with a viral infection only in the C10 strain and this was consistent with identification of appropriate dsRNA banding on a Northwestern blot for only C10.

5.2 To use Transmission Electron Microscopy and negative staining of supernatants to validate the presence of virus in the isolates identified in the screen.

The presence of increased dsRNA in an isolate need not necessarily reflect the presence of a capsid forming virus but can for instance be associated with transposons and transposon silencing. So, in order to evaluate further whether C10 and possibly C3 might be host to viral infections a visual confirmation of the virus and its capsid was sought. In doing so I was aware that the concentration of any capsid bound virus in the supernatant might be too low to be observable and so the virus might be most easily observed by TEM of sectioned parasites or by concentration of the supernatants and so sought to undertake all three methods. Supernatants were dried onto EM grids and negatively stained. No icosahedral structures were visible in the C3, C4 or A1 supernatants in comparison an icosahedral, virus like particle was observed in the C10 supernatant in the 30-40 nm size range consistent with other *Trichomonas* Viruses. I concentrated the supernatants and negatively stained the concentrates on EM grids. Interestingly exosomes were very apparent by this method in the C10 supernatant, but we not readily visualized from C3, C4 or C10 samples. Although naked icosahedral virus-like particles of the sort visualized from the unconcentrated supernatant were not obvious in the concentrate, in many

of the exosomes an electron dense core was consistent with virions being released as exosomes into the media which has been recently postulated for TVV release from *T. vaginalis*. In that study it was confirmed that TVV particles are released from infected *T. vaginalis* cells to the extracellular environment via sEVs and induced proinflammatory responses in human HaCaT cells. Considering the high prevalence of TVV harbouring *T. vaginalis* clinical isolates, the release of TVV via small exosomal vesicles (sEVs) might be critical for the development of pathologies related directly to trichomoniasis, as well as other pathologies related to modulation of the immune response such as the increased risk of preterm birth, susceptibility to HIV-1, and human papillomaviruses in *T. vaginalis*-infected patients (Rada *et al.*, 2022). Exosomes derived from virus-infected cells may contain various viral components with different functions together with altered protein and RNA cargo of host cell origin (Crenshaw *et al.*, 2018; Saad *et al.*, 2021). Moreover, exosomes from highly adherent parasite strains increase the adherence of poorly adherent parasites to vaginal and prostate epithelial cells. In contrast, exosomes from poorly adherent strains had no measurable effect on parasite adherence. Exosomes from parasite strains that preferentially bind prostate cells increased binding of parasites to these cells relative to vaginal cells. In addition to establishing that parasite exosomes act to modulate host:parasite interactions, these studies were the first to reveal a potential role for exosomes in promoting parasite:parasite communication and host cell colonization (Twu *et al.*, 2013). The effect of delivery of TGV1 in exosomes on avian mucosa and the immune response to *T. gallinae* is an interesting area for future research which may be relevant to avian mucosal vaccine delivery in the future.

5.3 To evaluate phenotypic differences between infected and closely related uninfected isolates using Scanning Electron Microscopy and Transmission Electron Microscopy.

In terms of growth and morphology, the C10 strain appeared smaller in size in the Giemsa-stained (surface area and volume) and grew less well in culture than the other isolates consistent

with the isolate being negatively affected by the presence of a virus. This stands in stark contrast to the paradigm for the other trichomonas viruses of *Trichomonas vaginalis* which are sometimes referred to as symbiotic and which are considered to exacerbate rather than attenuate pathogenesis.

All viruses are in fact obligate intracellular parasites and infection of any cell with a virus exacts a price on the host cell. Protozoa are very different from metazoans in how they can deal with virus threats because many metazoan cells rely on altruistic, programmed cell death as a means of protecting from being wiped out by a virus. In amoeboid protozoa like trichomonas, it is not obvious that a programmed cell death provides evolutionary advantage so trichomonas may have to live with any viruses it acquires until such time as it is able to find a way to inactivate them or is killed by them even if fitness suffers as a result. Our initial assays suggest that the infected C10 line may be less fit than the other cell lines and it is notable that the dove from which it was isolated was asymptomatic which may be an indication that a less fit cell line actually causes more, rather than less pathology which is intuitive but counter to the case proposed for TVV.

To look in more detail at the morphological and topological differences between C10 and the other lineages we used a Field Emission Scanning Electron Microscope. These images confirmed the considerable reduction in size of C10 compared to other lineages. At high resolution the increased blebbing from the C10 lineage is apparent and in some images a granulate surface by represent exosomes/virus being shed.

An interesting observation was that these parasites appear cannibalistic, able to devour each other in part (trogocytosis) or in whole (phagocytosis) into large vacuoles where they are degraded, and the membrane remnants excreted. During the course of the PhD an attempt unsuccessful attempts were made to infect, uninfected isolates with supernatant from C10 (not

shown). In the future it may be that by mixing infected and uninfected cells and allowing the uninfected cells to consume infected ones that the virus can be transmitted more successfully.

5.4 To determine the genomic sequences of any novel viruses identified.

The current study has used transcriptomics to confirm the presence on a novel virus in *T. gallinae*. The C10 subtype expresses viral transcripts at a high level which were absent in the three other isolates (C3, C4 and A1) for which transcriptomes were also obtained. Within the *Totiviridae* family, the genera named *Giardiavirus*, *Trichomonasvirus*, *Leishmanivirus*, *Totivirus*, and *Victorivirus*, are currently recognised which share common characteristics (Hillman and Cohen, 2021). Their genomes are linear uncapped dsRNA encoding for two partially overlapping proteins; the capsid protein (Schantz *et al.*, 1995) and the RNA-dependent RNA polymerase (RdRp). The RdRp is generally expressed as a CP/RdRp fusion protein by means of a -1 or, more rarely, $+1/-2$ ribosomal frameshift or by ribosomal hopping (Hillman and Cohen, 2021). The viral genome is never found free in the protozoan cell and the positive strand viral transcript is synthesized within the viral particle by CP/RdRp and translocated to the cell cytoplasm to be translated (Hillman and Cohen, 2021). To date our investigation of the novel TGV shows it to be a typical *Trichomonas* virus with its major features entirely consistent with other TVV1 viruses.

A Neighbour-Net analysis indicates that the TGV 1 isolate and TVV isolates appear to have evolved independently with little evidence for genetic exchange between the major lineages (TVV1, TGV1, TVV2, TVV3, TVV4) although some genetic exchange may have occurred between viruses within TVV lineages. Strong similarities in the capsid proteins between TGV and TVV lineages enabled the design of primers and epitopes to the conserved regions which may enable PCR and mAb based diagnosis of the virus in infections with avian trichomoniasis.

5.5 Afterword

T. vaginalis often harbours double-stranded RNA (dsRNA) viruses from the genus *Trichomonas virus* of the *Totiviridae* family (Wendel *et al.*, 2002; Weber, 2003). Given the widespread prevalence of TVV infections and the demonstration that TVV infections can modulate host translation and expression of immunogenic proteins (Alderete *et al.*, 1986), it is possible that underlying TVV infections may modulate the pathogenesis of *T. vaginalis* infections and possibly underlie differences in symptomatology, drug resistance, parasite load, transmissibility, etc. There is precedence in the literature for endobiotic viruses modulating the pathogenicity or behaviour of their parasitic hosts; for example, a virus infecting *Cryptosporidium parvum* has been shown to increase the fecundity of its protozoan host (levels of oocysts shed in faeces) during *C. parvum* infection of dairy calves (Jenkins *et al.*, 2008). And in *Leishmania* where the presence of virus has been correlated with the severe mucocutaneous pathology, virus has been described to have a major impact on the protein content of parasite's exosomes via modulation of mRNA translation and exploits *Leishmania* for packing viral particles into the exosomes to be released into the extracellular environment (Atayde *et al.*, 2019).

Virus infection of the cell leads to activation of innate immune responses that are accountable for impeding early virus replication and facilitating the establishment of adaptive immunity that comprise the generation of neutralizing antibodies and cytotoxic T cells (Su *et al.*, 1998). These innate cellular sentinels include a number of molecules that recognize dsRNA species, usually generated by viruses following infection of the cell (Biron, 1999).

T. vaginalis carries viruses which contribute to their transmission to a new host, as viruses internalised by *T. vaginalis* were shown to be infectious for human cells for 2–6 days. The viruses are either released upon parasite death or secreted from *T. vaginalis* -loaded viruses through the recycling route of the endocytic pathway. There is no evidence that any virus

specific for the vertebrate host can replicate in *Trichomonads*, but *T. vaginalis* is thought to be able to act as a Trojan horse for HIV and possibly other viruses (Hirt *et al.*, 2007) and by extension *T. gallinae* could harbour other pathogens. Nevertheless, my findings suggest that the TGV1 infection of the genotype C10 isolate that I have discovered it in, is an active infection detrimental to the parasite and this correlates with its lack of virulence in the host from which it was taken. The properties it induces in this isolate suggest that it could have an adjuvant like effect in bolstering immunity to *T. gallinae* and so may effectively act as a live attenuated vaccine strain. In the future it is worth considering whether this isolate is actually apathogenic and whether it elicits a strong mucosal immunity to avian trichomonas in otherwise susceptible hosts.

5.6 References:

- A Biron, C. (1999) 'Initial and innate responses to viral infections — pattern setting in immunity or disease', *Current Opinion in Microbiology*, 2(4), pp. 374–381. doi: 10.1016/S1369-5274(99)80066-6.
- Alderete, J. F. *et al.* (1986) 'Phenotypic variation and diversity among *Trichomonas vaginalis* isolates and correlation of phenotype with trichomonal virulence determinants', *Infection and Immunity*, 53(2), pp. 285–293. doi: 10.1128/iai.53.2.285-293.1986.
- AMIN, A. *et al.* (2014) 'Trichomonads in birds – a review', *Parasitology*, 141(6), pp. 733–747. doi: 10.1017/S0031182013002096.
- Atayde, V. D. *et al.* (2019) 'Exploitation of the *Leishmania* exosomal pathway by *Leishmania* RNA virus 1', *Nature Microbiology*, 4(4), pp. 714–723. doi: 10.1038/s41564-018-0352-y.
- Crenshaw, B. J. *et al.* (2018) 'Exosome Biogenesis and Biological Function in Response to Viral Infections', *The Open Virology Journal*, 12(1), pp. 134–148. doi: 10.2174/1874357901812010134.
- Grunenwald, C. *et al.* (2018) 'Tetratrichomonas and *Trichomonas* spp.-Associated Disease in Free-Ranging Common Eiders (*Somateria mollissima*) from Wellfleet Bay, MA and Description of ITS1 Region Genotypes', *Avian Diseases*, 62(1), pp. 117–123. doi: 10.1637/11742-080817-Reg.1.
- Hillman, B. I. and Cohen, A. B. (2021) 'Totiviruses (totiviridae', in *Encyclopedia of Virology*, pp. 648–657.
- Hirt, R. P. *et al.* (2007) 'Trichomonas vaginalis surface proteins: a view from the genome', *Trends in Parasitology*, 23(11), pp. 540–547. doi: 10.1016/j.pt.2007.08.020.
- Jenkins, M. C. *et al.* (2008) 'Fecundity of *Cryptosporidium parvum* is correlated with intracellular levels of the viral symbiont CPV', *International Journal for Parasitology*, 38(8–9), pp. 1051–1055. doi: 10.1016/j.ijpara.2007.11.005.
- Rada, P. *et al.* (2022) 'Double-Stranded RNA Viruses Are Released From *Trichomonas vaginalis* Inside Small Extracellular Vesicles and Modulate the Exosomal Cargo', *Frontiers in Microbiology*, 13, p. 893692. doi: 10.3389/fmicb.2022.893692.
- Saad, M. H. *et al.* (2021) 'A Comprehensive Insight into the Role of Exosomes in Viral Infection: Dual Faces Bearing Different Functions', *Pharmaceutics*, 13(9), p. 1405. doi: 10.3390/pharmaceutics13091405.
- Stabler, R. M. (1954) 'Trichomonas gallinae: A review', *Experimental Parasitology*, 3(4), pp. 368–402. doi: 10.1016/0014-4894(54)90035-1.
- Su, H. C. *et al.* (1998) 'CD4+ and CD8+ T Cell Interactions in IFN- γ and IL-4 Responses to Viral Infections: Requirements for IL-2', *The Journal of Immunology*, 160(10), pp. 5007–5017. doi: 10.4049/jimmunol.160.10.5007.
- Twu, O. *et al.* (2013) 'Trichomonas vaginalis Exosomes Deliver Cargo to Host Cells and Mediate Host:Parasite Interactions', *PLoS Pathogens*. Edited by W. A. Petri, 9(7), p. e1003482. doi: 10.1371/journal.ppat.1003482.

- Weber, B. (2003) 'Double stranded RNA virus in South African *Trichomonas vaginalis* isolates', *Journal of Clinical Pathology*, 56(7), pp. 542–543. doi: 10.1136/jcp.56.7.542.
- Wendel, K. A. *et al.* (2002) 'Double-Stranded RNA Viral Infection of *Trichomonas vaginalis* Infecting Patients Attending a Sexually Transmitted Diseases Clinic', *The Journal of Infectious Diseases*, 186(4), pp. 558–561. doi: 10.1086/341832.

Appendix 2.1 The growth of *T. gallinae* over the five days for samples from 1-10

Lineages of 21 samples	AVERAGE cells/mL OF WHAT				
	1st	2nd	3rd	4th	5th
1-Tawny owlAA1	110	275000	550000	260000	175000
2-feral pigeon AA1	85000	210000	935000	325000	250000
3-Wood pigeon NN1	80000	195000	600000	260000	195000
4-Wood pigeon C C4 2017	115000	225000	550000	285000	185000
5-Wood pigeon AA1	115000	245000	735000	235000	130000
6-ChaffinchAA1	105000	260000	775000	310000	175000
7-feral pigeon CC8	105000	195000	525000	295000	190000
8-GoldfinchAA1	135000	200000	595000	200000	165000
9- Black naped fruit dove MA1	105000	255000	425000	335000	185000
10-Bullfinch AA1	80000	120000	450000	260000	180000

Appendix 2.2. The growth of *T. gallinae* in the five days for samples from 11-2110 9-C3 12-A1 13-C420

Lineages of 21 samples	AVERAGE cells/mL				
	1 st day	2 nd day	3 rd day	4 th day	5 th day
11-Siskin AA1	80000	170000	450000	180000	155000
12- Pink pigeonCC3	85000	200000	850000	310000	210000
13-GreenfinchAA1	85000	220000	750000	230000	195000
14-feral pigeon AA1 2015	110000	235000	550000	245000	155000
15-Wood pigeon CC4 2016	120000	245000	780000	235000	160000
16-feral pigeon CC4. 2017	105000	145000	775000	350000	170000
17-Collared dove AA1	110000	195000	625000	310000	190000
18-Feral pigeon CC4	140000	225000	595000	220000	155000
19-Brambling AA1	115000	255000	480000	310000	175000
20-BuzzardCC4	101000	135000	455000	270000	165000
21- Socorro dove CC10	85000	135000	540000	255000	190000